Vol. 71, Part III, 2001

ISSN 0369-8211

National Academy of Sciences, India, Allahabad

राष्ट्रीय विज्ञान अकादमी, भारत, इलाहाबाद

The *Proceedings of the National Academy of Sciences, India*, is published in two Sections: Section A (Physical Sciences) and Section B (Biological Sciences). Four parts of each section are published annually (since 1960).

The Editorial Board in its work of examining papers received for publication is assisted, in an honorary capacity by a large number of distinguished scientists. The Academy assumes no responsibility for the statements and opinions advanced by the authors. The papers must conform strictly to the rules for publication of papers in the *Proceedings*. A total of 25 reprints is supplied free of cost to the author or authors. The authors may ask for a reasonable number of additional reprints at cost price, provided they give prior intimation while returning the proof.

Communication regarding contributions for publication in the *Proceedings*, books for review, subscriptions etc. should be sent to the Managing Editor, The National Academy of Sciences, India, 5 Lajpatrai Road, Allahabad-211 002 (India).

Annual Subscription for both Sections : Rs. 500.00; for each Section Rs. 250.00; Single Copy : Rs. 100.00. Foreign Subscription : (a) for one Section : US $100, (b) for both Sections U.S.$ 200.

(Air-Mail charges included in foreign subscription)

Co-Sponsored by C.S.T., U.P. (Lucknow)

PROCEEDINGS

OF THE

NATIONAL ACADEMY OF SCIENCES, INDIA
2001

VOL. LXXI SECTION–A PART III

Synthesis of some new azo-coumarins and Schiffs bases as possible antibacterial agents

SANGEETA BHATNAGAR, KAUSIK GHOSH and D.S. SETH*

Department of Chemistry, St. John's College, Agra - 282 002,India

Received September 20, 1999; Revised January 28, 2000; Accepted June 30, 2000

Abstract

Several substituted coumarins and Schiffs bases have been prepared by the condensation of N-(2-chloro-5-tri fluoromethyl) phenyl malonamic acid with 2-hydroxy-5-(R)-phenyl azo benzaldehyde.

(**Keywords** : spectral studies/coumarin derivatives/Schiffs bases/N-(2-chloro-5-tri fluoromethyl) phenyl malonamic acid).

Introduction

Compounds bearing azo groups and azo coumarins are known to have various biological activities[1-8]. Mishra *et al.*[9] have observed that some coumarin possessed anti-bacterial activity against *Pseudomonas aeruginosa, E-coli* and *B-subtilis.*

The present work describes the condensation of N-(2-chloro-5-tri fluoromethyl) phenyl malonamic acid with some azo salicylaldehydes to form new coumarins bearing azo group at position 6 and new Schiff bases.

$R=R_1=R_2=R_3=H$. $R=CH_3$, $R_1=R_2=R_3=H$. $R_1=CH_3$, $R=R_1=R_3=H$. $R=CH_3$. $R=R_1=R_3=H$. $R=Cl$, $R_1=R_2=R_3=H$. $R_2=Cl$, $R_1=R=R_3=H$. $R_2=Br$. $R=T_1=R_3=H$. $R_1=R_3=H$. $R_1=NO_2$, $R=R_2=R_3=H$.

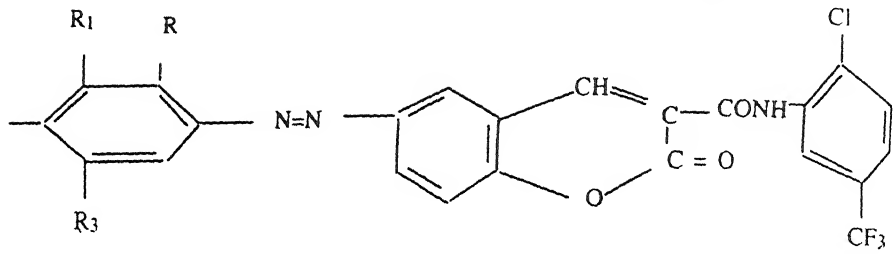

Coumarin

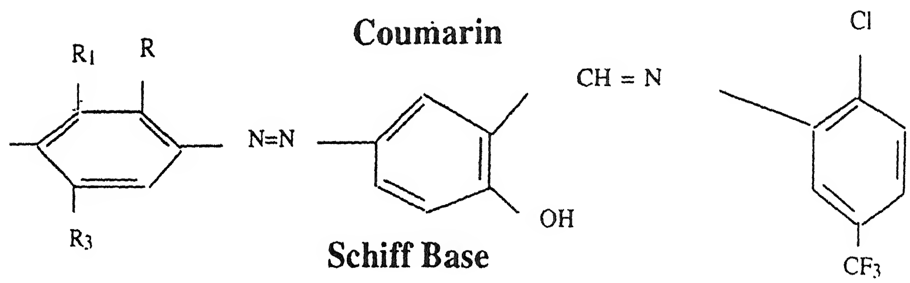

Schiff Base

Materials and Method

The general method for the preparation of coumarin and Schiff bases is to heat an equimolecular quantity of acid and aldehyde along with a drop or two of pyridine at 105 to115°C in an oil bath for 4 h. The mass first melted to a clear liquid which soon set to a solid. After completion of heating this was extracted with sodium bicarbonate solution to remove unreacted acid and the solid product left was invariably deeply coloured (yellow, orange, or mud brown). It was found to be a mixture of corresponding coumarins and Schiff bases. The Schiff base was easily separated from the coumarin being soluble in ethanol, while the coumarins remained insoluble. The coumarins were purified be repeated washing with boiling solvents such as ethanol, methanol and acetone. The Schiff bases were recrystallised from ethanol.

The melting points were determined using sulphuric acid bath. I. R. Spectra in Nujol were recorded on a Perkin Elmer spectrophotometer. ^{1}H-NMR spectrum were recorded on Brucker 300 MHz and TMS as an internal standard (chemical shifts in δ ppm).

Results and Discussion

The molecular formula, M.P., % yield, percentage of nitrogen, ^{1}H-NMR and HRMS of various coumarins and Schiffs bases are reported in Tables (1 and 2).

The filter paper disc method[10] was used for screening the compounds for antimicrobial activity. Standard size discs of Whatman filter paper No. 3 with a diameter of 6.5 mm were

Table 1 – Coumarins obtained by the condensation of N-(2-chloro-5-trifluoromethyl) phenyl malonamic acid with 2-hydroxy-5-(R)-phenyl azo benzaldehyde.

S.No	R	Mol. Formula of the Coumarin	M.P. (°C)	Yield (%)	Nitrogen (%) Found	Calc.	^{1}H - NMR data (300 MHz, $CDCl_3$, δ ppm)	Mass (API-300 ion spray) =m/z
1.	H	$C_{23}H_{13}F_3Cl\ N_3O_3$	Above 250	38.13	9.49	8.89	9.60 (S, 1H, CO-NH, D20 Exchangeable), 8.10 - 8.00 (m, 3H, Ar-H) 7.92-7.00 (broad m, 5H, Ar-H), 7.49 - 7.11 (dd, 3H, Ar-H), 6.40 (S, 1H,-CH=)	472.6 $[M+H]^+$ (+Ve ion mode)
2.	2—CH_3	$C_{24}H_{15}F_3Cl\ N_3O_3$	Above 250	26.74	8.85	8.64	9.58 (S, 1H, -CONH, D_2O Exchangeable), 8.00-7.98 (dd, 4H, J=8.0 Hz, Ar-H), 7.90—7.55 (m, 3H, Ar-H) 7.10-7.38 (m, 3H, Ar-H), 6.48 (s, 1H,-CM=) and 1.33 (S, 3H, -CH_3)	486.5 $[M+H]^+$ (+Ve ion mode)
3.	3—CH_3	$C_{24}H_{15}F_3Cl\ N_3O_3$	Above 250	31.25	8.77	8.64	9.42 (S, 1H,-CONH, D_2O exchangeable), 8.00-8.08 (m, 5H, Ar-H), 7.86-7.22 (m, 3H, Ar-H), 7.11 - 7.16 (brs, 2H, Ar-H), 6.46 (S, 1H, - CH=) and 1.40 (S, 3H, -CH_3)	486.6 $[M+H]^+$ (+Ve ion mode)
4.	4—CH_3	$C_{24}F_{15}F_3Cl\ N_3O_3$	Above 250	39.09	9.01	8.64	9.48 (S, 1H, - CONH, D_2O exchangeable), 7.92-7.90 (d, J=6.0 Hz, 2H, Ar-H), 7.88-7.86 (d, J=6.2 Hz, 2H, Ar-H), 7.22 - 7.68 (m, 6H, Ar-H), 6.45 (S, 1H, -CH=) and 1.46 (S, 3H, -CH_3)	486.7 $[M+H]^+$ (+Ve ion mode)
5.	2, 3$(CH_3)_2$	$C_{25}H_{17}F_3Cl\ N_3O_3$	Above 250	20.00	8.89	8.40	9.50 (S, 1H, -CONH, D_2O Exchangeable), 7.98-7.88 (m, 6H, Ar-H), 7.70-7.52 (broad m, 3H, Ar-H), 6.42 (S, 1H, -CH=C), 1.28 (S, 3H, 2-CH_3) and 1.22 (S, 3H, 3-CH_3)	400.5 $[M+H]^+$ (+Ve ion mode)
6.	3,4$(CH_3)_2$	$C_{25}H_{17}F_3Cl\ N_3O_3$	Above 250	30.00	8.69	8.40	9.46 (S, 1H, -CONH, D_2O exchangeable), 7.88-7.90 (m, 5H, Ar-H), 7.64-7.67 (m, 4H, Ar-H), 6.48 (S, 1H, CH=), 1.50(S, 3H, - CH_3) and 1.48 (S, 3H, - CH_3)	400.6 $(M+H)^+$ (+Ve ion mode)
7.	2—OCH_3	$C_{24}H_{15}F_3Cl\ N_3O_4$	190	19.92	8.51	8.36	9.61 (S, 1H, - CONH, D_2O exchangeable) 7.96 - 7.88 (dd, 4H, Ar-H), 7.70 - 7.80 (m, 3H, Ar - H) 7.28 - 7.38 (m, 3H, Ar-H), 6.52 (S, 1H, - CH=C) and 3.89 (S, 3H, - OCH_3	502.5 $[M+H]^+$ (Ve ion mode)
8.	3—NO_2	$C_{23}H_{12}F_3Cl\ N_4O_5$	Above 250	32.88	11.06	10.83	9.56 (S, 1H,-CONH, D_2O exchangeable), 7.94 - 7.46 (m, 6H, Ar - H) 7.21 - 7.31 (m, 4H, Ar-H) and 6.48 (S, 1H, - CH=C)	515.4 $[M-H]^+$ (-Ve ion mode)
9.	2—F	$C_{23}H_{12}F_4Cl\ N_3O_3$	Above 250	32.67	8.79	8.57	9.60 (S, 1H, - CONH, D_2O exchangeable), 7.89 - 7.69 (m, 4H, Ar - H) 7.51 -7.60 (broad m, 6H, Ar-H) and 6.54 (S, 1H - CH=C)	58.5 $[M-H]^+$ (-Ve ion mode)
10.	2—Cl	$C_{23}H_{12}F_3Cl2\ N_3O_3$	Abve 250	19.76	8.53	8.30	9.58 (S, -CONH, D_2O exchageable), 7.90-7.80 (m, 5H, Ar-H) 7.40 - 7.52 (m, 5H, Ar-H) and 6.47 (S, 1H, - CH=C-)	504.8 $[M-H]^+$ (-Ve ion made)
11.	4—Cl	$C_{23}H_{12}F_3Cl_2\ N_3O_3$	Above 250	29.64	8.72	8.30	9.52 (S, 1H,-CONH,-CONH, D_2O exchangeable), 7.98-8.00 (d, J=8.0 Hz, 2H, Ar-H), 7.90 - 7.92 (d, J=8.0 Hz, 2H, Ar-H) 7.78 - 7.81 (m, 4H, Ar-H), 7.60 - 7.62 (m, 2H, Ar-H), and 6.52 (S, 1H, - CH=)	507 $[M+H]^+$ (+Ve ion made)
12.	4—Br	$C_{23}H_{12}F_3ClBr\ N_3O_3$	Above 250	49.00	8.91	7.62	9.50(S, 1H, - CONH, D_2O exchangeable), 7.98 - 7.98 (d, J=7.8 Hz, 2H, Ar-H), 7.93 - 7.95 (d, J= 8.0 Hz, 2H, Ar-H), 7.74-7.77 (m, 4H, Ar-H), 7.59 - 7.62 (m, 2H, Ar-H) and 6.50 (S, 1H, - CH=)	551.6 $[M+H]^+$ (+Ve ion made)

Table 2 – Schiff bases obtained by the condensation of N–(2–chloro–5–trifluoromethyl) phenyl malonamic acid with 2–hydroxy 5 (R)- phenyl azo benzaldehyde

S No	R	Mol. Formula of the Schiff base	M.P (^{0}C)	Yield (%)	Nitrogen (%) Found	Nitrogen (%) Calc.	^{1}H - MNR data (300 MHz, $CDCl_3$, δ ppm)	Mass (API-300 ion spray):m/z
1	H	$C_{20}H_{13}F_3Cl\ N_3O$	Above 250	27 22	10 64	10 39	7 70 - 7 76 (m, 6 H, Ar-H), 7 68 - 7 53 (m, 5H, Ar-H), 6.60 (S, 1H,-CH=N) and 5 30 (broad S, -OH, D_2O exchangeable)	404 5[M+H]$^+$ (+Ve ion mode)
2.	4—CH_3	$C_{21}H_{15}F_3Cl\ N_3O$	Above 250	50.23	10 46	10 04	7.80 - 7.82 (d, J=6.0 Hz, 2H, Ar-H), 7.86 - 7.88 (d, J=6.0 Hz, 2H, Ar-H), 7.60 - 7.66 (m, 6H, Ar-H), 6 62 (S, 1H, CH=N), 5.38 (broad S, 1H, -OH, D_2O exchangeable) and 1.20 (S, 3H, -CH_3)	418.6[M+H]$^+$ (+Ve ion mode)
3.	2, 3—$(CH_3)_2$	$C_{22}H_{17}F_3Cl\ N_3O$	105	32 40	9.87	9.72	7.81 - 7.78 (m, 5H, Ar-H), 7.41 - 7.99 (m, 4H, Ar-H) 6.61 (S, 1H, -CH=N), 5.28 (broad S, -OH, D_2O exchangeable) and 1.20 & 1.24 (Two S, 6H, 2X-CH_3)	432.7[M+H]$^+$ (+Ve ion mode)
4	3,4—$(CH_3)_2$	$C_{22}H_{17}F_3Cl\ N_3O$	Above 250	48.61	10.04	9.72	7.78 - 7.75 (m, 5H, Ar-H), 7.40-7.60 (m, 4H, Ar-H), 6.60 (S, 1H,-CH=N) 5.28 (broad S, 1H, -OH, D_2O, exchangeable) and 1.22 & 1.24 (Two S, 6H, 2X-CH_3)	432.5[M+H]$^+$ (+Ve ion mode)
5	2—OCH_3	$C_{21}H_{15}F_3Cl\ N_3O_2$	Above 250	27.64	9.92	9.67	7.79 - 772.(dd, J = 9.0 Hz, 4H, Ar-H), 7 40-7.48 (m, 6H, Ar-H), 6.44 (S, 1H, -CH=N), 5.48 (broad S, 1H, -OH, D_2O exchangeable) and 3.90 (S, 3H, -OCH_3)	434.7[M+H]$^+$ (+Ve ion mode)
6	3—NO_2	$C_{20}H_{12}F_3Cl\ N_4O_3$	Above 250	31 18	12.61	12.47	7.80 - 7.74(m, 5H, Ar-H), 7 48-7.40 (m, 5H, Ar-H), 6.40 (S, 1H, - CH=N) and 5.36 (broad S, 1H,-OH, D_2O exchangeable).	449.5[M+H]$^+$ (+Ve ion mode)
7	2—F	$C_{20}H_{12}F_4Cl\ N_3O$	Above 250	73.45	10 08	9.95	7.88 - 7.84 (m, 5H, Ar-H), 7 51-7.46 (m, 5H, Ar-H), 6.39 (S, 1H, -CH=N) and 5.44 (broad S, 1H,-OH, D_2O exchangeable)	422 6[M+H]$^+$ (+Ve ion mode)
8	2-Cl	$C_{20}H_{12}F_3Cl_2\ N_3O$	170	43 37	9 81	9.58	7.66-7 60 (m, 5H, Ar-H), 7.42-7.38 (m. 5H, Ar-H), 6.28 (S, 1H, -CH=N) and 5 20 (broad S, 1H, OH, D_2O, exchangeable)	437 (M-H)$^+$ (-Ve ion mode)
9	4—Cl	$C_{20}H_{12}F_3Cl_2\ N_3O$	Above 250	22 83	9 92	9 58	7.89-7.91 (d, J=8 0 Hz, 2H, Ar-H), 7.86-7.88 (d, J=8 0 Hz, 2H, Ar-H), 7 65-7 68 (m, 6H, Ar-H), 6.66 (S, 1H, CH=N) and 5 42 (broad 5, 1H,-OH, D_2O exchangeable)	436.9[M-H)$^+$ (- Ve ion mode)
10	4—Br	$C_{20}H_{12}F_3ClBrN_3O$	Above 250	31.05	8 82	8 69	7.86-7.88 (d, J=8 0 Hz, 2H, Ar-H), 7.82-7.80 (d, J=80 Hz, 2H, Ar-H), 7 60-7.63 (m, 6H, Ar-H), 6.63(S, 1H, CH=N) and 5.40 (broad S, 1H,-OH, D_2O exchangeable)	481.3[M-H]$^+$ (-Ve ion mode)

sterilised by dry heat at 140°C for 1 h and were saturated with the solution of compound. These were air dried at room temperature to remove any residual solvent, which interfere with the determination. The discs were then placed on the surface of the sterilised solidified culture medium that had been innoculated with the test organism (using a sterile cotton swab) and air dried to remove the surface moisture. The thickness of the culture medium was kept equal in all petridish (20 ml). For each of the experiment a petridish innoculated withthe organism but without disc containing the compound was taken and incubated as control. These were incubated at 28 ± 1°C after which the zone of inhibition or depressed growth were measured.

The data of antibacterial screening is reported in Table 3. The effectiveness of these compounds were tested against *S. aureus, E. coli, Pseudomonas and Klebsiella.*

Table 3 – Anti-bacterial activity screening of coumarin.

Name of the coumarin and dilution	Zone of Inhibition (mm)			
	S. aureus	*E. coli*	*Pseudomonas*	*Klbsiella*
6-(4-chloro)phenyl azo-coumarin-3-carboxy-(2-chloro-5-tri fluoromethyl) phenyl amide				
1 : 5	R	R	R	R
1 : 10	R	R	24	R
1 : 20	R	R	R	R
1 : 50	R	18	22	R
1 : 100	R	R	R	R

R = Resistant

None of the other coumarins showed antibacterial activity.
None of the schiff bases showed antibacterial activity.

The purity of the compounds were checked by T.L.C. 5% benzene/methanol for Schiff bases and 10% benzene/methanol for coumarins.

IR spectrum of 6-(2, 3-dimethyl) phenyl azo-coumarin-3-carboxy-(2- chloro-5-tri fluoromethyl) phenyl amide shows absorption at 3400 cm^{-1} (-NH stretching vibrations), 1720 cm^{-1} (C=O of secondary amide), 1660 cm^{-1} (C=C stretching), 1580 cm^{-1} (N=N stretching), 1320 cm^{-1} (-CH_3 bending), 1110 cm^{-1} (aromatic character), 1070 cm^{-1} (C-F linkage), 810 cm^{-1} (C-Cl linkage).

Materials and Method

SMZ (m.p. 169°C) used in the present study was procured from Matta Remedies, Ludhiana (India). All the metal salts i.e. $AgNO_3$, $CdCl_2$, $HgCl_2$, $CoCl_2.6H_2O$, $VOSO_4.H_2O$ and $UO_2(NO_3)_2.6H_2O$ employed were reagent grade chemicals. All the complexes were prepared as follows[5]. A solution containing 5 mmol of SMZ in aqueous sodium hydroxide (pH 8-10) was added to a solution of 2.5 mmol metal ion namely VO(II), UO_2(II), Co(II), Hg(II), Cd(II) and Ag(I). The precipitates that formed immediately or after a few minutes of stirring were filtered, washed with distilled water and dried in a vacuum desiccator.

Method of Analysis : Melting points were determined with a Thiele's apparatus using open capillary tube. Carbon, hydrogen and nitrogen were analysed with a Perkin Elmer 240C elemental analyser. Sulphur and metals were estimated by the standard methods reported in the literature[7,8]. Infrared spectra of the ligand and its metal complexes were recorded in nujol mull on a Perkin Elmer 1430 double-beam spectrophotometer.

The magnetic susceptibilities of the metal complexes prepared were measured with Gouy's method at room temperature using $Hg[Co(NCS)_4]$ as calibrant. Conductivity measurements were carried out on bridge type CM82T conductometer. Differential scanning calorimetric (DSC) studies were carried out on a Stanton Rederoft differential scanning calorimeter using Al_2O_3 as a standard and zinc as reference. The heat of fusion of the metal complexes was determined using well known standard formula[9].

$$\frac{H_f^{Zn}}{H_f^s} = \frac{(K\ \Delta A_{Zn}/m_{Zn})\ M_{Zn}}{K\ \Delta A_s/m_s)\ M_s}$$

where H_f^{Zn} = heat of fusion of Zn, 7.28 kJ mol^{-1}, [10], H_f^s = heat of fusion of sample, K = calorimeter constant, m_{Zn} = mass of zinc, m_s = mass of sample, ΔA_{zn} = area of the Zn peak, ΔA_s = area of the sample peak, M_{Zn} = atomic mass of Zn, M_s = molecular mass of sample. The area of each DSC peak was determined by paper weight method.

Results and Discussion

The analytical and nonspectral physical data of the ligand and metal complexes have been listed in Table 1. The stoichiometry (M : L) of the complexes as deduced from elemental analysis has been found to be 1:2 in case of Cd(II), Co(II), VO(II), UO_2(II) and Hg(II) complexes while 1:1 in Ag(I) complex. The stoichiometry of the complexes also conforms to the thermogravimetric and differential thermal analysis data[11]. These complexes

Table 1 – Analytical and physical data of sulphamethoxazole and its metal complexes.

Compound	Yield (%)	Formula weight	Stoich-iometry	Colour	M.P. (°C)	Elemental analysis (%)[a]					λ_M (ohm^{-1} cm^2 mol^{-1})
						M	C	H	N	S	
$C_{10}H_{11}N_3O_3S$		253.27		White	169	–	47.25 (47.42)	4.30 (4.38)	16.29 (16.59)	12.60 (12.65)	–
$[Ag(SMZ)H_2O]$ $AgC_{10}H_{12}N_3O_4S$	67	378.15	1:1	Brown	>245	28.31 (28.52)	31.93 (31.76)	2.91 (3.17)	11.22 (11.11)	8.35 (8.48)	19.3
$[Cd(SMZ)_2(H_2O)_2]$ $CdC_{20}H_{24}N_6O_9S_2$	75	652.98	1:2	White	203	17.68 (17.21)	36.45 (36.79)	3.98 (3.70)	12.57 (12.87)	9.38 (9.82)	32.0
$[VO(SMZ)_2(H_2O)_2]$ $VC_{20}H_{24}N_6O_9S_2$	70	607.51	1:2	Green	174	7.92 (8.38)	39.54 (39.54)	3.53 (3.98)	13.62 (13.83)	10.30 (10.55)	–
$[UO_2(SMZ)_2]H_2O$ $UC_{20}H_{22}N_6O_9S_2$	73	792.58	1:2	Light green	172	30.57 (30.03)	30.88 (30.30)	2.77 (2.80)	10.87 (10.60)	7.85 (8.09)	–
$[Co(SMZ)_2(H_2O)_2]H_2O$ $CoC_{20}H_{26}N_6O_9S_2$	65	617.51	1:2	Violet	155	9.40 (9.54)	38.98 (38.90)	3.90 (4.24)	13.37 (13.61)	10.88 (10.38)	45.5
$[Hg(SMZ)_2(H2O)_2]$ $HgC_{20}H_{24}N_6O_8S_2$	80	741.16	1:2	White	240	27.12 (27.06)	32.41 (32.41)	3.11 (3.26)	11.41 (11.34)	8.96 (8.65)	4.5

SMZ′ – deprotonated sulphamethoxazole; [a]The quantities within parentheses are the calculated values.

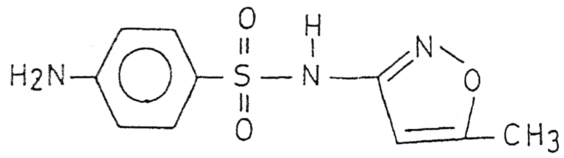

Fig. 1 – Structure of sulphamethoxazole.

have high melting point and are insoluble in water and common organic solvents namely chloroform, ether, benzene, carbon tetrachloride and ethanol. The molar conductivity value of complexes in DMF of Ag(I), 19.3; Cd(II), 32.0; Co(II), 45.5 and Hg(II), 4.5 ohm^{-1} cm^2 mol^{-1} show these compounds to be non-electrolytes.

IR spectra : The sulphamethoxazole moiety is expected to behave as chelating ligand with the metal ions. Just like its other analogues, the chelation[12,13] occur mainly through (i) nitrogen of NH_2 and sulphonyl oxygen of – SO_2NH groups, (ii) nitrogen of $-NH_2$ as well as $-SO_2NH$ groups, (iii) sulphonyl oxygen and nitrogen atom of $-SO_2NH$ group and (iv) sulphonamide nitrogen and ring nitrogen of isoxazole ring. The NH_2 stretching, NH_2 bending, NH and SO_2 stretching (– SO_2NH), C-N stretching (– SO_2NH and NH_2) and C=C stretching (phenyl ring), O-H stretching (water) vibrations of the ligand and its metal complexes has been assigned[5,14]. and recorded in Table 2. A perusal of IR data in Table 2 reveal that $-NH_2$ and – SO_2NH groups of SMZ are involved in coordination since the region corresponding to the vibrational bands of these groups are affected on complexation. The bands of medium intensity of SMZ at 3480 and 3387 cm^{-1} due to asymmetric and symmetric $-NH_2$ stretching vibrations of the amino group except Co(II) and Cd(II) are not influenced significantly on complexation. This suggests the participation of nitrogen atom of $-NH_2$ group in Co(II) and Cd(II) complexes. This is also in accordance with the observations of Narang and Gupta[12] on the metal complexes of the related sulpha drugs i.e. sulphanilamide, sulphaguanidine, sulphathiazole, sulphamerazine, sulphadiazine and sulphapyridine. The nitrogen of the isoxazole ring of SMZ is not involved in coordination in the present complexes since the C=N stretching frequency is not affected at all on complexation. Further in the Co(II) and Cd(II) complexes, the significant shift in the SO_2 symmetric stretching frequency and with change in intensity also infer the involvement of oxygen of sulphonamide group (Table 2). This conforms to the observations of Kanagaraj and Rao[5] on Cr(III), Mn(II), Ni(II) and Cu(II) complexes. In view of it, we would like to point out that the observations of Kanagaraj and Rao[5] on the basis of infrared and NMR spectral data that absence of (i) vibrational band at 3300 cm^{-1} (due to sulphonamide N-H

Table 2 – The characteristic IR (cm^{-1}) and electronic absorption (nm) bands of sulphamethoxazole and its metal complexes.

Compound	ν_{N-H} (Aniline-NH_2)	ν_{N-H} (Sulphonamide NH)	$\delta_{NH2} + \nu_{C=N}$ (Isoxazole ring)	Phenyl ring C=C stretching	ν_{SO2} (asym)	ν_{SO2} (sym)	ν_{C-N} (Sulphonamide & aniline)	ν_{O-H} (H_2O)
$C_{10}H_{11}N_3O_3S$	3480 m(asym) 3387 m(sym)	3307 s	1625 m	1605 m 1505 sh	1320 s 1310 s	1159 s 1147 m	1270 s	–
$[Ag(SMZ)H_2O]$	3495 m(asym) 3385 m(sym)	–	1625 m	1605 m 1505 sh	– 1290 s	– 1142	1275 w 1255 s	3250 w
$[Cd(SMZ)_2(H_2O)_2]$	3470 m(asym) 3370 m(sym)	–	1665 m	1635 w 1505 sh	1320 s 1310 s	1235 s 1225 s 1185 s 1123 s	1270 s	3160 w
$[VO(SMZ)_2(H_2O)_2]$	3475 s(asym) 3390 m(sym)	–	1625 m	1600 s 1519 m 1503 sh	1310 s 1305 s	1155 s 1135 g	1260 m	3200 m
$[UO_2(SMZ)_2].H_2O$	3480 m(asym) 3390 m(sym)	–	1625 m	1595 m 1500 sh	1308 s 1295 sh	1155 s 1135 s	1257 m	3210 m
$[Co(SMZ)_2(H_2O)_2].H_2O$	3460 m(asym) 3365 m(sym)	–	1620 m	1600 sh 1500 sh	1315 s 1295 s	1205 m 1165 s	1260 m	3165 vw
$[Hg(SMZ)_2(H_2O)_2]$	3480 m(asym) 3385 m(sym)	–	1630 m	1610 m 1600 m 1505 m	1305 sh 1292 s	1142 s 1132 s	1263 m	3150 m

s – strong; m – medium; w – weak; vw – very weak; sh – shoulder.

stretching of the free ligand) in the metal complexes and (ii) N-H proton signal at 11.19δ, ppm (which disappears on deuterium exchange) in the zinc complex due to deprotonation seem to be erroneous because the complexes were prepared in the alkaline medium (pH 8-10) and the pKa of the ligand is 6[15]. In this pH range, the ligand itself undergoes deprotonation. Hence the absence of N-H band at 3300 cm^{-1} in the infrared and proton signal at 11.19δ, ppm in the NMR spectra cannot be fixed as criterion for the deprotonation of sulphonamide proton of SMZ on complexation and hence the binding of metal ion to nitrogen of the SO_2NH group as proposed by the authors. Most probably inadvertently Kanagaraj and Rao[5] has misquoted Gogorishvili *et al.*[13] In sulphonamide ligand, the latter have suggested the binding of metal ions to the ligand through the nitrogen of the isoxazole ring since the C=N band of the ligand at 1600 cm^{-1} appears as doublet (1598-1605 and 1587-1595 cm^{-1}) in the metal ion complexes. At no stage, they have mentioned that the missing of the band at 1380 cm^{-1} and a positive shift of the band at 1460 to 1480 cm^{-1}, indicate that the involvement of isoxazole ring in the coordination of the ligand (possibly through nitrogen) to metal ion. In fact, they have assigned a band at 1380 cm^{-1} to S=O asymmetric stretch in the IR spectra of sulphanilamide. This band appears in the range 1378-1385 cm^{-1} in complexes. Thus, the isoxazole ring vibrations of SMZ at 1460 and 1380 cm^{-1} appearing at 1490 and 1480 cm^{-1} in its copper complex may not be fixed as criterion as suggested by Kanagaraj and Rao[5] for the coordination of the metal ion to the ring nitrogen since the C=N stretching vibration of the same very ring remains unaltered in the complexes.

Just like Co(II) and Cd(II) complexes of SMZ, Ag(I), VO(II), UO_2(II) and Hg(II) also bind to SMZ through oxygen of the SO_2NH group since S=O (symmetric/asymmetric or both) are influenced on going from ligand to the respective complexes (Table 2). However, in the case of UO_2(II) and Hg(II) complexes, nitrogen of SO_2NH is also involved in coordination as is evident from the C-N stretching frequency shift and intensity changes in passing from the ligand to the complexes (Table 2). The shift is found to be of the order of 4-12 and 17-19 cm^{-1} in the Hg(II) and UO_2(II) complexes respectively. All the metal complexes except that of Co(II) were found to be diamagnetic. Though there are various factors i.e., steric, pH, electronic state of the metal, which govern the extent of co-ordination of a multidentate ligand with various metal ions, no single factor in this case can explain the extent of co-ordination of SMZ with different metal ions because of their diverse nature.

Thermal behaviour of complexes : The characteristic parameters of the DSC curves of SMZ and its metal complexes are recorded in Table 3. Heat changes associated with various steps of dissociation of the metal complexes as deduced from characteristic parameters of DSC curves are also recorded in Table 3. The broad character of some of the DSC peaks as observed in various complexes suggests that a number of reactions are occurring

Table 3 – Characteristic parameters of DSC curves and heat of fusion of SMZ and its metal complexes.

Compound	Temperature (°C) range	Peak temp. (°C)	ΔA^b (mg)	H_f (kJ mol^{-1})	ΔS (Jmol^{-1}K^{-1})
$C_{10}H_{11}N_3O_3S$	170^a – 198 (s, endo)	180	2.20	38.18^c	68.18
	230–290 (s, exo)	265	8.80	152.73	
	325–610 (b, exo)				
$[Ag(SMZ)H_2O]$	249^a-310 (s, exo)	280	9.00	233.22	446.78
	500-570 (b, exo)				
	570-620 (b, exo)				
	650-720 (b, exo)				
$[Cd(SMZ)_2(H_2O)_2]$	160-200^a (s, endo)	189	3.00	134.23^c	280.20
	280-309 (s, exo)	295	0.35	15.66	
	310-360 (s, exo)	330	2.70	120.80	
	500-670 (b, exo)				
$[VO(SMZ)_2(H_2O)_2]$	100-130 (s, endo)	110	1.82	34.13	133.79
	175^a-205 (s, endo)	190	1.44	59.94^c	
	240-285 (s, exo)	265	7.68	319.68	
	360-525 (b, exo)				
	605-700 (b, exo)				
$[UO_2(SMZ)_2].H_2O$	100-135 (s, endo)	120	0.70	38.11	157.28
	177^a-210 (s, endo)	190	1.30	70.78^c	
	235-350 (s, exo)	290	6.00	326.68	
	440-700 (b, exo)				
$[Co(SMZ)_2(H_2O)_2].H_2O$	152^a-215 (s, endo)	185	3.95	167.13^c	393.24
	245-305 (s, exo)	279	5.00	211.56	
	500-570 (b, exo)				
	660-700 (b, exo)				
$[Hg(SMZ)_2(H_2O)_2]$	198-230^a (s, endo)	210	0.40	20.31^c	40.37
	250-315 (s, exo)	280	4.30	218.38	
	600-700 (b, exo)				

s-symmetrical: b-broad; exo-exothermic, endo-endothermic, H_f-heat of fusion; ΔG=0; ΔA^b-area under the DSC curve; ΔA_m - 1.3 mg; ^{a}melting temperature.

simultaneously with the formation of unstable intermediate species in the decomposition process, as expected. The value of H_f (with superscript c) in column five (Table 3) corresponds to the heat of fusion of the respective systems while the second value corresponds to some sort of decomposition of the respective systems. The heat of fusion (H_f) reflects on the thermal stability of a metal complex in a particular state[16]. Thus the

trend of the thermal stability of the metal complex on the basis of H_f (Table 3) is : Co(II) > Cd(II) > UO_2(II) > VO(II) > Hg(II).

Conclusions

On the basis of spectroscopic and differential scanning calorimetric studies on the prepared metal complexes of SMZ, the following aspects of the behaviour of SMZ are demonstrated. SMZ acts as (a) monodentate ligand binding the Ag(I) and VO(II) through the oxygen of the SO_2NH group, (b) bidentate ligand binding the metal through nitrogen of NH_2 and oxygen of SO_2NH group in case of Co(II) and Cd(II) complexes while *via* both oxygen and nitrogen of SO_2NH group in UO_2(II) and Hg(II) complexes, (c) the absence of N-H band at 3300 cm^{-1} in the infrared and proton signal at 11.19δ, ppm in the NMR spectra cannot be fixed as criterion for the deprotonation of sulphonamide proton of SMZ on complexation and hence the binding of metal ion to nitrogen of SO_2NH group as proposed by Kanagaraj and Rao[5], (d) the thermal stability of the metal complexes follows the order : Co(II) > Cd(II) > UO_2(II) > VO(II) > Hg(II).

Acknowledgements

The authors are indebted to Dr. Rajini Lakhani, Scientist, C.B.R.I., Roorkee, for her generous help in DSC and magnetic susceptibility measurements. Thanks are also due to RSIC, Chandigarh for elemental analysis and infrared spectral studies.

References

1. Stecher, P.G. (1960) *The Merck Index of Chemicals and Drugs,* Merck & Co. Inc., Rahway, New Jersey, USA, p. 992.
2. Burger, A. (1960) *Medicinal Chemistry,* Interscience, New York, p. 801.
3. Deorge, R.F. (1982) *Wilson and Gisvold's Textbook of Organic Medicinal and Pharmaceutical Chemistry,* 8th Edn., J.B. Lippincott, Philadelphia, p. 162.
4. Florey, K. (1973) *Analytical Profiles of Drug Substances,* Vol. 2, Academic Press, New York, p. 469.
5. Kanagaraj, G. & Rao, G.N. (1992) *Synth. React. Inorg. Met.-Org. Chem.* **22** : 559.
6. Sekhon, B.S., Sahai, H.K. & Randhawa, H.S. (1998) *Nat. Acad. Sci. Letters* **21** : 282.
7. Vogel, A.I. (1975) *Elementary Practical Organic Chemistry,* Part 3, *Quantitative Organic Analysis,* Longman, London.
8. Vogel, A.I. (1978) *Text Book of Quantitative Inorganic Analysis,* ELBS, London.
9. Murphy, C.B. (1968) *Treatise on Analytical Chemistry,* Part I, Vol. 13, Interscience, New York, p. 5949.
10. Weast, R.C. (1974-75) *Handbook of Chemistry and Physics,* 55th Edn., CRC Press.

11. Randhawa, H.S., Sekhon, B.S., Sahai, H. & Lakhani, R. (1999) *J. Therm. Anal. Cal.* **57** : 551.

12. Narang, K.K. & Gupta, J.K. (1975) *Indian J. Chem.* **13** : 705.

13. Gogorishvili, P.V., Tskitishvili, M.G., Machkhoshvili, R.I. & Kharitonov, Y.Y. (1975) *Russian J. Inorg. Chem.* **20** : 798.

14. Nakamoto, K. (1978) *Infrared and Raman Spectra of Inorganic and Coordination Compounds*, 3rd, Edn., John Wiley & Sons, New York, p. 244.

15. Wolff, M.E. (Ed.) (1979) *Burger's Medicinal Chemistry*, Part II, 4th Edn., John Wiley & Sons, New York, p. 30.

16. Randhawa, H.S. & Lakhani, R. (1993) *J. Therm. Anal.* **39** : 457.

PROC. NAT. ACAD. SCI. INDIA, 71 (A), III, 2001

Synthesis and characterization of 8-hydroxy-quinoline-oxamide-formaldehyde tercopolymers*

PETER S. LINGALA, L.J. PALIWAL and H.D. JUNEJA**

Department of Chemistry, Hislop College, Nagpur-440 001, India.

***Department of Chemistry, Nagpur University Campus, Nagpur-440 010, India.*

***Author for correspondence.*

Received October 25, 1999; Revised September 19, 2000; Accepted May 14, 2001

Abstract

The title tercopolymer (8-HQOF) have been prepared by refluxing a mixture of 8-hydroxy quinoline (8-HQ), oxamide (O) and formaldehyde (F) in presence of 2M HCl as a catalyst for 4-5h at 127 (± 1°C) with varying molar ratio of reactants. The four differnt tercopolymer thus obtained using different molar ratios are all amorphous in nature with four different-shades of light brown colour. They have high melting points and exhibit high thermal stability. The tercopolymers were analysed for C, H and N. Their purity was established by thin layer chromatography (TLC). The viscosity measurements, in dimethylformamide (D.M.F.) have been carried out with a view to ascertain characteristic function and constants. The molecular weight of tercopolymers were determined by non-aqueous conductometric titrations against alcoholic KOH in DMF and also ultra-violet, infra-red and nuclear magnetic resonance spectral studies have been undertaken for synthesized resins to elucidate their structure.

(**Keywords :** 8 HQOF/tercopolymer)

Introduction

A large number of synthetic resins derived from hydroxy and amino compounds have attracted the attention of many research workers due to their versatile use as ion exchangers,[1,2] photographic binders[3] and thermal stabilizers[4-6] etc.

Chelating resins containing oxine group have been synthesized either from oxine, formaldehyde and resorcinol by condensation[7,8] or by diazotization of poly (amino styrene) resins followed by coupling with oxine[9]. Their properties were later improved by Pennington and Williams, and also by Parrish and Stevenson[10]. Aristov and Kostaintinov reported preparation of chelating ion-exchanger by copolycondensation of 8-hydro xyquinoline or

*Paper presented at "The National Academy of Sciences, India, 68th Annual Session, CDRI, Lucknow. (Oct. 23-25, 1998)

phenol derivatives like amino phenol, β-resorcyclic acid or resorcinol with formaldehyde[11]. Purohit, *et al.* prepared a resin from 8-hydroxyquinoline, hydroquinone and formaldehyde[12]. 8-Hydroxy quinoline, resorcinol, formaldehyde and 8-hydroxyquinoline, resorcinol, salicyclic acid, formaldehyde, chelating resins were prepared and studied for its ion-exchange properties by Kim Don *et al.*[13] Kapadia and co-workers have prepared many resins containing 8-hydroxyquinoline by using 8-hydroxyquinoline and poly (vinyl acetate) in glacial acetic acid[14], 8-hydroxyquinoline and poly (vinyl alcohol) in DMF[15], 8-hydroxyquinoline and epichlorohydrine with dimethyltetramine[16], and 8-hydroxyquinoline and acetaldehyde with thiourea[17].

However, literature survey revealed that no tercopolymers have been synthesized from 8-hydroxyquinoline, oxamide and formaldehyde. Therefore, we have undertaken the synthesis and characterization of these tercopolymers and the results of our studies are reported in this paper.

Materials and Method

All chemicals used were of AR Grade. The solvents like dimethyl formamide and dimethylsulphoxide were double distilled under reduced pressure.

Synthesis of 8-hydroxyquinoline-oxamide-formaldehyde (I) tercopolymer : A mixture of 0.1 mole 8-hydroxyquinoline, 0.1 mole oxamide, and 0.2 mole formaldehyde in 100 ml of 2M HCl was refluxed on oil bath, at 127 (± 1°C) for 4-5 h with occasional shaking. The contents were then cooled to room temperature and neutralized with dil. NaOH. The greenish yellow resinous product so obtained was filtered and repeatedly washed with cold water, hot water and alcohol and dried in air. The powder was then purified by dissolving it in 8% NaOH solution, filtered and reprecipitated by gradual dropwise addition of ice cold 1:1 (v/v) concentrated HCl and distilled water with constant and rapid stirring to avoid lump formation. The tercopolymer resin so obtained finally was filtered, washed several times with hot water, dried in air, powdered and kept in vacuum desiccator over silica.

Similarly, other tercopolymer resins *viz.* 8-HQOF (II), 8-HQOF (III) and 8-HQOF (IV) were synthesized by varying the molar proportion of the starting materials i.e. 8-hydroxyquinoline, oxamide and formaldehyde in the ratios 2:1:3, 3:1:4 and 4:1:5 respectively.

Characterization :

Methods : The purity of each tercopolymer sample was checked and confirmed with thin layer chromatography. Elemental analysis of all the tercopolymers for carbon, hydrogen

and nitrogen were carried out in CARLO ERBA STUM, DP 200 at CDRI Lucknow. Molecular weights of the resins were determined by non-aqueous conductometric titration in DMF. The viscosity measurements were carried out in DMF at 35°C using Tuan-Fuoss viscometer. Electonic absorption spectra of all the newly synthesized tercopolymer resins were recorded in DMSO on Shimadzu double beam spectophotometer. The Infrared spectra of all the newly synthesized tercopolymer resins have been scanned on Perkin-Elmer 983 spectrophotometer in KBr pellets in the wave number region of 4000-400 cm^{-1}. Proton NMR spectra of all the newly synthesized tercopolymer resins have been scanned on Varian-EM 360 A 60 MHz proton, NMR spectrophotometer using deuterated dimethylsulphoxide (DMSO-D_6) as a sovent.

Results and Discussion

All the tercopolymers were light brown in colour and were completely soluble in DMF, DMSO, HCl and aq. NaOH. The details of synthesis and analytical data of all the tercopolymers are presented in Table 1.

Molecular weight determination ($\overline{Mn}$) : The results of conductometric titrations were used to determine number average molecular weight ($\overline{Mn}$) of the tercopolymer samples using alcoholic KOH as titrant[18,19]. From the plots of specific conductance against milliequivalents of titrant (alc. KOH) added, the first breaks and the last breaks were noted. The degree of polymerization ($\overline{DP}$) of the tercopolymer samples was obtained from the values of the breaks. Table 2 shows that the molecular weights increase as proportion of 8-hydroxyquinoline increases in the tecopolymer resins[20].

Viscosity measurements : The measurements of viscosity have been carried out in DMF at 35°C using Tuan-Fuoss viscometer. The reduced viscosity versus various concentrations is plotted for each set of data. The intrinsic viscosity [η] has been determined from the following equations.

Huggin's equation

$$\eta_{sp/c} = [\eta] + k_1 [\eta]^2 C \tag{1}$$

Kraemer equation

$$\ln (\eta_r/C) = [\eta] - k_2 [\eta]^2 C \tag{2}$$

The intrinsic viscosity of 8-hydroxyquinoline–oxamide–formaldehyde tercopolymer determined from both the plots using eqn. (1) and (2) is identical and it increases with the

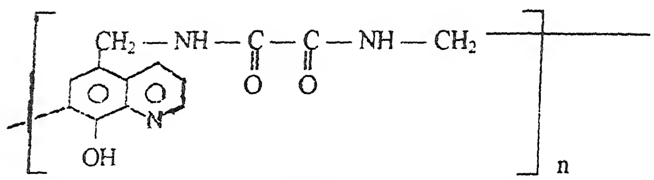

Fig. 1 – Structure of 8–HQOF – I tercopolymer

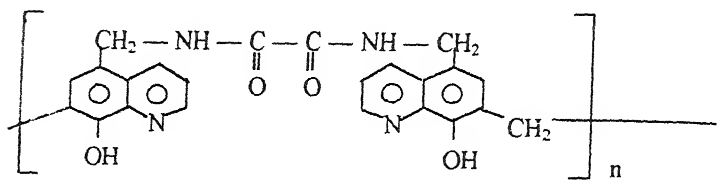

Fig. 2 – Structure of 8–HQOF – II tercopolymer

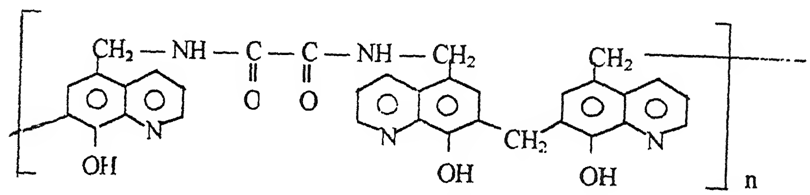

Fig. 3 – Structure of 8–HQOF – III tercopolymer

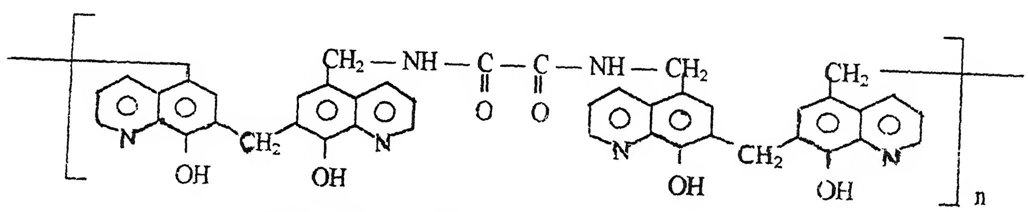

Fig. 4 – Structure of 8–HQOF – IV tercopolymer

Table 1 – Synthesis and analytical data of 8-hydroxyquinoline – oxamide – formaldehyde (8–HQOF) tercopolymers.

Tercopolymer	Reactants			Colour	Yield %	C % Obs (Cal)	H % Obs (Cal)	N % Obs (Cal)
	8-HQ mol	Oxamide mol	HCHO mol					
8–HQOF – I	1	1	2	Light brown	65	61.10 (61.88)	4.30 (4.34)	16.34 (16.42)
8 – HQOF – II	2	1	3	Light brown	67	67.20 (67.78)	4.34 (4.81)	13.32 (13.62)
8 – HQOF – III	3	1	4	Light brown	72	69.30 (69.66)	4.38 (4.71)	12.30 (12.64)
8 – HQOF – IV	4	1	5	Light brown	80	70.88 (70.52)	4.40 (4.52)	11.54 (11.86)

increase in molecular weights of tercopolymer samples under investigation (Table 2). Similar trends have been reported by earlier workers[20,21].

UV-visible spectra : UV-visible spectra of all the four 8-hydroxyquinoline-oxamide-formaldehyde tercopolymers show two characteristic bands at 330 nm and 270 nm. The intense band with some dimnished fine structues at 330 nm is due to ($\pi \rightarrow \pi^*$) allowed transition of the benzenoid system of heteroaromatic compounds (quinoline). The bathochromic shift from the basic value of 308 nm may be due to presence of phenolic hydroxy group (auxochrome). The second less intense band at 270 nm is due to ($n \rightarrow \pi^*$) forbidden transition in saturated aliphatic carbonyl compounds[26]. The appearance of phenolic hydroxyl group as well affects the rise of $\in_{max}$ value, i.e. hyperchromic effect. The log $\in_{max}$ value gradually increases in the order : 8-HQOF (I) (log $\in_{max}$, 0.41) < 8–HQOF (II) (log $\in_{max}$, 0.45) < 8–HQOF (III) (log $\in_{max}$, 0.46) < 8–HQOF (IV) (log $\in_{max}$, 0.55) which is due to introduction of more and more chromophores (hetero aromatic system) and auxochromes (phenolic OH group) in the repeat unit of the tercopolymer resins[20].

IR-Spectra : IR-Spectra of all the tercopolymer resins recorded in KBr matrix resembled each other and assigned to the tercopolymer on the basis of nature and reactive positions

Table 2 – Molecular weight determination, viscometric data and IR frequencies of 8-hydroxyquinoline-oxamide-formaldehyde (8-HQOF) tercopolymers.

Tercopolymers 8-HQOF	Number average mol. weight ($\overline{Mn}$)	Intrinsic viscosity [η] (dl/g)	Important	IR frequencies
			Wave number	Assignment's
8–HQOF–I	5140	8.50	3371 (mbr) 2930 (m) 3050 (mbr) 1621 (s)	– OH Stretching – CH_2 Stretching > NH. Stretching >C=O Stretching
8–HQOF–II	5970	10.00	1418 (m) 1230 (m) 1579 (m)	–C=N– Stretching –OH in plane bending Aromatic ring
8–HQOF–III	10,849	11.50	2850 (w) 1466 (m) 1267 (m)	–CH_2 Stretching –CH_2 Scissoring 5,7,8 - trisubstituted aromatic ring coxinet
8–HQOF–IV	11,070	13.00	70 (m)	–CH_2 rocking

m – medium; s – strong; w – weak; br – broad.

Table 3 – ^{1}H NMR spectral data of 8-hydroxyquinoline–oxamide–formaldehyde (8–HQOF) tercopolymers (in DMSO – D_6)

Nature of proton assigned	Observed chemical shifts. (δ) ppm				Expected (δ) ppm
	8-HQOF-I	8-HQOF-II	8-HQOF-III	8-HQOF-IV	
Proton of phenolic – OH involved in hydrogen bonding	8.75 – 8.65	8.4 – 8.65	8.85 – 8.65	8.85 – 8.65	8.0 – 12.0
Aromatic proton (Ar – H)	8.33 – 8.14	8.49 – 8.23	8.36 – 8.24	8.44 – 8.24	7.3 – 8.8
Proton of – NH – bridges	7.34 – 6.65	7.49 – 7.08	7.51 – 6.14	7.53 – 6.11	5.0 – 8.5
Amido proton Ar–CH_2NH – CO – linkage	4.10 – 3.39	4.64 – 3.88	4.53 – 3.36	4.67 – 3.63	3.5 – 6.00
Methylene proton of Ar – CH_2 – Ar – linkage	–	3.48 – 2.49	2.81 – 2.48	2.50 – 2.48	2.0 – 3.0

of the monomers. A broad peak in the range 3360-3377 cm^{-1} was assigned to hydrogen bonded ν OH[24]. A broad band observed around 3000 cm^{-1} may be assigned to ν NH of the oxamide monomer[24,25]. A sharp and strong band observed at around 1621 cm^{-1} may be assigned to ν C=O of the tercopolymer[25,26]. A sharp peak around 1500-1580 cm^{-1} may be assigned to aromatic skeletal ring breathing modes[26]. The inflections at around 2800, 1460, 1260 and 700 cm^{-1} due to stretching, scissoring, wagging and rocking modes of $-CH_2-$ suggested the presence of methylene bridges in tercopolymer[26,27].

NMR Spectra : The three 8-hydroxyquinoline – oxamide – formaldehyde tercopolymers–II, III and IV exhibit signals in the region 2.5 to 2.8 δ (ppm) which are attributed to methylene proton of $Ar-CH_2-Ar$ linkage[26]. A broad signal at 3 to 4δ (ppm) may be assigned to methylenic proton of $Ar-CH_2-NH-CO$ linkage[26]. The presence of broad signal may be attributed to the presence of –NH–bridges[23]. The signal around 8.1 to 8.3 and 8.6 to 8.9δ (ppm) are attributed to proton of aromatic ring (Ar–H) and phenolic–OH involved in hydrogen bonding respectively[22,26].

On the basis of the nature and reactive positions of the monomers, elemental analysis, IR and NMR spectra and molecular weight, the following structures (Fig. 1–4) have been suggested for the tercopolymers.

References

1. Pennington, L.D. & Williams, M.B. (1959) *Ind. Eng. Chem.* **51** : 759.
2. Parmer, J.S., Patel, M.R. & Patel, M.M. (1981) *Angew. Makromol. Chem.* **93** : 11.
3. Guivetchi, N. (1963) *J. Rech. Sci., Lab Belle. Vul.* (Paris) **14(62)** : 73.
4. Fogg, A.N. & Lodge, R.M. (1940) *Trans. Faraday Soc.* **62** : 413.
5. Wallenberger, P.T. (1964) *Angew. Makromol. Chem.* **3** : 453.
6. Koton, M.M. (1961) *J. Polym. Sci.* **52** : 97.
7. Lillin, N. (1954) *Angew. Chem.* **66** : 649.
8. Parrish, J.R. (1955) *Chem. Ind. (Lond.)* : 386.
9. Idem, (1956) *ibid.* : 137.
10. Parrish, J.R. & Stevenson, R. (1974) *Anal. Chim. Acta.* **70** : 189.
11. Aristov, L.J., Kostantinov, V.V. (1961) *Inz. Tomsk. Plitekh,* **11** : 104.
12. Purohit, Rajesh & Devi, Surekha (1991) *Talanta* **38(7)** : 753.
13. Kim, Dongwon, Kim, Kong Soo, Kim, Hong Soo (1986) *Taehans Hwana Khoe Chi.* **30(1)** : 69.
14. Amin, Sushila & Kapadia, R.N. (1995) *Ind. J. Chem. Technol.* **2(1)** : 37.
15. Amin, Sushila & Kapadia, R.N. (1993) *J. Polym. Mater.* **10(3)** : 175.

16. Kapadia, R.N. & Vyas, M.V. (1983) *J. Appl. Polym. Sci.* **28(3)** : 983.
17. Vyas, M.V. & Kapadia, R.N. (1980) *Indian J. Technol.* **18(10)** : 411.
18. Chatterjee, S.K. & Mitra, R.P. (1970) *J. Poly Sc. (A)* **1(8)** : 1299.
19. Chatterjee, S.K. & Gupta, N.D. (1973) *J. Polym. Sci. (A)* **I(11)** : 1261.
20. Pal, T.K. & Kharat, R.B. (1989) *Die. Angewandte Makromolekulare Chemie.* **173** : 55.
21. Mitra, R.P. & Chatterjee, S.K. (1961) *J. Sc. Ind. Res.* **20(B)** : 310.
22. Kalsi, P.S. (1995) *Spectroscopy of Organic Compounds,* Second Edition, New age International Ltd., New Delhi.
23. Dyer, J.R. (1971) *Application of Absorption Spectroscopy of Organic Compounds,* Prentice Hall of India, 2nd Indian reprint, New Delhi, p. 33.
24. Kemp, William (1975) *Organic Spectroscopy,* The Macmillan Press Ltd., Hongkong.
25. Bellamy, J.J. (1956 & 1958) *The J.R. Spectr of Complex Molecules,* Methuen & Catt. Ltd. & John Willey & Sons Inc.
26. Silverstein, R.M. & Basler, G.C. (1969) *Spectroscopic Identification of Organic Compounds,* 2nd Edition, John Willey & Sons Inc., New York.
27. Nakanishi, K. (1967) *IR Absorption Spectroscopy–Practical,* Nolden Day Inc. & Nakodo Co. Ltd., Tokyo.

PROC. NAT. ACAD. SCI. INDIA, 71 (A), III, 2001

A uniform model for the storage utilization of *B*-tree-like structure

P.K. MISHRA and C.K. SHARMA

Department of Mathematics and Statistics, A.P.S. University, Rewa, India.

Received March 21, 1998; Revised November 4, 1999; Accepted February 15, 2000

Abstract

The approximate model introduced by Leung in 1984 was rediscussed by Gupta and Srinivasan, who point out that the model refers to a uniform distribution of B-trees, i.e., a distribution in which all possible configuration of B-trees with the same number of keys are equally likely. To be more precise, if f is the minimum storage utilization of each node, then each node can contain at least $2df$ keys and, obviously, at most $2d$ keys; Gupta and Srinivasan observe that the problem of finding the number of different B-tree configurations having an order d, n nodes and r keys is equivalent to the restricted occupancy problem when n different cells can contain more than v of P like objects, where $P = r - 2dnf$ and $v = (1\text{-}f)\, 2d$.

Unfortunately, this statement is not precise and Gupta and Srinivasan's model can not be considered to be a true model for B-trees. It makes sense to reconsider Gupta and Srinivasan's model from this point of view and in fact we obtain more precise results on storage utilization. By the way, from a mathematical point of view, these results conclusively show that the model cannot be considered a realistic B-tree model.

In the present paper, we want to show that it is possible to find the generating function for the sums $\sum_n Np\,(n, v)$ and $\sum_n nNp\,(n, v)$.

This allows us to give either approximate or asymptotic estimates for the expected value $E(u)$ and thus solve the storage utilization problem for this model. To this purpose we use the method of Riordan arrays. Riordan arrays constitute a flexible algebraic approach to the solution of combinatorial sums, to find either their closed form or their asymptotic estimate, and seem to have many applications to combinatorial analysis and to analysis of algorithms.

(**Keywords :** B-trees/Riordan array)

Introduction

B-trees are one of the most frequently used structures for storing information in a two level storage. Since there introduction in the early 1970's, they have been widely studied together with their main memory companion, the 2-3 trees, and therefore a vast literature exists, in which their performance is analyzed. Just to give some examples, we quote here the papers by Beaza-Yates[1], Chu and Knott[2], Mishra[3-4], Quitzow and Klopproge[5] and

Wright[6], which all refer to a distribution in which key permutations are all equally likely. This problem is quite hard, and therefore several approximate models have been proposed, in order to simplify the analysis, especially concerning their "occupancy problem", i.e. how much space is necessary to store a given number of keys. If we have r-keys, stored in a n nodes, each containing a maximum of $2d$ keys (d is the order of the tree), then the ratio $r/(2dn)$ is called the load factor for the B-tree and is the quantity of main interest.

Preliminaries

Gupta and Srinivasan's[7] paper shows that, if $Np\ (n, v)$ represents the number of B-trees with p keys distributed over n nodes such that each node can have a maximum of v vacancies, then

$$N_p\,(n, v) = \sum_{k=0}^{n} (-1)^k \binom{n}{k} \binom{P-kv-k+n-1}{P-kv-k} \tag{1}$$

In this model, the number n of nodes varies between $n_{\min} = r/(2d)$ and $n_{\max} = r/(2df)$ and the expected storage utilization is :

$$E\,(u) = \frac{r \sum\limits_{n=n_{\min}}^{n_{\max}} N_p\ (n, v)}{2d \sum\limits_{n=n_{\min}}^{n_{\max}} n\, N_p\,(n, v)} = r/2d\ E\,(1/n).$$

This definition of $E(1/n)$ is slightly different from Gupta and Srinivasan's[7] but it is more appropriate from a probabilistic point of view. The sums can be extended from 0 to ∞ because by (1) the value of $N_p\ (n, v)$ is zero when n is outside the range $n_{\min} \ldots. n_{\max}$.

Riordan Arrays

The technique we use to solve the occupancy problem relies on the concept of Riordan array[8]. A Riordan array[8] $\{a_{pk} \mid p, k \varepsilon N, k \leq p\}$ is an infinite, low triangular array defined by

Table 1 – $E(u)$ = approximate storage utilization.

D	$f = 1/2$		$f = 2/3$		$f = 3/4$	
	s	$E(u)$	s	$E(u)$	s	$E(u)$
6	90.796544	67.72%	0.849077	80.64%	0.865395	86.12%
12	0.859757	66.71%	0.894105	80.28%	0.910745	85.95%
24	0.908698	65.50%	0.930175	79.80%	0.940164	85.72%
48	0.943159	64.21%	0.956165	79.25%	0.961960	85.43%
96	0.965760	62.92%	0.973493	78.64%	0.976783	85.10%
192	0.979948	61.70%	0.984418	78.01%	0.986260	84.76%

means of two analytic functions ($b(t)$; $h(t)$), in the sense that the generic element $a_{p,k}$ is given by

$$ca_{p,k} = [t^p]\ b(t)\ (t\,(h\,(t))^k)$$

$[t_p]$ being the "coefficient of" operator.

In other words, $b(t)\ (t(h)(t))k$, $k = 0.1.....$, is the generating function of the kth column of the Riordan array. Riordan arrays allow us to solve combinatorial sums like $\sum_k a_{p,k}\, g_k$ in terms of generating functions according to the following rule :

$$G\left\{\sum_{k=o}^{\infty} a_{p,k}\, g_k\right\} = b(t)\,(t\,(h\,(t)) \tag{2}$$

where the symbol G denotes the generating function operator i.e.

$$g(t) = G\,\{g_k\}_{k\in \mathrm{N}}$$

$$= G\,\{g_k\}$$

$$= \sum_{k=0}^{\infty} g_{kt}^{k}$$

is the generating function of the sequence $\{g_k\}_{k \in N}$.

In particular, the arrays row sums and weighted row sums in which $g^k = 1$ and $g^k = k$, have the following generating functions :

$$G\left\{\sum_k a_{p,k}\right\} = \frac{b(t)}{1 - th(t)}$$

$$G\left\{\sum_k k\, ap, k\right\} = \frac{t\, b(t)\, h(t)}{(1 - th\,(t))^2}$$

we wish to point out that in formula (1),

$$a_{p,k} = \binom{(p+n-1-k(v+1)}{p-k\,(v+1)}$$

is the Riordan array $D = (1/(1\text{-}t)^n, t^v)$ and by a simple application of rule (2), with $g(t) = (1\text{-}t)n$. The generating function of binomial coefficients with alternating signs, we obtain:

$$N_{p(n,v)} = \sum \binom{(p+n-1-k(v+1)}{p-k\,(v+1)} \binom{n}{k} (-1)^k.$$

$$= [t^{p+n-1}]\, \frac{t^{n-1}}{(1-t)^n}\, (1 - t^{v+1})^n.$$

$$= [t^p] \left(\frac{1 - t^{v+1}}{(1-t)}\right)^n.$$

$$= [t^{r-2dnf}]\, (1 + t + \ldots + t^{2(1-f)d})^n.$$

$$= [t^r]\, (t^{2fd}\,(1 + \ldots + t^{2(1-f)d})^n.$$

This proves that, when $2df$ and $2(1\text{-}f)d$ are integer numbers, then $N_p\,(n, v)$ is the genetic element of the Riordan array[8] defined by $b(t) = 1$ and $h(t) = t^{2df-1}\,(1+t+\ldots+t^{2(1-f)d})$.

This immediately gives

$$S = \sum_n N_p\,(n, v)$$

$$= [t^r]\ \frac{1}{(1-t^{2df}\,(1+t+\ldots.+t^{2(1-f)d})},$$

$$W = \sum_n n\ N_p\ (n, v)$$

$$= [t^r]\ \frac{t^{2df}\,(1+t+\ldots+t^{2(1-f)d})}{(1-t^{2df}\,(1+t+\ldots.+t^{2(1-f)d})^2}$$

The most important cases are

(i) $f = 1/2$

This corresponds to (B)-trees whose analogue is the standard definition of B-trees.

(ii) $f = 2/3$.

This corresponds to (B)-trees with left [right] rotations. In the B-tree analogue, when a node is full, its keys are "rotated" into the left [right] sibling. Node splitting is performed only when the two nodes are full.

(iii) $f = 3/4$.

This corresponds to (B)-trees with left and right rotations. In the B-tree analogue, when a node is full, its keys are "rotated" into the left or right sibling, according to whichever has room. Node splitting is performed only when the three nodes are full.

(iv) $f = 1/3$.

This also corresponds to (B)-trees, since the circles of radii exist between 1/2 and 2 and 2 in B-trees. In any case, we can always, choose d in such a way that both $2df$ and $(21\text{-}f)\,d$ are integers. The expected storage utilization is given by

$$E(u) = \frac{rs}{2dw}.$$

If we now set

$$P(t) = 1 - t^{2df}\,(1 + t + \ldots + t^{2d(1-f)})$$

$$= 1 - t^{2df}\left(\frac{1 - t^{2d(1-f)} + 1}{1 - t}\right),$$

$$Q(t) = 1 + t + \ldots + t^{2d(1-f)}$$

It is obvious that the asymptotic values of S and W are connected to the zeroes of $P(t)$ of minimal modules for a detailed explanation of singularity analysis for generating functions. By applying the results about the location of the zeros of polynomials, we find that the zeros of $P(t)$ lie in the annulus bounded by the two concentric circles of radii 1/2 and 2, centered at the origin. We observe that, by adding the root $t = 1$ to $P(t)$, we get the equivalent equation.

$$(1 - t)\,P\,(t) = 1 - t - t^{2df} + t^{2d+1} = 0 \tag{3}$$

This implies that only two real roots exist for $P(t) = 0$, and $\bar{s}$, with $1/2 < S < 1$ and $-2 < S < -1$ and multiplicity 1.

The other $2d-2$ roots are all complex. Since the coefficients of the Taylor expansion of $P(t)^{-1}$ around $t = 0$ are all positive (i.e. our $N_p\,(n, v)$, s should be the root of minimal modules) and thus we have :

$$\frac{1}{P(t)} \sim \frac{A}{1 - t/s}\,S \sim \frac{A}{s^r}$$

$$\frac{Q(t)}{P(t)^2} \sim \frac{B}{(1 - t/s)^2} + \frac{C}{1 - t/s}$$

$$W \sim \frac{B(r - 2df + 1)}{S^{r-2df}} + \frac{C}{s^{r-2df}} .$$

for suitable constants A, B and C which are easily computed in terms of S :

$$A = -\frac{1}{sp^1(s)}, \quad B = \frac{Q(s)}{(sp^1(s))^2}$$

$$C = \frac{Q(s)P''(s) - Q'(s)P'(s)}{sp(s)^2}$$

A's and B's values are the most important ones, and can be described in further detail by observing that

$$Q(s) = 1 + s + s^2 + \ldots + s^{2d(1-f)}$$

$$= \frac{1 - s^{2d(1-f)+1}}{(1 - s)}$$

$$P'(s) = \frac{-2dfs^{2df-1}(1 - s^{2d(1-f)+1})}{(1 - s)} - \frac{s^{2df}.(1 - s^{2d(1-f)+1} - 2d(1 - f)s^{2d(1-f)}(1 - s)}{(1 - s)^2}$$

$$= \frac{-2dfs^{2df-1}.(1 - s^{2d(1-f)+1})}{1 - s}$$

$$= \frac{-1 - (2d(1 - f) + 1)s^{2d}}{1 - s}$$

$$A = -\frac{1}{sp^1(s)}, \quad B = \frac{Q(s)}{(sp^1(s))^2} .$$

$$C = \frac{Q(s)P''(s) - Q'(s)\,P'(s)}{sp(s)^2}$$

Here we use the identity $s^{2df}(1 - s^{2d(1-f)+1}) = 1 - s$, (4)

because s is a root of $P(t)$. We can now compute the expected values of storage utilization as follows :

$$E(u) \sim \frac{rA}{s^{2df}\,2d\,(B\,(r - 2df + 1) + C)}$$

$$\sim \frac{A}{2ds^{2df}B} = \frac{-P'(s)}{2ds^{2df-1}\,Q(s)}$$

We set $r \to \infty$, i.e. we assumed that our (B) trees contain a large number of keys. By inserting the values of $P'(s)$ and $Q(s)$ in this expression, we have

$$E(u) \sim f + \frac{s(1 - (2d\,(1-f) + 1)\,s^{2d})}{2d\,(1-s)}$$

which is our most significant result. It gives us the expected value of storage utilization in terms of s, the unique real solution of $P(t) = 0$ *s.t.* $1/2 < s < 1$. This result gives us some further information : by construction, we know that $E(u) > f$, and this means that $1 - (2d\,(1-f) + 1 + s^2 d \geq 0$. This provides us with an upper limit for s :

$$s \leq \frac{1}{\sqrt{2d\,/\,\{2d\,(1-f) + 1\}}}$$

If we set $e^h = 2d\,(1-f) + 1$ or

$$h = \ln\ (2d\,(1-f) + 1)$$

In the relation $(1 + h\,/\,(2d)^2 d \sim e^h$, we obtain the approximation

$$2d\sqrt{\{2d}\,(1-f)+1\} \sim 1+\ln(2d\,(1-f)+1/2\,. \quad \text{or}$$

$$s \leq 1 - \frac{1+\ln(2d\,(1-f)+1/2\,d.}{2d} \tag{5}$$

Actually, this is a good approximation of s which can also be used to show that $E(u) \to f$, when $d \to \infty$, and obviously remains $d = O(r)$. Fortunately, when d is in a practical range (for example, when the nodes contain from 10 to 400 keys), the expected storage utilization is much larger than f, as Table 1 shows. However, it can be noted that in this model, storage utilization decreases as the dimension of the nodes increases. These results agree with intuitive idea that, if we have r keys ($r \to \infty$), which have to be randomly distributed in n cells containing at least $2df$ keys and at most $2d$ keys, the more d increases, the more empty space is left in the cells.

(v) *the $f = 0.5$ case* :

When $f = 0.5$, that is, when the B-tree analogues have their standard formulation, the formulae involved simplify and therefore allow us to be more precise. In particular, the relation $P(t) = 0$ can be written in the form

$$t^d\,(1-t^{d+1}) = 1-t \quad \text{or} \quad t\,(1-t^{2d}) = 1-t^d$$

which simplifies to $t\,(1+t^d) = 1$.

It is worth noting that in the former form, we add the root $t = 1$ to $P(t)$, while in the latter, we eliminate the dth roots of unity.

Theefore, $1 - t - t^{d+1}$ has the same roots as $P(t)$, except for the dth roots of unity. The latter, however, are not significant in the asymptotic evaluation of S and W. The real root evaluation of s ($1/2 < s < 1$) satisfies the identity

$$s^{d+1} + 1 - s, \tag{6}$$

and this can be used to simplify all our expressions. We can also easily prove a stronger limitation for s, as follows :

Using the equation (4) (5) and (6), we get the result

$$1 - \frac{\ln(d+1)}{(d+1)} < s < 1 - \frac{\ln(d+1)}{(d+1)} + \frac{\ln(\ln(d+1))}{(d+1)} \tag{7}$$

In fact, if we denote the two values by x and y, i.e. $x,\ s < y$, we can show that $1 - x - x^{d+1} > 0$ and $1 - y - y^{d+1} < 0$ which means that x and y separate for root s. In fact, by writing m for d+1, we find

$$1 - \left(1 - \frac{\ln m}{m}\right) - \left(1 - \frac{\ln m}{m}\right)^m = \left(\frac{\ln m}{m}\right) - \exp\left(m \ln\left(1 - \left(1 - \frac{\ln m}{m}\right)\right)\right).$$

$$= \left(\frac{\ln m}{m}\right) - \exp\left((-\ln m) - \left(\frac{(\ln m)^2}{2m}\right) - \left(\frac{\ln m}{3m^2}\right)^3 + \ldots\right).$$

$$= \left(\frac{\ln m}{m}\right) - \left(\frac{1}{m}\right) + \left(\frac{(\ln m)^2}{2m^2}\right) + O\left(\left(\frac{(\ln m)^4}{m^2}\right)\right)$$

$$\left[\text{since} \quad \exp(-\ln m) = \frac{1}{m} \quad \text{etc.}\right].$$

which is positive for $m \geq 3$, or $d \geq 2$. In a similar way, we can show that $1 - y - y^{d+1} < 0$.

By applying the rule $s^{d+1} = 1 - s$, we find the values :

$$Q(s) = \frac{s}{1-s)}, \quad P(s) = \frac{(2s-1)\ (d - ds + 1)}{s^2(1-s)}$$

and therefore,

$$E(u) \sim = \frac{(2s-1)(d-ds+1)}{2ds(1-s)}$$

$$= \left(1 - \frac{1}{2s}\right)\left(1 + \frac{1}{d(1-s)}\right).$$

By means of this formula, we deduce the asymptotic behaviour $E(u) \sim 1/2 + 1/2 \ln(d+1)$, which explains the slow convergence towards 1/2 of the expected storage utilization.

We conclude by pointing out that we only examined the root s of minimal modules. As previously mentioned, we also have $2d$–2 complex conjugate roots, some of which have modules less than 1. By applying Euclid's algorithm to $P(t)$ and $P'(t)$, we can show that all roots have multiplicity one. These roots produce oscillations in the behaviour of $E(u)$, which tends to disappear as r increased. For example, when $d = 10$, complex roots having minimal modules are :

$s_1 \cong 0.831630 - 0.415552i$

$s_2 \cong 0.831630 - 0.415552i$

$|s_1| = |s_2| \cong 0.929673$

and the minimal modules real root is

$s_3 \cong 0.8444398$

In this case, S and W are more accurately described by the formulae :

$$S \sim \sum_{I}^{3} \frac{Ai}{S_i^r},$$

$$W \sim \sum_{i=1}^{3} \frac{Bi\,(r-2df+1)}{s_i^{r-2df}} + \frac{C}{s_i^{r-2df}}$$

In which the constants A_i, B_i, C_i correspond to A, B, C evaluated in $s = s_i$, $i = 1, 2, 3$ respectively.

Acknowledgements

The authors thanks the referee for his useful suggestions.

References

1. Baeza-Yeates, R.A. (1989) *Acta Inform*, **26** : 439.
2. Chu, J.H. & Knott, G. (1989) *Inform. Systems* **14** : 359.

3. Mishra, P.K. (1995) *M. Phil. Thesis,* A.P.S. University, Rewa, India.

4. Mishra, P.K. & Sharma, C.K. (1997) *5th International Conf.* HPC-97, Spain.

5. Quitzow, K.H. & Klopprogge (1980) *Inform. Systems* **5** : 7.

6. Wright, W.E. (1985) *Acta Inform.* **21** : 541.

7. Gutpa, G.K. & Srinivasan, B. (1986) *Inform. Process. Lett.* **22** : 243.

8. Riordan, J. (1958) *An Introduction to Combinatorial Analysis,* Wiley, New York.

PROC. NAT. ACAD. SCI. INDIA, 71 (A), III, 2001

Non-linear effects in the motion and stability of an inter-connected satellites system orbiting an oblate Earth

B.M. SINGH*, ASHUTOSH NARAYAN*+, and R.B. SINGH

Department of Mathematics, J.M. College Muzaffarpur-842 001, India.

+Department of Mathematics, Bhilai Institute of Technology, Durg-491 001, India.

Department of Mathematics, Bihar University, Muzaffarpur, India.

*+*Author for correspondence.*

Received November 3, 1998; Revised April 23, 1999; Re-revised January 4, 2000; Accepted March 9, 2000

Abstract

The motion and stability of a system of two satellites, connected by a light, flexible and inextensible string, have been studied under the central gravitational field of the Earth. The non-linear effects due to earth oblateness have been analysed using method due to Bogoliubov and Mitropolsky.

(**Keywords** : inter connected satellites/earth oblateness/non-linear oscillation)

Introduction

The present paper deals with the study of non-linear effects of the Earth's oblateness, on the motion of the system of two satellites connected by a light, flexible and in-extensible string in the central gravitational field of force, for the elliptical orbit, relative to the centre of mass.

The relative motion of two satellites connected by a light, flexible and inextensible string in the central gravitational field of Earth was studied by Beletsky[1,2] and Beletsky and Novikova[3]. The study was based on the assumptions that the orbit of the centre of mass of the system is a circular and the system itself moves in the plane of the orbit of the centre of mass, Singh[4,5] generalized the work by studying it in the two dimensional as well as three dimensional cases.

Manazirudin and Singh[6,7], studied the non-linear effects of small external forces on the motion and stability of the system of two satellites, connected by a light, flexible and in-extensible string. Narayan and Singh[8-10], studied the non-linear oscillation of two inter-connected satellites system under the solar radiation pressure. Finally Singh *et al.*[11]

studied non-linear parametric resonance oscillation of the system of two inter-connected satellites orbiting around an oblate earth.

We have in this paper, studied the effects of Earth's oblateness on the non-linear oscilltion of two artificial satellites connected by a light, flexible and in-extensible string relative to its centre of mass moving in elliptical orbit under the central gravitational field of oblate Earth.

A system in space cannot escape perturbing forces and therefore even an infinitesimal perturbing force can change the circular orbit into an elliptical one. The complexity of the elliptical motion of the system of two inter-connected satellites in space, forced us to restrict our analysis in two dimensional case of the motion of the system.

Equation of Motion

The equation of two dimensional motion of one of the satellites, when the centre of the mass moves along Keplarian elliptical orbit in Nechvill's coordinate system[12] has been obtained in the form Singh[13].

$$X'' - 2Y' - 3X\rho = \lambda_\alpha X - \frac{4AX}{\rho}$$

$$Y'' + 2X' = \lambda_\alpha Y + \frac{AY}{\rho} \tag{1}$$

where X-axis is the direction of the position vector joining the centre of mass and the attracting center and Y-axis along the direction normal to the position vector in the orbital plane of the centre of mass and in the direction of the motion of the satellite.

In the case the condition for constrained motion is given by the inequality.

$$X^2 + Y^2 \leq \frac{1}{\rho^2}$$

where $$\rho = \left(\frac{R}{p}\right) = \frac{1}{1 + e\cos v} \tag{2}$$

where p is the focal parameter, e and v are respectively the eccentricity and the true anomaly of the orbit of the centre of mass of the system. Prime (/) denotes the differentiation with respect to the true anomaly v

$$\lambda_\alpha = P^3 \frac{\lambda}{\mu} = \frac{P^3}{\mu} \rho^4 \left(\frac{(m_1 + m_2)}{(m_1 m_2)} \lambda \right. \tag{3}$$

where λ is the undetermined Langrange's multiplier, A is the Earth oblateness parameter and μ is the product of mass of attracting centre (Earth) and the gravitional constants. When the motion of the satellite m_1 is determined with the help of eqn. (1), the motion of the satellite m_2 is easily determined with the help of identity.

$$m_1 \overrightarrow{\rho_1} + m_2 \overrightarrow{\rho_2} = 0 \tag{4}$$

where $\overrightarrow{\rho_1}$ and $\overrightarrow{\rho_2}$ are the radius vectors of satellites of masses m_1 and m_2 respectively with respect to the centre of mass of the system.

As free motion is bound to be converted into constrained motion with lapse of time, we shall analyse the constrained motion. In the case of constrained motion the equality sign holds in eqn. (2) i.e., the system will be moving along the circle of variable radius given by

$$X^2 + Y^2 = \frac{1}{\rho^2} \tag{5}$$

Now, the equation for motion (1) can be transformed to the polar form, which is best suited for our further investigation of the problem given by :

$$X = (1 + e \cos v) \cos \psi$$

$$Y = (1 + e \cos v) \sin \psi \tag{6}$$

where ψ is the angular deviation of the line joining the satellites with stable position of equilibrium of the system.

Now, differentiating eqn. (6) with respect to true anomaly, putting the derivatives obtained above in eqn. (1), multiplying the first equation obtained above by sin ψ and the second equation by cos ψ, subtracting, we get :

$$(1 + e\cos v)\,\psi'' - 2e\,\psi'\sin v + 3\sin\psi\cos\psi = 2e\sin v + 5A\,(1 + e\cos v)^2\sin\psi\,.\,\cos\psi \quad (7)$$

The eqn. (7) is the equation of motion of a dumbell satellite in the central gravitational field of the oblate earth. The eqn. (7) will be the starting point for our subsequent discussion of the problem of oscillation. Again, differentiating eqn. (6) with respect to true anomaly v, putting the derivatives in eqn. (1) multiplying the first equation obtained above by $\cos\psi$ and the second equation by $\sin\psi$ and adding we get :

$$(1 + e\cos v)(\psi' + 1)^2 - (1 - 3\cos^2\psi) - A(1 + e\cos v)^2(4\cos^2\psi - \sin^2\psi) = \lambda_\alpha(1 + e\cos v) \quad (8)$$

The eqn. (8) determines the undetermined Lagrange's multiplier λ_α. The mechanical implication of the λ_α is that, the motion will be constrained so long as $\lambda(t) > 0$ i.e. $\lambda_\alpha(t) < 0$. Boundaries between the regions of constrained motion and the regions of free motion are given by :

$$(\psi' + 1)^2 - \frac{1 - 3\cos^2\psi}{(1 + e\cos v)} - A\,(1 + e\cos v)\,(4\cos^2\psi - \sin^2\psi) = 0 \quad (9)$$

Equation Characterizing the Non-linear Oscillation of the System

The non-linear oscillation of the system in the central grvitational field of oblate Earth is determined by the equation Singh[13]

$$(1 + e\cos v)\psi'' - 2e\psi'\sin v + 3\sin\psi\cos\psi = 5A\,(1 + e\cos v)^2\sin\psi\cos\psi + 2e\sin v \quad (10)$$

where $$A = 3\left[\alpha_R - \frac{\Omega^2 R_e}{2g_e}\right]\frac{R_e^2}{P^2};$$

α_r = oblateness of the Earth = $(R_e - R_P)/R_e$;

Ω = angular velocity of the rotation of the Earth;

g_e = force of the gravity at equator of the Earth;

R_p = polar radius of the Earth;

R_e = equatorial radius of the Earth.

It has been established that there exists a stable position of equilibrium given by :

$$\varphi = 0$$

$$\psi = 0 \tag{11}$$

The position was found to be Liapunov stable[13].

In the present paper, assuming e to be a very small parameter instead of zero; Now we shall study the oscillation of the system in above mentioned stable position equilibrium.

$$\psi = \psi_0 + \eta$$

$$\psi'' = \eta''$$

$$\sin\psi = \eta - \frac{\eta^3}{3l} + \tag{12}$$

$$\cos\psi = 1 - \frac{\eta^2}{2l}$$

Retaining the terms up to third order in the expansion of sin ψ and cos ψ in the ascending power of ψ, the eqn. (10) takes the form :

$$(1 + e\cos\nu)\,\eta'' - 2e\eta'\sin\nu - 2e\sin\nu - 3\eta - 2\eta^3 =$$

$$\left[5A\eta - \frac{10}{3}A\eta^3 + 10Ae\eta\cos\nu - \frac{20}{3}Ae\cos\nu\eta^3 + 5A\eta e^2\cos^2\nu - \frac{10}{3}Ae^2\eta^3\cos^2\nu\right] \tag{13}$$

Since, the non-linearity has been assumed to be sufficiently weak, $2\eta^3$ is supposed to be of the order of e.

Now $2\eta^3 \sim 0(e)$ and $10/3\ A\eta^3 \sim 0\,(e)$.

Setting $2\eta^3 = ek_2\eta^3$, $\frac{10}{3}A\eta^3 = ek_1\,\eta^3$, let us introduce the substitution.

$$\eta = \frac{z}{(1 + e\cos\nu)} = (z\rho) \tag{14}$$

Differentiating eqn. (14) with respect to ν, we get :

$$z'' = (1 + e\cos\nu)\,\eta'' - 2e\,\eta'\sin\nu - e\,\eta\cos\nu$$

$$z'' + e\,\eta\cos\nu = (1 + e\cos\nu)\,\eta'' - 2e\,\eta'\sin\nu \tag{15}$$

With the help of eqn. (14) and (15) the equation of motion given by (13) takes the form

$$z'' + n^2 z = e\left[2z\cos\nu + 5Az\cos\nu + 2\sin\nu - k_1 z^3 + \frac{20}{3}Az^3\cos\nu - 6z^3\cos\nu + k_2 z^3\right]$$
$$+ e^2\left[-2z\cos^2\nu + 3k_1 z^3\cos\nu + 15Az^3\cos^2\nu \,\ldots\ldots\ldots\right] + e^3\left[\ldots\ldots\ldots\ldots\right] \tag{16}$$

Here $n^2 = 3 - 5A$; where $k_2 = (2/e)$ and $k_1 = 10/3e$

The eqn. (16) is the variational equation describing non-linear oscillation of the system about the position of equilibrium. We shall use this equation in our further discussions.

We shall construct an approximate solution of eqn. (16) in the non-resonance case exploiting the method[14] of Bogoliubov Krilov and Mitropolsky. After some lengthy calculations, we obtain the solution in the first approximation as

$$z = a\cos\theta \tag{17}$$

where $\theta = n\nu + \theta*$ where, the phase θ^* is a constant quantity. The amplitude a and the phase θ are given by the equations

$$\frac{da}{d\theta} = O i.e. a. = \text{Constant} \tag{18}$$

$$\frac{d\theta}{d\nu} = n + \frac{3e}{8n}(k_1 - k_2)\,a^2$$

and in the second approximation the solution is

$$z = a\cos\theta + e\left[\frac{2}{(n^2-1)}\sin\nu - \frac{(4a+10Aa-10Aa^3-9a^3)}{4(2n+1)}\cos(\nu+\theta) + \frac{(4a+10Aa-10Aa^3-9a^3)}{4(2n-1)}\cos(\nu-\theta)\right]$$

$$e\left[+\frac{(10A-9)a^3}{12(4n+1)(2n+1)}\cos(\nu+3\theta)+\frac{(10A-9)a^3\cos(\nu-3\theta)}{12(4n-1)(2n-1)}\right]+\left[\frac{(3-5A)a^3\cos 3\theta}{72n^2}\right] \quad (19)$$

where the amplitude and the phase are determined by the equations : $da/dv = 0$; $a = a_\theta$ (constant) in the second approximation.

$$\frac{d\theta}{dv} = n + \frac{(3-5A)}{4n}a^2 - e^2\left[\frac{(4a-10Aa-10Aa^3-9a^3)\,(12-45a^2-10Aa^2-120A}{96n\,(4n^2-1)}\right]+$$

$$e^2\left[\frac{a^5\,(100A^2-81)}{144(16n^2-1)\,(4n^2-1)\,n}\right]-\frac{3e\,(3-5A)\,a^5}{8n^2} \quad (20)$$

From the above solution we come to the conclusion that the amplitude a of the system remained constant up to the second approximation. The phase of the oscillation of the system in the case of non-linear non-resonance oscillation varies with respect to time; However, the variation of the phase of the system is of the order of the square of the eccentricity, if the orbit of the centre of mass of the system which is a small quantity.

We arrive at the conclusion that the system experiences main resonance at $n = \pm 1$ the parametric resonance at $n = \pm 1/2$ up to the second approximation.

Non-Linear Oscillation of the System about the Position of Stable Equilibrium for Small Eccentricity in the neighborhood of Main Resonance.

In the previous section, we have observed that the system experiences main resonance at $n = 1$. Now we proceed to construct the asymptotic solution of (16) for the case of main resonance $n = 1$, in the form :

$$z = a\cos(\nu+\theta) \quad (21)$$

where the amplitude a and the phase θ are given by the system of differential equations :

$$\frac{da}{d\nu} = -\frac{2e}{(n+1)}\cos\theta \quad (22)$$

$$\frac{d\theta}{d\nu} = (n-1) + \frac{2e}{a(n+1)}\sin\theta - \frac{(3-5A)a^2}{4n}$$

We conclude that the oscillation of the system in the first approximation is depending upon the form of the orbit of the centre of mass.

The equation can be integrated in a close form as it can be reduced to the Hamilton canonical form;

$$\frac{da}{d\nu} = \frac{1}{a}\left(\frac{\partial H}{\partial \theta}\right) \;\&\; \frac{d\theta}{d\nu} = -\frac{1}{a}\left(\frac{\partial H}{\partial a}\right) \tag{23}$$

where
$$H = -2a\frac{e}{(n+1)}\sin\theta - \frac{(n-1)}{2}a^2 + \frac{(3-5A)}{16n}a^4 \tag{24}$$

Obviously, the system of the eqn. (23) has a first integral of the form $H = Co$ (25)

which reduces the problem to quadrature. Here Co' is the constant of integration. However, it is preferable to analyse the integral curves in the phase plane (a,θ). In order to plot the integral curves in the phase plane (a,θ) let us put the eqn. (24) in the form :

$$(n^2-1)\,a^2 + 4ae\sin\theta - \frac{(n+1)}{8n}(3-5A)\,a^4 + Co = 0 \tag{26}$$

where $Co = 2\,(n+1)\,Co'$

The integral curve (26) has been plotted in Fig. 1 for $n = 0.8$, $e = 0.01$ and $A = 0.18$ (i.e. Earth oblateness parameter). The integral curves drawn in the phase plane (a, θ) clearly indicate that there exists only one stationary regime of the amplitude i.e. $a = 0.046$ and $\theta = (81)^\circ$ and it is stable as the integral curves are closed curves. For any other initial conditions, we shall obtain periodic change in the amplitude a which will be bounded. But the maximum values of a in this case will always be greater than its values at the stationary regime. We conclude therefore, that for a gravity gradient stabilisation of such a space system in elliptical orbit, we need to bring the amplitude of oscillation near the stationry regime which gives, smallest deflection of the system from the relative equilibrium position in comparison, to any other regime of oscillation.

In the Fig. 2 the integral curves, (26) for $n = 1.2$, $e = 0.01$ and $A = 0.18$ (Earth oblateness parameters) has been plotted and it is found that the stationary regime of the amplitude a exists. In this case also there exists only one stationary regime which gives, smallest deflection of the system from the relative equilibrium position in comparison, to any other regime of oscillation. We also conclude that the period passes through the position of main

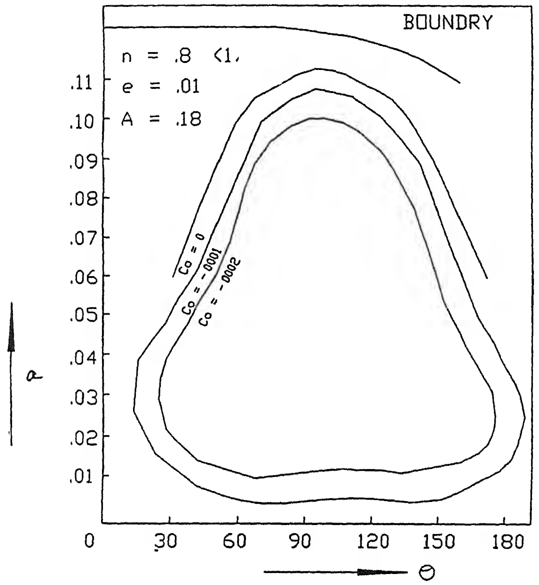

Fig. 1 – Oscillation of an inter connected satellites system in elliptical orbit, amplitude phase characteristic.

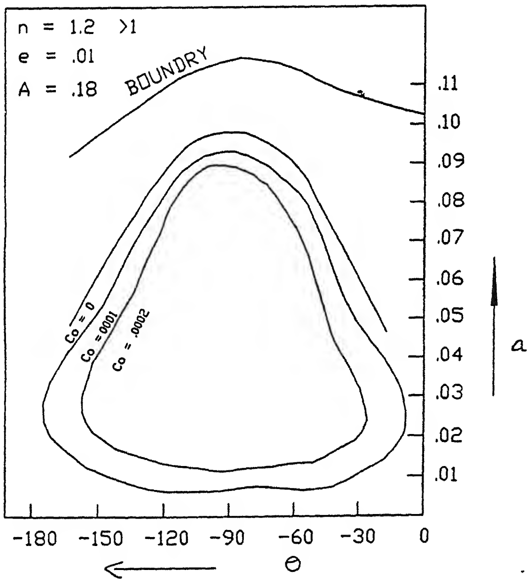

Fig. 2 – Oscillation of an inter connected satellites system in elliptical orbit, amplitude phase characteristic.

resonance stationary amplitude declines steadily, which is obvious from Fig. (1 & 2) plotted for $n = 0.8$ and $n = 1.2$ respectively.

In order to see, whether the oscillation of the system in this stationary regime always takes place with tight string, we shall consider the eqn. (9). This condition divides the phase plane into two regions which are regions for free and constrained motions. The boundary of these regions is given by :

$$(1 + e\cos\nu)(\eta' + 1)^2 - 3\cos^2\eta + 1 - A(1 + e\cos\nu)^2(5\cos^2\eta - 1) = 0 \tag{27}$$

$$\cos^2\eta = \cos^2(a\cos k) = \cos^2[a\cos(\nu + \theta)]$$

$$J_0(a) - 2J_2(a)\cos(2\theta + 2\nu) + 2J_4(a)\cos(4\theta + 4\nu)$$

$$1 - \frac{a^2}{2} - \frac{a^2}{2}\cos(2\theta + 2\nu)$$

$$\sin\eta = 2J_1(a)\cos k - 2J_3(a)\cos 3k + 2J_5(a)\cos 5k \tag{28}$$

$$= a^3\cos(\nu + \theta)$$

where $$J_\gamma(a) = \sum_{m=0}^{\infty} \frac{(-1)^m\left(\frac{a}{2}\right)^{m+\gamma}}{m\sqrt{\gamma + m + 1}} \tag{29}$$

Now substituting the value of $\eta, \eta' \cos^2\eta$ in the above eqn. (25) neglecting the terms containing e^2 and higher order of e and averaging with respect to ν in the interval $(0, 2\pi)$ keeping θ and A to be constant we get,

$$\left[\frac{a^2n^2}{2} - \frac{(3 - 5A)}{4}a^4 \frac{ane}{(n+1)}\cos\theta - 1 + \frac{3}{2}a^2 - 4A + \frac{5Aa^2}{2} - ane\sin\theta\right] = 0 \tag{30}$$

In the process of tracing out the average eqn. (30) for $n = 0.8$, $e = 0.01$ and $A = 0.18$ find that the boundary line does not intersect any of the integral curves but passes just above them. Also, from the figure in which the averaged equation (30) for $n = 1.2$, $e = 0.01$ and $A = 0.18$ has been traced we find that the line does not intersect the integral curves.

Therefore, the motion of the system in the whole phase plane (a, θ) will be non-evolutional.

Discussion and Conclusion

We thus, conclude that the amplitude of the oscillation of the system in the case of non-linear non-resonance oscillation remained constant up to the second approximation. The phase of the oscillation of the system varies with respect to time. However, the variation of the phase of the system is of the order of the square of the eccentricity, if the orbit of the centre of mass of the system which is a small quantity. We observe that the system experiences main resonance at $n = \pm 1$ and parametric resonance at $n = \pm 1/2$ up to the second approximation.

We further conclude that if a system of two cable connected satellites oscillating at and near the main resonance $n = 1$ under the gravitational field of oblate Earth, there exists only one stationary stable regime of amplitude for both $n < 1$ and $n > 1$. We have established that at the resonance oscillation at and near $n = 1$, the motion remains non-evolutional i.e. the system moves like dumbell satellite. However, the stationary amplitude declines steadily as it passes through two values of n given by $n < 1$ and $n > 1$. Thus, we arrive at the conclusion that oblateness of the Earth, however small, may cause periodic changes in the amplitude of the oscillating system in case of slight deflection from stationary regime of oscillation.

References

1. Beletsky, V.V. (1969) *Iskussivennjic sputniki Zeml., lzd ANSSSR* 3.
2. Beletsky, V.V. (1969) *Koswicheskiya Issaledovania* **7** : 827.
3. Beletsky, V V. & Novikova, E.T. (1969) *Koswiecheskiya Issledovania* **7** : 377.
4. Singh, R.B. (1971) in *Problem of Guided Motion in Mechanics*, Russian Collechov : 210.
5. Singh, R.B. (1973) *Astronautica Acta* **18** : 301.
6. Manazirudin & Singh, R.B. (1985) *Proc. Nat. Acad. Sci. India* **55(A)** : 261.
7. Manazirudin & Singh, R.B. (1992) *Celestial Mechanics* **53** : 219.
8. Narayan, A. & Singh, R.B. (1987) *Proc. Nat. Acad. Sci. India* **57(A)** : 427.
9. Narayan, A. & Singh, R.B. (1990) *Proc. Nat. Acad. Sci. India* **60(A)** : 307.
10. Narayan, A. & Singh, R.B. (1992) *Proc. Nat. Acad. Sci. India* **62(A)** : 241.
11. Singh, B.M., Narayan, A. & Singh, R.B. (1997) *Proc. Nat. Acad. Sci. India*, **67(A)** : 245.
12. Nechvill, V. (1926) *Acad. Paris compt Rend. 37D.* : 182.
13. Singh, C.P. (1984) *Dissertation for Ph.D.*, University of Bihar, Muzaffarpur, India.
14. Bogoliubov, N.N. & Mitropolosky, Y.A. (1961) *Asymptotic Method in the Theory of Non-Linear Oscillation*, Hindustan Publishing Corporation, Delhi.

PROC. NAT. ACAD. SCI. INDIA, 71 (A), III, 2001

A common fixed point theorem in complete metric spaces by altering distances

K.P.R. SASTRY and G.V.R. BABU

Department of Mathematics, Andhra University, Visakhapatnam-530003, India.

Received March 12, 1999; Revised September 16, 1999, Accepted March 9, 2000

Abstract

A unique common fixed point theorem for a sequence of selfmaps of a complete metric space by altering distances between the points under a certain continuous control function is established.

(**Keywords** : complete metric space/Hilbert space/selfmaps/common fixed points)

Introduction

Existence and uniqueness of fixed points for selfmaps of a metric space by altering distances between the points with the use of a certain control function was established by Khan *et al.*[1] Some contributions in this direction are due to Pathak and Sharma[2], Sastry and Babu[3,4].

Throughout this paper, (X, d) denotes a complete metric space, H a Hilbert space, R^+ the set of all non-negative real numbers and N the set of all positive integers. Φ denotes the set of all continuous selfmaps ϕ of R^+ satisfying (i) ϕ is increasing (ii) $\phi(t) = 0$ if and only if $t = 0$.

Existence and uniqueness of fixed points for a sequence of selfmaps of a Hilbert space H is established by Pandhare and Waghmode[5].

Theorem 1 : Pandhare and Waghmode.[5] : Let C be a closed subset of H and $\{T_n\}_{n=1}^{\infty}$ a sequence of selfmaps of C satisfying

(A) : For any two maps T_i, T_j

$$\| T_i x - T_j y \|^2 \leq a \|x-y\|^2 + b\left(\|x - T_i x\|^2 + \|y - T_j y\|^2\right)$$

for all distinct x, y in C where $a \geq 0$, $0 < b < 1$ and $a + 2b < 1$.

(B) : There is a point $x_0 \in C$ such that any two consecutive members of the sequence $\{x_n\}$ defined by $x_n = T_n x_{n-1}$, $n \geq 1$ are distinct.

Then $\{T_n\}_{n=1}^{\infty}$ has a unique common fixed point in C.

Babu[6] obtained a partial generalization of theorem 1 to complete metric spaces by assuming more stringent hypothesis that all the members of the sequence $\{x_n\}$ in (B) are distinct. In this paper, we obtain a generalization to theorem 1 in complete metric spaces under hypothesis (B1) (stated in hypothesis of theorem 2) by altering distinces between the points, with the use of a certain continuous control function ϕ in Φ, which is our main theorem.

Examples are also provided to justify the study of the mappings under condition (A) (in the Hilbert space setting) and the generalized version under condition (A1) in metric space setting. In fact, Example 3 shows the applicability of theorem 2 in l_1-norm setting.

Main Theorem

Theorem 2 : Let $\{T_n\}_{n=1}^{\infty}$ be a sequence of selfmaps on (X, d). Assume

(A1) : There exists a ϕ in Φ such that

$$\phi(d(T_i x, T_j y)) \leq a\,\phi(d(x, y)) + b\,(\phi(d(x, T_i x)) + \phi(d(y, T_j y)))$$

for all i, j in N and for all distinct x, y in X where $a \geq 0$, $0 < b < 1$ with $a + 2b < 1$.

(B1) : There is a point x_0 in X such that any two consecutive members of the sequence $\{x_n\}$ defined by $x_n = T_n x_{n-1}$, $n \geq 1$ are distinct.

Then $\{T_n\}_{n=1}^{\infty}$ has a unique common fixed point in X. Infact, $\{x_n\}$ is Cauchy and the limit of $\{x_n\}$ is the unique common fixed point of $\{T_n\}_{n=1}^{\infty}$

Proof : Write $\alpha_n = d(x_n, x_{n+1})$ and $\beta_n = \phi(\alpha_n)$. From (A1) and (B1), we have $\beta_1 = \phi(d(x_1, x_2)) = \phi(d(T_1 x_0, T_2 x_1)$

$$\leq a\,\phi(d(x_0, x_1)) + b\,(\phi(d(x_0, x_1)) + \phi(d(x_1, x_2)))$$

so that $\beta_1 \leq k\,\beta_0$ where $k = \dfrac{a+b}{1-b} < 1$, since $a + 2b < 1$.

By induction, follows that $\beta_n \leq k\,\beta_{n-1}$ for all $n \geq 1$ (1)

so that $\beta_n \downarrow 0$ as $n \to \infty$ and $\alpha_n < \alpha_{n-1}$ for $n = 1, 2, \ldots$ Therefore $\{\alpha_n\}$ is a decreasing sequence of non-negative reals. Thus $\{\alpha_n\} \downarrow \alpha$ (say). Then

$\beta_n = \phi(\alpha_n) \downarrow \phi\,(\alpha)$ so that $\phi(\alpha) = 0$ and hence $\alpha = 0$. Therefoe $\{\alpha_n\} \downarrow 0$. (2)

The crucial part of the theorem is to show that $\{x_n\}$ is Cauchy in X. Otherwise, there is an $\in > 0$ and sequences $\{m\,(k)\}$ and $\{n\,(k)\}$ such that $m(k) < n(k)$, $d\,(x_{n(k)}, x_{m(k)}) \geq \in$ and $d(x_{n(k)-1}, x_{m(k)}) < \in$.

Assume that $x_{n(k)-1} = x_{m(k)-1}$ for infinitely many k. Then, for such k,

we have

$$\begin{aligned} \in \leq d(x_{n(k)}, x_{m(k)}) &\leq d\,(x_{n(k)}, x_{m(k)-1}) + d\,(x_{m(k)-1}, x_{m(k)}) \\ &= d\,(x_{n(k)}, x_{n(k)-1}) + d\,(x_{m(k)-1}, x_{m(k)}) \to 0 \text{ as } k \to \infty \text{, a contradiction.} \end{aligned}$$

Hence, for large k, $x_{n(k)-1} \neq x_{m(k)-1}$, consequently

$$\begin{aligned} \phi(\in) &\leq \phi\,(d\,(x_{n(k)}, x_{m(k)})) = \phi\,(d\,(T_{n(k)}\,x_{n(k)-1}, T_{m(k)}\,x_{m(k)-1})) \\ &\leq a\,\phi\,(d\,(x_{n(k)-1}, x_{m(k)-1})) + b\,(\phi\,(d\,(x_{n(k)-1}, x_{n(k)})) + \phi\,(d\,(x_{m(k)-1}, x_{m(k)}))) \\ &\leq a\,\phi\,(x_{n(k)-1}, x_{m(k)})) + d\,(x_{m(k)}, x_{m(k)-1})) \\ &\qquad + b\,(\phi\,(d\,(x_{n(k)-1}, x_{n(k)})) + \phi\,(d\,(x_{m(k)-1}, x_{m(k)}))) \\ &\leq a\,\phi\,(\in + d\,(x_{m(k)}, x_{m(k)-1})) + b\,(\phi\,(d\,(x_{n(k)-1}, x_{n(k)})) + \phi\,(d\,(x_{m(k)-1}, x_{m(k)}))) \\ &\to a\,\phi\,(\in) \text{ as } k \to \infty, \text{ by (2).} \end{aligned}$$

Hence $\phi(\in) \leq a\,\phi(\in) < \phi(\in)$, a contradiction.

This shows that $\{x_n\}$ is a Cauchy sequence in X. As X is complete, limit of $\{x_n\}$ exists,

There is a sequence $\{n(k)\}$ such that $y \neq x_{n(k)-1}$. Otherwise, $y = x_{n-1}$ for large n, which is not the case, since consecutive terms are different. With this subsequence $\{x_{n(k)}\}$, we have, for any positive integer m,

$$\begin{aligned}\phi(d(T_m y, x_{n(k)})) &= \phi\ (d(T_m y, T_{n(k)}\, x_{n(k)-1})) \\ &\leq a\,\phi\ (d\ (y, x_{n(k)-1})) + b\ (\phi\ (d\ (T_m y, y)) + \phi\ (d\ (x_{n(k)}, x_{n(k)-1})))\end{aligned}$$

Taking limits as $k \to \infty$, we have $\phi\ (d\ (T_m y, y)) \leq b\ \phi\ (d\ (T_m y, y))$.

Since $0 < b < 1$, it follows that $\phi\ (d\ (T_m y, y)) = 0$ so that $d\ (T_m y, y) = 0$.

This shows that y is a fixed point for T_m . Thus y is a common fixed point for the sequence $\{T_n\}_{n=1}^{\infty}$.

Uniqueness of the fixed point follows trivially from (A1).

Remark : When X is a Hilbert space, we get theorem 1 due to Pandhare and Waghmode[5] from the above theorem, by taking $\phi(t) = t^2$ for $t \geq 0$.

Generalization of Theorem 2

Theorem 2 can be further generalized (the proof being similar) as follows.

Theorem 3 : Let $\{T_n\}_{n=1}^{\infty}$ be a sequence of selfmaps on (X, d) and assume (B1) holds. Further assume that

(A2) : There exists ϕ in Φ such that

$$\phi(d\,(T_i x, T_j y)) \leq k\ \max\ \{\phi\ (d\,(x, y)),\ \frac{1}{2}(\phi\ (d\,(x, T_i x)) + \phi\ (d\ (y, T_j y)))\}$$

for some $0 < k < 1$, and for all i, j in N and for all distinct x, y in X.

Then the sequence $\{T_n\}_{n=1}^{\infty}$ has a unique common fixed point in X. In fact, $\{T_n\}$ $\{x_n\}$ is Cauchy and the limit of $\{T_n\}$ $\{x_n\}$ is the unique common fixed point of $\{T_n\}_{n=1}^{\infty}$.

Examples

The following is an example to show the applicability of theorem 2 with $\phi(t) = t$.

Example 1 : Let $X = [0, 0.2]$ with the usual metric. Define $T_n : X \to X$ by $T_n x = x^{4n}$ for $n = 1, 2, \ldots$ Define $\phi(t) = t$, $t \geq 0$ that $\phi \in \Phi$. Then, $\{T_n\}_{n=1}^{\infty}$ satisfies the condition (A1) with $a = 0.5$ and $b = 0.125$. Observe that, for any non-zero x_0 in X, the sequence $\{x_n\}_{n=1}^{\infty}$ defined by $x_n = T_n x_{n-1}$, $n \geq 1$ has all its elements distinct so that (B1) also holds; thus hypothesis of theorem 2 is satisfied and 0 is the unique common fixed point of $\{T_n\}_{n=1}^{\infty}$.

Example 2, below shows the applicability of theorem 2 with $\phi(t) = t^2$. This example may be taken as an application of theorem 1 in Hilbert space setting.

Example 2 : Let $X = [0, 0.1]$ with usual metric. Define $T_n : X \to X$ by $T_n x = x^{2n}$ for $n = 1, 2. \ldots$ Define $\phi(t) = t^2$, $t \geq 0$ so that $\phi \in \Phi$, Let $x, y \in X$, $x \neq y$. Then

$$\phi(d(T_n x, T_m y)) = (x^{2n} - y^{2m})^2 \leq (0.04)(x^n - y^m)^2 \leq (0.04)(x^{2n} + y^{2m}) \tag{3}$$

and
$$\begin{aligned}
&(0.04)(x^{2n} + y^{2m}) + 2(0.05)(x^{2n+1} + y^{2m+1}) \\
&= (0.04 + (0.1)x)x^{2n} + (0.04 + (0.1)y)y^{2m} \\
&\leq (0.05)(x^{2n} + y^{2m}) \\
&\leq (0.05)(x^2 + y^2) \\
&\leq (0.01)(x-y)^2 + (0.05)(x^2 + y^2) + (0.05)(x^{4n} + y^{4m})
\end{aligned}$$

for all $m \geq 1$ and $n \geq 1$,

so that
$$(0.04)(x^{2n} + y^{2m}) \leq (0.01)(x-y)^2 + (0.05)\left[(x - x^{2n})^2 + (y - y^{2m})^2\right] \tag{4}$$

From (3) and (4), it follows that the inequality (A1) holds with $a = 0.01$ and $b = 0.05$.

Condition (B1) holds trivially for any $0 \neq x_0 \in X$, and 0 is the unique common fixed point for $\{T_n\}_{n=1}^{\infty}$.

In the above example, we observe that (A1) does not hold with $\phi(t) = t$ and $a = 0.01$ and $b = 0.05$ (take $x = 0$ and $y = 0.1$).

We now give an example as an application of theorem 2, with $\phi(t) = t^2$ in metric space setting, in general and l_1-norm setting, in particular.

Example 3 : Let $X = \left[0, \frac{1}{18}\right] \times \left[0, \frac{1}{18}\right]$ with l_1-norm, $\|\,.\,\|_1$ being defined by $\|(x, y)\|_1 = |x| + |y|$ for $(x, y) \in X$. Define $\phi : R^+ \to R^+$ by $\phi(t) = t^2$, $t \geq 0$ so that $\phi \in \Phi$. Define $T_n : X \to X$ by $T_n(x, y) = (x^{4n}, y^{4n})$ for $n = 1, 2, \ldots$ Then $\{T_n\}$ satisfies (A1) with $a = 0.5$ and $b = 0.1$. Condition (B1) holds trivially for any nonzero (x_0, y_0) in X and $(0, 0)$ is the unique common fixed point for $\{T_n\}_{n=1}^{\infty}$.

Open Problem

Is the conclusion of theorem 2 valid if (A1) is replaced by (A3) : There exists ϕ in Φ such that

$$\phi(d(T_i x, T_j y)) \leq a\,\phi(d(x, y)) + b\,(\phi(d(x, T_i x)) + \phi(d(y, T_j y)))$$
$$+ c\,(\phi(d(x, T_j y)) + \phi(d(y, T_i x)))$$

for all i, j in N and for all distinct x, y in X where $a \geq 0$, $c \geq 0$, $0 < b < 1$ with $a + 2b + 2c < 1$.

Acknowledgements

This work is supported by the UGC Minor Research Project Grant No. U4/4997/97-98. One of the authors (G.V.R.B.) thanks the University Grants Commission, New Delhi for the financial support.

References

1. Khan, M.S., Swaleh, M. & Sessa, S. (1984) *Bull. Austra. Math. Soc.* 30 : 1.
2. Pathak, H.K. & Sharma, Rekha (1994) *The Mathematics Education* 28 : 151.
3. Sastry, K.P.R. & Babu, G.V.R. (1998) *Bull. Cal. Math. Soc.* 90(4) : 175.
4. Sastry, K.P.R. & Babu, G.V.R. (1999) *Indian J. Pure Appl. Math.* 30(6) : 641.
5. Pandhare, D.M. & Waghmode, B.B. (1998) *The Mathematics Education* 32 : 61.
6. Babu, G.V.R. (1999) *The Mathematics Education* 33 : 4.

PROC. NAT. ACAD. SCI. INDIA, 71 (A), III, 2001

Hall current effects on heat and mass transfer in flow of a viscous fluid

N.P. SINGH*

Department of Mathematics, C.L. Jain (P.G.) College, Firozabad-283 203, India.

**Address for correspondence : H.No. 236, Durga Nagar, Firozabad-283 203, India.*

Received October 8, 1999; Accepted April 6, 2000

Abstract

In the present paper Hall current effects on unsteady free convection and mass transfer flow of a viscous, electrically conducting fluid past an infinite, porous, non-conducting, vertical plate under the influence of uniform transverse magnetic field in the presence of constant normal suction velocity at the plate is considered. It is assumed that the free stream, plate temperature, species concentration oscillates about a non-zero mean and the concentration level of the diffusing species is small compared with other concentrations. Momentum, energy and concentration equations are solved. The effects of the various parameters, entering into the problem, on the primary and secondary velocities are depicted graphically while the skin-friction coefficient, Nusselt number and Sherwood number are shown in tabular form followed by a discussion.

(**Keywords** : Hall current/mass transfer/heat source/Soret number/Sherwood number)

Introduction

The studies on MHD free convection analysis appear in literature because of its important applications in meteorology, solar physics, cosmic fluid dynamics, motion of earths core, planetary magnetospheres, aeronautics, chemical engineering, electronics etc. Along with the free convection currents caused by the temperature difference, the flow is also affected by the difference in concentration on material constitution. Gebhart and Pera[1-4] made extensive studies of combined heat and mass transfer flow. The effect of suction parameter on free convection and mass transfer MHD flow being an effective method of controlling the boundary layer has been studied by several authors[5-7]. In all these studies thermal effect has been neglected. Eckert and Drake[8] have pointed out that in a convective fluid when the flow of mass is caused by a temperature difference one can not neglect the thermal diffusion effect (commonly known as Soret effect) due to its practical application in engineering sciences. For instance thermal diffusion effect has been utilized for isotope separation and in mixtures between gases with very light molecular weight (H_2, He) and medium molecular weight (N_2, air) and it was found to be of a such magnitude that it can

not be neglected. In view of the importance of this diffusion thermo effect, Jha and Singh[9] presented study for a free convection and mass transfer flow past an infinite vertical plate moving impulsively in its own plane taking into account the Soret effect. Kafoussias[10] extended this work to MHD free convective flow. Recently Sattar and Alam[11] have discussed Soret effects on MHD free convection and mass transfer flow past an impulsively started vertical porous plate in a rotating fluid with out taking into account the Hall current effect. However, when the strength of the magnetic field is strong, the Hall effects play a significant role in determining the flow feature. More recently Singh and Singh[12] have discussed Hall current effects in convective flow of a viscous liquid. Hence our aim is to study Soret effects as well as heat source effects on MHD free convection and mass transform flow of a viscous fluid past an infinite porous non-conducting vertical plate with constant suction normal to the plate taking Hall currents into account.

Formulation of the Problem

Let x-axis be chosen along the plate and y-axis normal to it. A uniform magnetic field B_0 is taken to be acting along the y-axis and the induced magnetic field is assumed to be negligible so that $B = (0, H_0, 0)$. The plate temperature and concentration oscillate about a constant mean and the species concentration is assumed at low level. The plate temperature and concentration are instantaneously raised or lowered to T_w $(> T_\infty)$ and C_w $(> C_\infty)$, T_∞ and C_∞ are the temperature and concentration of the uniform flow. The equation of conservation of electric charge is $\vec{\nabla}.\vec{J} = 0$ which gives J_y = constant, where $\vec{J} = (J_x, J_y, J_z)$. Since the plate is electrically non-conducting, $J_y = 0$ and is zero every where in the flow. When the magnetic field is large, the generalized Ohms law, in absence of electric field, neglecting the ion slip and thermo electric effect (Meyer[13]) yields

$$J_x - w_e \tau_e J_z = -\sigma\mu_e H_0 w \tag{1}$$

$$J_z + w_e \tau_e J_x = \sigma \mu_e H_0 u \tag{2}$$

The solution of eqn. (1) and (2) is

$$J_x = \frac{\sigma \mu_e H_0}{1 + m^2} (mu - w) \tag{3}$$

$$J_z = \frac{\sigma \mu_e H_0}{1 + m^2} (u + mw) \tag{4}$$

where $m(= w_e \tau_e)$ is Hall parameter, w_e : the cyclotron frequency, τ_e : the electron collision time, μ_e : the magnetic permeability, σ : the electrical conductivity of the fluid. Within the frame work of such assumptions, neglecting the Joule heating and viscous dissipation terms and assuming that all the fluid properties are constant except that the density variation with temperature is considered only in the body force term, the basic equations governing the boundary layer flow past the plate under Boussinesq's approximation in non-dimensional form (ignoring the stars introduced ahead) are

$$\frac{1}{4}\frac{\partial u}{\partial t} - \frac{\partial u}{\partial y} = \frac{1}{4}\frac{\partial U}{\partial t} + \frac{\partial^2 u}{\partial y^2} - \frac{M}{1+m^2}(u - U + mw) + G_r T + G_m \theta \tag{5}$$

$$\frac{1}{4}\frac{\partial w}{\partial t} - \frac{\partial w}{\partial y} = \frac{\partial^2 w}{\partial y^2} + \frac{M}{1+m^2}[m(u-U) - w] \tag{6}$$

$$\frac{1}{4}\frac{\partial T}{\partial t} - \frac{\partial T}{\partial y} = \frac{1}{P_r}\frac{\partial^2 T}{\partial y^2} + ST \tag{7}$$

$$\frac{1}{4}\frac{\partial \theta}{\partial t} - \frac{\partial \theta}{\partial y} = \frac{1}{S_c}\frac{\partial^2 \theta}{\partial y^2} + S_0 \frac{\partial^2 T}{\partial y^2} \tag{8}$$

The non-dimensional boundary conditions are

$$\left.\begin{array}{llll} u = w = 0, & T = \theta = 1 + \in \exp(int) & at & y = 0 \\ u = 1 + \in \exp(int), & w \to 0 \quad t = \theta = 0 & as & y \to \infty \end{array}\right\} \tag{9}$$

where G_r : Grashof number, G_m : modified Grashof number, P_r : Prandtl number, S_c : Schmidt number, S_0 : Soret number, S : heat source parameter, β : volumetric coefficient of thermal expansion, β^* : volumetric coefficient of thermal expansion with concentration, K : thermal conductivity, D : molecular diffusivity, D_1 : thermal diffusivity and all the other quantities have their usual meanings[11,14].

The non-dimensional quantities introduced in the above equations are defined as

$$u^* = \frac{u}{U_0},\ w^* = \frac{w}{U_0},\ y^* = \frac{yv_0}{\gamma},\ t^* = \frac{tv_0^2}{4\upsilon},\ U^* = \frac{U}{U_0},\ n^* = \frac{4\upsilon n}{v_0^2},$$

$$T^* = \frac{T - T_\infty}{T_w - T_\infty}, \quad \theta^* = \frac{C - C_\infty}{C_w - C_\infty}, \quad G_r = \frac{g\beta\upsilon(T_w - T_\infty)}{U_0\, v_0^2}, \quad G_m = \frac{g\beta^*\upsilon\,(C_w - C_\infty)}{U_0\, v_0^2}$$

$$M = \frac{\mu_e^2 H_0^2 \sigma\upsilon}{v_0^2 \rho}, \quad S = \frac{Q\upsilon}{v_0^2}, \quad P_r = \frac{\mu C_p}{K}, \quad S_c = \frac{\upsilon}{D}, \quad S_0 = \frac{D_1\,(T_w - T_\infty)}{\upsilon\,(C_w - C_\infty)}$$

Introducing $q = u + iw$, the equations (5) and (6) transform to

$$\frac{1}{4}\frac{\partial q}{\partial t} - \frac{\partial q}{\partial y} = \frac{1}{4}\frac{\partial U}{\partial t} + \frac{\partial^2 q}{\partial y^2} - \frac{M(1 - im)}{(1 + m^2)}\,(q - U) + G_r T + G_m \theta \tag{10}$$

Solution of the Problem

In order to solve the system of eqn. (7), (8) and (10) under the boundary conditions (9), we assume

$$\begin{aligned} q\,(y, t) &= (1 - q_0) + \in (1 - q_1)\ \exp\,(int) \\ T\,(y, t) &= T_0\,(y) + \in T_1\,(y)\ \exp\,(int) \\ \theta(y, t) &= \theta_0\,(y) + \in \theta_1\,(y)\ \exp\,(int) \end{aligned} \tag{11}$$

Substituting (11) in (7), (8), (10) and equating harmonic and non-harmonic terms, we get six equations. The solutions of these equations under the boundary conditions obtained after substituting (11) in (9) give q_0, q_1, T_0, T_1, θ_0 and θ_1. Using these in (11), we get

$$q = (M_r - iM_i) + \in (L_r - iL_i)\ \exp\,(int) \tag{12}$$

$$T = \exp\,(-C_0 y) + \in (X_1 - iY_1)\ \exp\,(int) \tag{13}$$

$$\theta = (1 + d_1 S_0 S_c)\exp\,(-S_c y) - d_1 S_0 S_c \exp\,(-C_0 y) + \in (N_r - iN_i)\exp\,(int) \tag{14}$$

where $M_r = 1 - D_3 + a_4\,(G_r - G_m S_0 S_c)\exp\,(-C_0 y) + a_6\, G_m \exp\,(-S_c y)$

$$M_i = F_3 - b_4\,(G_r - G_m S_0 S_c)\exp\,(-C_0 y) + b_6 G_m \exp\,(-S_c y)$$

$$L_r = 1 - D_4 + G_r C_1 + (1 + d_1 S_0 S_c)\, G_m C_2 - E_3 G_m S_0 S_c \exp(-C_0 y)$$

$$L_i = F_4 + G_r D_1 + (1 + d_1 S_0 S_c)\, G_m D_2 - E_4 G_m S_0 S_c \exp(-C_0 y)$$

$$N_r = X_2 + (X_2 - X_1)\, e_3 S_0 S_c + e_4 S_0 S_c (Y_2 - Y_1)$$

$$N_i = Y_2 + (Y_2 - Y_1)\, e_3 S_0 S_c - e_4 S_0 S_c (X_2 - X_1)$$

$$(X_n, Y_n) = (\cos\beta_n y, \sin\beta_n y)\, \exp(-\alpha_n y) \qquad n = 1, 2$$

$$(C_n, D_n) = (A_n \cos\beta_n y \mp B_n \sin\beta_n y)\, \exp(-\alpha_n y) \qquad n = 1, 2, 3, 4$$

$$F_n = (B_n \cos\beta_n y - A_n \sin\beta_n y)\, \exp(-\alpha_n y) \qquad n = 3, 4$$

$$a_n = \alpha_n^2 - \beta_n^2 - \alpha_n - b_0 \qquad n = 1, 2$$

$$b_n = 2\alpha_n \beta_n - \beta_n + E_2 \qquad n = 1, 2$$

$$\alpha_1 = \frac{P_r}{2} + \frac{1}{2\sqrt{2}}\left[\sqrt{A_0^2 + B_0^2} + A_0\right]^{1/2}, \qquad \beta_1 = \frac{1}{2\sqrt{2}}\left[\sqrt{A_0^2 + B_0^2} - A_0\right]^{1/2}$$

$$\alpha_2 = \frac{S_c}{2} + \frac{1}{2\sqrt{2}}\left[S_c\sqrt{(1+n^2)} + S_c\right]^{1/2}, \qquad \beta_2 = \frac{1}{2\sqrt{2}}\left[S_c\sqrt{(1+n^2)} - S_c\right]^{1/2}$$

$$\alpha_3 = \frac{1}{2} + \frac{1}{2\sqrt{2}}\left[\sqrt{a_0^2 + n^2 b_0^2} + a_0\right]^{1/2}, \qquad \beta_3 = \frac{1}{2\sqrt{2}}\left[\sqrt{a_0^2 + n^2 b_0} - a_0\right]^{1/2}$$

$$\alpha_4 = \frac{1}{2} + \frac{1}{2\sqrt{2}}\left[\sqrt{a_0^2 + d_0^2} + a_0\right]^{1/2}, \qquad \beta_4 = \frac{1}{2\sqrt{2}}\left[\sqrt{a_0^2 + d_0^2} - a_0\right]^{1/2}$$

$$a_0 = 1 + \frac{4M}{1+m^2}, \qquad b_0 = \frac{M}{1+m^2}, \qquad d_0 = n + b_0, \qquad d_1 = \frac{C_0}{C_0 - S_c}$$

$$C_0 = P_r + \sqrt{A_0}, \qquad A_0 = P_r(P_r - 4S), \qquad B_0 = -nP_r, \qquad a_3 = C_0^2 - C_0 - b_0$$

$$b_3 = mb_0, \quad a_4 = \frac{a_3}{a_3^2 + b_3^2}, \quad b_4 = \frac{b_3}{a_3^2 + b_3^2}, \quad a_5 = d_1 a_4$$

$$b_5 = d_1 b_4, \quad a_6 = \frac{(1 + d_1 S_0 S_c) E_1}{E_1^2 + b_3^2}, \quad b_6 = \frac{(1 + d_1 S_0 S_c)\, b_3}{E_1^2 + b_3^2}, \quad E_1 = S_c^2 - S_c - b_0,$$

$$E_2 = b_3 - \frac{n}{4}, \quad E_3 = \frac{a_3}{a_3^2 + E_2^2}, \quad E_4 = \frac{E_2}{a_3^2 + E_2^2}, \quad e_1 = \alpha_1^2 - \beta_1^2 - S_c \alpha_1,$$

$$e_2 = 2\alpha_1 \beta_1 - S_c \beta_1 + \frac{n S_c}{4}, \qquad e_3 = \frac{(\alpha_1^2 - \beta_1^2)\, e_1 + 2 e_2 \alpha_1 \beta_1}{e_1^2 + e_2^2}$$

$$e_4 = \frac{2 e_1 \alpha_1 \beta_1 - (\alpha_1^2 - \beta_1^2)\, e_2}{e_1^2 + e_2^2}, \qquad A_3 = 1 - G_r a_4 + G_m (S_0 S_c a_5 - a_6)$$

$$B_3 = G_r b_4 - G_m (S_0 S_c b_5 - b_6), \qquad A_4 = 1 - A_1 G_r - A_2 G_m - G_m S_0 S_c (d_1 A_2 - E_3)$$

$$B_4 = B_1 G_r + B_2 G_m + G_m S_0 S_c (d_1 B_2 + E_4)$$

Shear Stress, Nusselt Number and Sherwood Number

The non-dimensional expressions for shear stress τ, rate of heat transfer in terms of Nusselt number Nu and rate of mass transfer in terms of Sherwood number Sh are

$$\tau = \left(\frac{\partial q}{\partial y}\right)_{y=0} \tag{15}$$

$$Nu = -\left(\frac{\partial T}{\partial y}\right)_{y=0} \tag{16}$$

$$Sh = -\left(\frac{\partial C}{\partial y}\right)_{y=0} \tag{17}$$

Table 1 – Transient primary (τ_p) and secondary (τ_s) shear stress.
($\in = 0.01$, $n = 10$, $P_r = 0.71$ and $nt = \pi/2$)

m	M	S	G_r	G_m	S_0	S_c	τ_p	τ_s
0.5	5.0	1.0	5.0	4.0	1.0	0.60	1.4695	0.6937
1.0	5.0	1.0	5.0	4.0	1.0	0.60	1.3932	0.7528
0.5	10.0	1.0	5.0	4.0	1.0	0.60	1.3887	0.5167
0.5	5.0	2.0	5.0	4.0	1.0	0.60	1.5482	0.6521
0.5	5.0	– 2.0	5.0	4.0	1.0	0.60	1.3817	0.7289
0.5	5.0	1.0	10.0	4.0	1.0	0.60	1.3548	0.5098
0.5	5.0	1.0	– 5.0	4.0	1.0	0.60	1.5897	0.7139
0.5	5.0	1.0	5.0	8.0	1.0	0.60	1.3482	0.4973
0.5	5.0	1.0	5.0	4.0	2.0	0.60	1.3466	0.4836
0.5	5.0	1.0	5.0	4.0	1.0	0.75	1.6183	0.6892

Table 2 – Primary (Nu_p) and secondary (Nu_s) Nusselt number.
($\in = 0.01$ and $nt = \pi/2$)

S	P_r	n	Nu_p	Nu_s
0.10	0.71	5.0	0.9236	1.0422
0.15	0.71	5.0	0.7815	1.0296
– 0.10	0.71	5.0	0.4921	1.1018
1.00	7.00	5.0	27.9842	6.2801
0.10	7.00	5.0	53.1879	7.1088
0.10	0.71	10.0	0.9208	1.3118
0.10	0.71	15.0	0.9187	1.5209

Table 3 – Transient primary (Sh_p) and secondary (Sh_s) Sherwood number.
($\in = 0.01, P_r = 0.71, n = 5.0$ and $nt = \pi/2$)

S_0	S_c	S	$10^{-2} \times Sh_p$	$10^{-2} \times Sh_s$
0.0	0.22	0.10	0.3358	0.5196
1.0	0.22	0.10	0.2895	0.4206
2.0	0.22	0.10	0.2433	0.3216
0.0	0.60	0.10	0.5548	0.9764
1.0	0.60	0.10	0.5384	0.9723
2.0	0.60	0.10	0.5331	0.9681
0.0	0.75	0.10	0.6199	1.1313
1.0	0.75	0.10	0.5621	1.2055
2.0	0.75	0.10	0.5042	1.2796
1.0	0.22	0.15	0.2855	0.4001
1.0	0.22	– 0.10	0.3001	0.3843
1.0	0.22	– 0.15	0.3053	0.3819

Discussion

To understand the physical depth of the problem, some numerical calculations are carried out for the non-dimensional primary velocity field (u) and secondary velocity field (w). To be realistic, the values of the Prandtl number (P_r) is chosen to be 0.71 and 7.00 which corresponds to water vapour and water respectively. The value of Schimdt number (S_c) is chosen to represent hydrogen (S_c = 0.22), water vapour (S_c = 0.60) and oxygen (S_c = 0.75) respectively. The values of Grashof number (Gr), modified Grashof number (Gm), Soret number (S_0), magnetic parameter (M), Hall parameter (m), heat source parameter (S) and frequency parameter (n) are chosen arbitrarily.

The variations of primary velocity (u) and secondary velocity (w) are shown in Fig. (1&2) respectively. A deep study of these figures reveals that (i) an increase in M leads to a decrease in primary velocity but an increase in secondary velocity. (ii) an increase in Soret number S_0 increases the primary velocity but decreases the secondary velocity. (iii) an increase in heat source parameter (absorption type) increases primary velocity but decreases the secondary velocity and *vice-versa* for generation type heat source parameter.

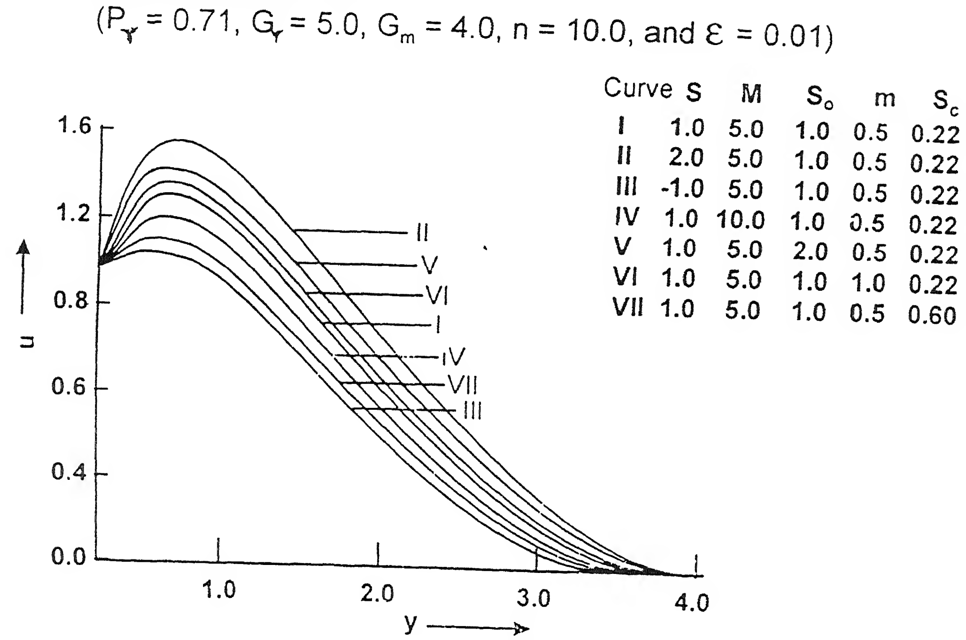

Fig. 1 – Primary velocity profiles.

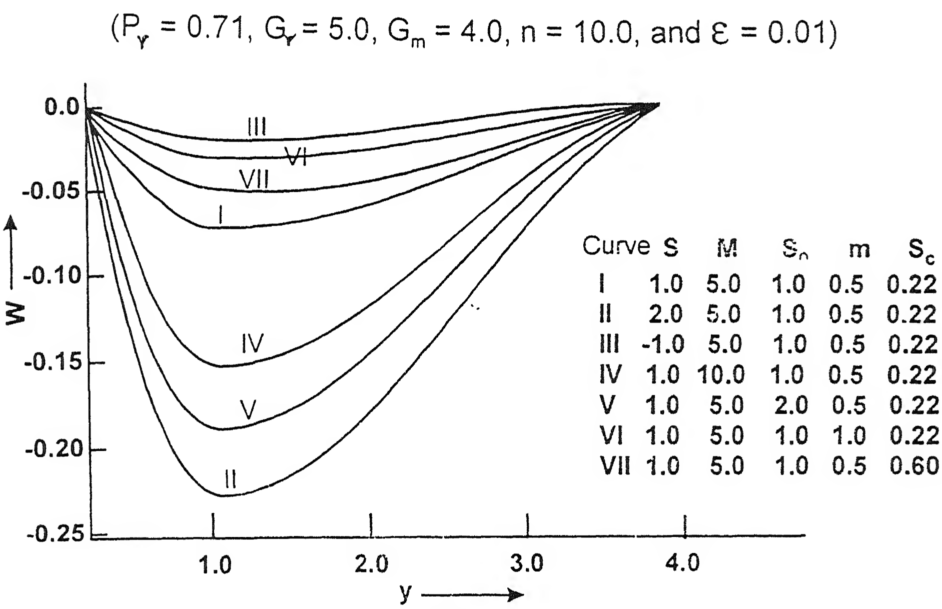

Fig. 2 – Secondary velocity profiles.

(iv) an increase in m increases primary as well as secondary velocity. (v) an increase in S_c decrease primary velocity but increases the secondary velocity.

The variations in non-dimensional transient primary and secondary shear-stress (denoted by τ_p and τ_s), rate of primary and secondary heat transfer in terms of Nusselt number (denoted by Nu_p , Nu_s), transient primary and secondary mass transfer rate (denoted by Sh_p and Sh_s) are shown in Tables 1, 2 and 3 respectively. The conclusion regarding the behaviour of the parameters on shear-stress, Nusselt number and the Sherwood number are self evident from the tables. Therefore any further discussion about them seems to be redundant.

References

1. Gebhart, B. & Pera, L. (1971) *Int. J. Heat Mass Transfer* **14** : 957.
2. Gebhart, B. & Pera, L. (1971) *Int. J. Heat Mass Transfer* **14** : 2025.
3. Gebhart, B. & Pera, L. (1973) Int. J. Heat Mass Transfer **16** : 1131.
4. Gebhart, B. & Pera, L. (1973) *Int. J. Heat Mass Transfer* **16** : 1147.
5. Nanousis, N.D., Kafoussias, N.G. & Georgantapoulos, G.A. (1979) *Astrophys. Space. Sci.* **64** : 391.
6. Singh, A.K. (1982) *Astrophys. Space. Sci.,* **87** : 455.
7. Raptis, A.A. & Perdikis, C.P. (1982) *Atrophys Space. Sci.* **84** : 457.
8. Eckert, E.R.C. & Drake, R.M. (1972) *Analysis of Heat and Mass Transfer.* Mc GrawHill Co., New York.
9. Jha, B.K. & Singh, A.K. (1990) *Atrophys. Space. Sci.* **173** : 251.
10. Kafoussias, N.G. (1992) *Astrophys. Space. Sci.* **192** : 11.
11. Sattar, M.A. & Alam, M.M. (1995) *Ind. J. Theo. Phys.* **43** : 169.
12. Singh, N.P. & Singh, Ajay Kumar *Bull. Cal. Math. Soc.* (Communicated).
13. Meyer, R.C. (1958) *J. Aero/Space Sci.* **25** : 561.
14. Jha, B.K. (1991) *Int. J. Energy Res.* **15** : 79.

PROC. NAT. ACAD. SCI. INDIA, 71 (A), III, 2001

Unsteady flow of visco-elastic Oldroyd fluid with transient pressure gradient through a rectangular channel

SHYAMAL KUMAR KUNDU and P.R. SENGUPTA

Indian Institute of Mechanics of Continua, 201 Manicktala Main Road, Suit No. 42, Calcutta-700054, India

Received August 31, 1999; Revised February 16, 2000; Accepted May 3, 2000

Abstract

The aim of this paper is to investigate the flow of visco-elastic Oldroyd fluid with transient pressure gradient through a rectangular channel. Firstly, the first order Oldroyd fluid has been considered. Secondly, the authors propose a second order Oldroyd fluid and investigate the same problem in this new visco-elastic model. The numerical computation of the velocity profiles have been presented for both the first and second order fluids in the form of tables and graphs. The result for visco-elastic Maxwell fluid and purely viscous fluid have been determined from the first order Oldroyd fluid simply by passing to the limit as $\mu_1 \rightarrow 0$ (Maxwell fluid) and $\lambda_1 \rightarrow 0,\ \mu_1 \rightarrow 0$ (purely viscous fluid). Finally a new generalized model of visco-elastic fluid has been proposed.

(Keywords : visco-elastic Oldroyd fluid/unsteady flow/transient pressure gradient/rectangular channel/generalized visco-elastic fluid)

Introduction

In the classical theory of viscous flow tremendous development have been observed as evidenced by the informative monographs of Lamb[1] and various other authors[2-7]. In recent years the development of new areas of fluid mechanics are very remarkable. For this one may refer to the review literature[8-10] in connection with non-Newtonian fluids, polymeric liquids and visco-elastic liquids of different types. Moreover some interesting problems in this area have been investigated by Sengupta and his research collaborators[11-17].

Basic Theory and Equations of Motions for First Order Oldroyd Fluid

For slow motion, the rheological equations for Oldroyd visco-elastic fluid are

$$\tau_{ij} = -p'\delta_{ij} + \tau_{ij}'$$

$$\left(1+\lambda_1' \frac{\partial}{\partial t'}\right) \tau_{ij}' = 2\mu \left(1+\mu_1' \frac{\partial}{\partial t'}\right) e_{ij}$$

$$e_{ij} = \frac{1}{2} (v_{i,j} + v_{j,i})$$

where τ_{ij} is the stress tensor, τ_{ij}' is the deviatoric stress tensor, e_{ij} the rate of strain tensor, p' the pressure, λ_1' the stress relaxation time parameter, μ_1' the strain rate retardation time parameter, δ_{ij} the metric tensor in cartesian co-ordinates and μ, the co-efficient of viscosity and v_i the velocity components.

Let us now consider the walls of the rectangular channel to be the planes $x' = \pm a$ and $y' = \pm b$ where z'-axis is taken towards the direction of motion. 0, 0, $w'(x', y', t')$ are respectively the velocity components along x', y', z' directions where $w'(x', y', t')$ is axial velocity of the fluid. A transient pressure gradient $-Pe^{-\omega' t'}$ varying with time is applied to the fluid.

Following the stress-strain relations, the equation for unsteady motion is given by

$$\left(1+\lambda_1' \frac{\partial}{\partial t'}\right) \frac{\partial w'}{\partial t'} = -\frac{1}{\rho}\left(1+\lambda_1' \frac{\partial}{\partial t'}\right) \frac{\partial p'}{\partial z'} + \nu \left(1+\mu_1' \frac{\partial}{\partial t'}\right) \nabla^2 w' \tag{1}$$

Introducing the non-dimensional quantities

$$w = w' \frac{a}{\nu},\; p = p' \frac{a^2}{\rho \nu^2},\; t = t' \frac{\nu}{a^2},\; \omega = \omega' \frac{a^2}{\nu},\; (x, y, z) = \frac{1}{a}(x', y', z'),$$

$$\lambda_1 = \lambda_1' \frac{\nu}{a^2},\; \mu_1 = \mu_1' \frac{\nu}{a^2}.$$

eqn. (1) becomes

$$\left(1+\lambda_1 \frac{\partial}{\partial t}\right) \frac{\partial w}{\partial t} = -\left(1+\lambda_1 \frac{\partial}{\partial t}\right) \frac{\partial p}{\partial z} + \left(1+\mu_1 \frac{\partial}{\partial t}\right) \nabla^2 w \tag{2}$$

We have considered those type of situations of the flow which is transient in nature with respect to time and periodic in nature with respect to y. From the nature of the boundary conditions we have chosen the solution of (2) as

$$w = W(x) \cos mye^{-\omega t} \tag{3}$$

The boundary conditions of the fluid are

(i) $W = 0$ when $x = \pm 1, -\frac{b}{a} \le y \le \frac{b}{a}$ (4)

(ii) $w = 0$ when $y = \pm \frac{b}{a}, -1 \le x \le 1$ (5)

Condition (5) will be satisfied if $\cos m \frac{b}{a} = 0$

$$\text{or} \qquad m = (2n+1) \frac{\pi a}{2b} \quad n = 0, 1, 2, 3 \ldots\ldots \tag{6}$$

We construct the solution as the sum of all possible solutions for each value of n.

$$w = \sum_{n=0}^{\infty} W(x) \cos mye^{-\omega t} \tag{7}$$

By putting $\frac{\partial p}{\partial z} = -Pe^{-\omega t}$ $(\omega > 0)$ in (2) and using (7), we get,

$$\sum_{n=0}^{\infty} \left\{ \frac{d^2 W(x)}{dx^2} - m^2 W(x) \right\} \text{cosmy} + \sum_{n=0}^{\infty} \frac{\omega(1-\lambda_1 \omega)}{(1-\mu_1 \omega)} W(x) \cos my + \frac{P(1-\lambda_1 \omega)}{(1-\mu_1 \omega)} = 0$$

and equating the co-efficient of cos my equal to zero, the value of W can be determined from

$$\frac{d^2 W}{dx^2} - \frac{K^2}{a^2} W + A_n = 0 \tag{9}$$

where
$$\left.\begin{aligned} A_n &= \frac{(-1)^n}{(2n+1)} \frac{4P(1-\lambda_1\omega)}{\pi(1-\mu_1\omega)} \\ K^2 &= \left\{m^2 - \frac{\omega(1-\lambda_1\omega)}{(1-\mu_1\omega)}\right\} a^2 \end{aligned}\right\} \tag{10}$$

Using the boundary condition (4), the solution is

$$W(x) = \frac{(-1)^n}{(2n+1)} \frac{4P(1-\lambda_1\omega)}{\pi(1-\mu_1\omega)K^2} \left\{1 - \frac{\cosh \frac{K}{a} x}{\cosh \frac{K}{a}}\right\}$$

So the velocity of the fluid is given by

$$W(x, y, t) = \sum_{n=0}^{\infty} \left[\frac{(-1)^n}{(2n+1)} \frac{4P(1-\lambda_1\omega)}{\pi(1-\mu_1\omega)K^2} \left\{1 - \frac{\cosh \frac{K}{a} x}{\cosh \frac{K}{a}}\right\}\right] e^{-\omega t} \cos(2n+1) \frac{\pi a y}{2b} \tag{11}$$

Basic Theory and Equations of Motions for Second Order Oldroyd Fluid

For slow motion, the rheological equations for second order Oldroyd visco-elastic fluid are

$$\tau_{ij} = -p' \delta_{ij} + \tau_{ij}'$$

$$\left(1 + \lambda_1' \frac{\partial}{\partial t'} + \lambda_2' \frac{\partial^2}{\partial t'^2}\right) \tau_{ij}' = 2\mu \left(1 + \mu_1' \frac{\partial}{\partial t'} + \mu_2' \frac{\partial^2}{\partial t'^2}\right) e_{ij}$$

$$e_{ij} = \frac{1}{2} (v_{i,j} + v_{j,i})$$

where τ_{ij} is the stress tensor, τ_{ij}' is the deviatoric stress tensor, e_{ij} the rate of strain tensor, p' the pressure, λ_1' the stress relaxation time parameter, μ_1' the strain rate retardation time parameter, λ_2' is the additional material constant, μ_2' is the additional material constant, δ_{ij} the metric tensor in cartesian co-ordinates and μ, the co-efficient of viscosity and v_i the velocity components.

Let us now consider the walls of the rectangular channel to be the planes $x' = \pm a$ and $y' = \pm b$ where z'-axis is taken towards the direction of motion. 0, 0, $w'(x', y', t')$ are

respectively the velocity components along x', y', z' directions where $w'(x', y', t')$ is axial velocity of the fluid. A transient pressure gradient $-Pe^{-\omega' t'}$ varying with time is applied to the fluid.

Following the stress-strain relations, the equation for unsteady motion is given by

$$\left(1+\lambda_1'\frac{\partial}{\partial t'}+\lambda_2'\frac{\partial^2}{\partial t'^2}\right)\frac{\partial w'}{\partial t'} = -\frac{1}{\rho}\left(1+\lambda_1'\frac{\partial}{\partial t'}+\lambda_2'\frac{\partial^2}{\partial t'^2}\right)\frac{\partial p'}{\partial z'}+$$

$$+\,\nu\left(1+\mu_1'\frac{\partial}{\partial t'}+\mu_2'\frac{\partial^2}{\partial t'^2}\right)\nabla^2 w' \qquad (12)$$

Introducing the non-dimensional quantities in eqn. (12)

$$w = w'\frac{a}{\nu},\ p = p'\frac{a^2}{\rho\nu^2},\ t = t'\frac{\nu}{a^2},\ \omega = \omega'\frac{a^2}{\nu},\ (x, y, z) = \frac{1}{a}(x', y', z'),$$

$$\lambda_1 = \lambda_1'\frac{\nu}{a^2},\ \mu_1 = \mu_1'\frac{\nu}{a^2},\ \lambda_2 = \lambda_2'\frac{\nu^2}{a^4},\ \mu_2 = \mu_2'\frac{\nu^2}{a^4}$$

eqn. (12) becomes

$$\left(1+\lambda_1\frac{\partial}{\partial t}+\lambda_2\frac{\partial^2}{\partial t^2}\right)\frac{\partial w}{\partial t} = -\left(1+\lambda_1\frac{\partial}{\partial t}+\lambda_2\frac{\partial^2}{\partial t^2}\right)+\nu\left(1+\mu_1\frac{\partial}{\partial t}+\mu_2\frac{\partial^2}{\partial t^2}\right)\nabla^2 w \qquad (13)$$

Solution of the Problem

Let us assume the solution of (13) as

$$w = W(x)\ \cos mye^{-\omega t}$$

Here we have used the same boundary conditions of the fluid given by (4) and (5) and used the relation (6).

We construct the solution as the sum of all possible solutions for each value of n.

$$w = \sum_{n=0}^{\infty} W(x) \cos my e^{-\omega t} \tag{14}$$

Using (14) and putting $\frac{\partial p}{\partial z} = -Pe^{-\omega t}$ $(\omega > 0)$ in (13), we get,

$$\sum_{n=0}^{\infty} \left\{ \frac{d^2 W(x)}{dx^2} - m^2 W(x) \right\} \cos my + \sum_{n=0}^{\infty} \frac{\omega(1 - \lambda_1 \omega + \lambda_2 \omega^2)}{(1 - \mu_1 \omega + \mu_2 \omega^2)} W(x) \cos my +$$

$$\frac{P(1 - \lambda_1 \omega + \lambda_2 \omega^2)}{(1 - \mu_1 \omega + \mu_2 \omega^2)} = 0 \tag{15}$$

If we express $\frac{P(1 - \lambda_1 \omega + \lambda_2 \omega^2)}{(1 - \lambda_1 \omega + \lambda_2 \omega^2)}$ as a Fourier cosine series in the interval of $-\frac{b}{a} \le y \le \frac{b}{a}$ and equate the co-efficient of cos my to zero, the value of W can be determined from $\frac{d^2 W}{dx^2} - \frac{K^2}{a^2} W + A_n = 0$

where

$$A_n = \frac{(-1)^n}{(2n+1)} \frac{4P(1 - \lambda_1 \omega + \lambda_2 \omega^2)}{\pi (1 - \mu_1 \omega + \mu_2 \omega^2)}$$

$$K^2 = \left\{ m^2 - \frac{\omega(1 - \lambda_1 \omega + \lambda_2 \omega^2)}{(1 - \mu_1 \omega + \mu_2 \omega^2)} \right\} a^2$$

We now obtain the solution by using the boundary condition (4) as follows

$$W(x) = \frac{(-1)^n}{(2n+1)} \frac{4P(1 - \lambda_1 \omega + \lambda_2 \omega^2)}{\pi (1 - \mu_1 \omega + \mu_2 \omega^2) K^2} \left\{ \frac{1 - \cosh \frac{K}{a} x}{\cosh \frac{K}{a}} \right\}$$

So the velocity of the fluid is given by

$$w(x, y, t) = \sum_{n=0}^{\infty} \left[\frac{(-1)^n}{(2n+1)} \frac{4P(1 - \lambda_1\omega + \lambda_2\omega^2)}{\pi(1 - \mu_1\omega + \mu_2\omega^2) K^2} \left\{ 1 - \frac{\cosh \frac{K}{a} x}{\cosh \frac{K}{a} x} \right\} \right] e^{-\omega t} \cos(2n+1) \frac{\pi ay}{2b} \quad (16)$$

Deduction

Case I : If we put $\mu_1 = 0$ in the eqn. (11), we shall obtain Maxwell fluid which is given below

$$W(x, y, z) = \sum_{n=0}^{\infty} \left[\frac{(-1)^n}{(2n+1)} \frac{4P(1 - \lambda_1\omega)}{\pi K^2} \left\{ 1 - \frac{\cosh \frac{K}{a} x}{\cosh \frac{K}{a}} \right\} \right] e^{-\omega t} \cos(2n+1) \frac{\pi ay}{2b}$$

where $K^2 = \{m^2 - \omega(1 - \lambda_1\omega)\} a^2$

Case II : Putting $\mu_1 = 0$ and $\lambda_1 = 0$ in the eqn. (11), we shall obtain purely viscous fluid which is given below :

$$w(x, y, t) = \sum_{n=0}^{\infty} \left[\frac{(-1)^n}{(2n+1)} \frac{4P}{\pi K^2} \left\{ 1 - \frac{\cosh \frac{K}{a} x}{\cosh \frac{K}{a}} \right\} \right] e^{-\omega t} \cos(2n+1) \frac{\pi ay}{2b}$$

where $K^2 = (m^2 - \omega) a^2$

Numerical Calculation and Discussion

For numerical calculation of the velocity for Oldroyd first and second order fluid given by the eqn. (11) and (16) we take $\lambda_1 = 0.0023$, $\mu_1 = 0.0005$, $a = 0.5$, $b = 0.25$, $x = 0.75$, $y = 0.45$, $\omega = 10$, $m = 10$, $P = 8$, $\lambda_2 = 0.000023$, $\mu_2 = 0.000005$.

The velocity of a fluid element starts with a maximum value initially and thereafter it gradually diminishes asymptotically to a vanishingly small value as time advances and tends to infinity. It is represented in the forms of tables and graphs.

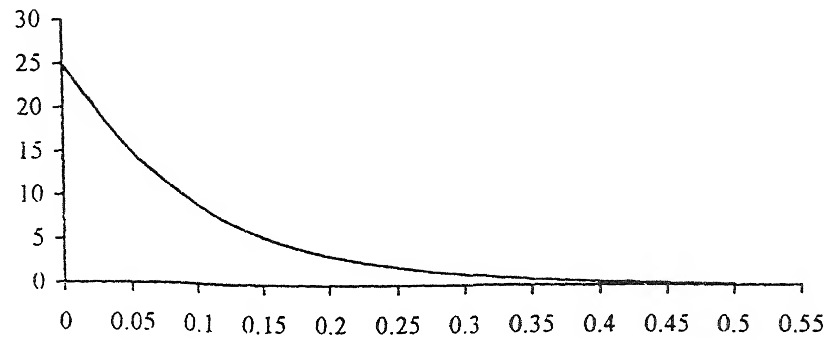

Fig. 1 – Velocity profile for first order Oldroyd fluid.

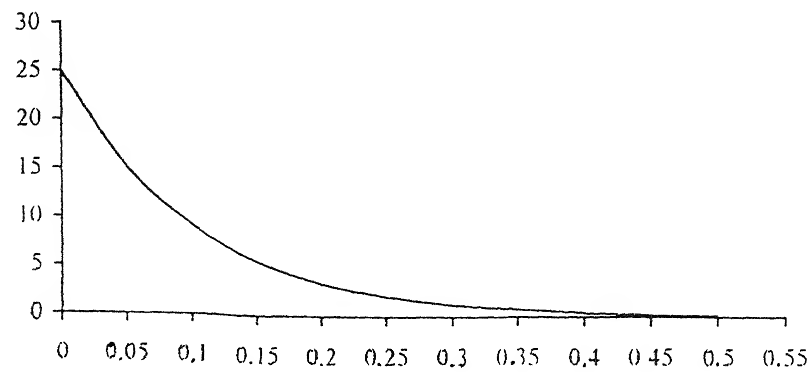

Fig. 2 – Velocity profile for second order Oldroyd fluid

	Table 1	Table 2
	Oldroyd fluid	Oldroyd fluid
	(1st Order)	(2nd Order)
t	W (x, y, t)/A	W (x, y, t)/A
0	24.8646136	24.9189382
0.05	15.0811504	15.1141
0.1	9.1471801	9.167165
0.15	5.5480452	5.5601666
0.2	3.3650595	3.3724115
0.25	2.0410117	2.045471
0.3	1.2379362	1.2406408
0.35	0.7508462	0.7524867
0.4	0.4554112	0.4564062
0.45	0.2762209	0.2768243
0.5	0.1675364	0.1679024

A General Visco-Elastic Model of Liquid

A new general empirical model of visco-elastic fluid has been suggested by one of the authors (P.R.S.) in the following form[18-20]

$$\tau_{ij} = -p\,\delta_{ij} + \tau_{ij}'$$

$$\left(1 + \sum_{j=1}^{n} \lambda_j \frac{\partial^j}{\partial t^j}\right) \tau_{ij}' = 2\mu \left(1 + \sum_{j=1}^{n} \mu_j \frac{\partial^j}{\partial t^j}\right) e_{ij}$$

$$e_{ij} = \frac{1}{2}\,(v_{i,j} + v_{j,i})$$

where τ_{ij} is the stress tensor, τ_{ij}' is the deviatoric stress tensor, e_{ij} the rate of strain tensor, p the fluid pressure, λ_j are new material constants of which the greatest value λ_1 represents the relaxation time parameter and λ_2, λ_3, ..., λ_n are additional material constants; μ_j are also new material constants of which the greatest value μ_1 represents the strain rate retardation time parameter and μ_2, μ_3, ... μ_n are additional material constants representing

the behaviour of a very wide class of visco-elastic liquids δ_{ij} the metric tensor in cartesian co-ordinates and μ, the co-efficient of viscosity and v_i the velocity components. The material constants λ_j and μ_j designating visco-elasticity satisfy the following conditions $\lambda_1 > \lambda_2 > \lambda_3 > .... > \lambda_n$ and $\mu_1 > \mu_2 > \mu_3 > .... > \mu_n$ i.e. they are arranged in descending order of magnitudes. These rheological equations are concerned with the description of the mechanical properties of numerous materials under various deformation conditions when the materials exhibit the ability to flow the accumulative recoverable deformations. In fact, materials satisfying elasticity of solids and viscosity of liquids fall into this category.

References

1. Lamb, H. (1945) *Hydrodynamics,* Dover Publication, New York.
2. Thomson, L.M. Milne (1962) *Antiplane Elastic System,* Academic Press, New York.
3. Gold Stein, S. (ed) (1938) *Modern Development in Fluid Dynamics,* 2 vols. Oxford University, New York.
4. Batchelor, G.K. (1967) *An Introduction to Fluid Dynamics,* Cambridge University Press.
5. Landau, I.D. & Lifshitz, E.M. (1959) *Theory of Elasticity,* Pergamon, London.
6. Kapur, J.N. & Shukla, J.B. (1962), *ZAMM* **44** : 268.
7. Huilgol, R.R. & Phan-Thien, N. (1997) *Fluid Mechanics of Visco Elasticity,* Elsevier, New York.
8. Kapur, J.N., Bhatt, B.S. & Sacheti, N.C. (1992) *Non-Newtonian Fluid Flows,* Pragati Prakashan, India.
9. Joseph, D.D. (1989) *Fluid Dynamics of Visco-Elastic Liquids.* University of Minnesota Minneapolis, MN Springer-Verlag, London.
10. Bhatnagar, P.L. (1967) *The Summer Seminar in Fluid Mechanics,* Department of Applied Mathematics, Indian Institute of Science, Bangalore, India.
11. Panja, S., Banerjee, M. & Sengupta, P.R. (1994) *Rev. Roum. Sci. Tech. Mec., Appl., Tome 39,* Bucharest, No. 4, p. 421.
12. Chakraborty, G. & Sengupta, P.R. (1994) *Rev. Roum. Sci. Tech. Mec. Appl. Tome 39,* Bucharest No. 6, p. 635.
13. Das, K.K. & Sengupta, P.R. (1993) *Proc. Nat. Acad. Sci., India* **63A** : 411.
14. Ghosh, B.C. & Sengupta, P.R. (1993) *Proc. Math. Soc. BHU* **9** : 89.
15. Sengupta, P.R. & Raymahapatra, J. (1971) *Rev. Roum. Sci. Tech. Mec. Appl. Tome 16,* Bucharest, No/ 5, p. 1023.
16. Chakraborty, G. & Sengupta, P.R. (1992) *Czechoslovak Jour. of Phys.* **42(5)** : 525.
17. Sengupta, P.R. & Roy, T.K. (1990) *Warsaw Arch. Mech. STOS* **42(6)** : 717.
18. Sengupta, P.R. & Kundu, S.K. (1999) *Proc. National Symposium,* Math. Dept., Kalyani University, p. 93.
19. Sengupta, P.R. & Kundu, S.K. (1999) *Jour. Pure & Applied Phys.* **11(2)** : 57.
20. Sengupta, P.R. & Kundu, S.K. (1999) *Proc. 4th ICOVP,* Jadavpur University, India.

PROC. NAT. ACAD. SCI. INDIA, 71 (A), III, 2001

Fluctuating free convective flow with radiation through porous medium having variable permeability

S.S. TAK and ARVIND MAHARSHI

Department of Mathematics and Statistics, J.N.V. University, Jodhpur-342001, India.

Received July 13, 1999; Revised July 10, 2000; Accepted August 16, 2000

Abstract

The object of the paper is to present a theoretical analysis of free convective two dimensional unsteady flow with radiation through a porous medium of variable permeability, bounded by an infinite vertical porous plate with uniform suction. The permeability of porous medium fluctuates with time about a constant mean. Using perturbation method, the expressions for velocity, temperature and skin-friction are obtained and the effects of radiation, variable permeability and Prandtl number on velocity, temperature and skin-friction amplitude and phase are presented graphically. It is found that the velocity decreases with radiation parameter and Prandtl number but increases with permeability.

Introduction

Raptis *et al.*[1] studied the steady free convective flow through porous medium bounded by an infinite plate. The same problem, when there is a constant heat flux on the plate, was studied by Raptis *et al.*[2] Thereafter, Raptis[3] and Raptis and Predikis[4] studied unsteady flow through porous medium, when the temperature of porous plate oscillates in time about a constant mean. In above problems, the permeability of porous medium was assumed to be constant. In fact, a porous material containing the fluid is a non homogeneous medium and the inhomogeneties which can be present in porous medium are numerous. Thus taking permeability variations into consideration, Chandrasekhara *et al.*[5] and Vedha Nayagam *et al.*[6] have studied the buoyancy induced flow behaviour adjacent to a horizontal surface in a porous medium. Singh *et al.*[7] and Singh and Suresh Kumar[8] have studied the effects of permeability variation on free convective flow through a porous medium bounded by an infinite vertical porous plate with constant suction. When the temperature of the plate is high, the radiation effects are not negligible. Recently, the effect of radiation and magnetic field on the free convective flow along semi-infinite vertical plate bounded by non-porous medium has been studied by Takhar *et al.*[9]

The purpose of this paper is to study the effects of radiation and permeability variation on free convective flow through porous medium bounded by an infinite porous plate with uniform suction.

It has been pointed out by Rudraiah *et al.*[10] that the results of this type of problem are of interest in metal production, underground bed flow, oil recovery from partially depleted reservoirs, agriculture engineering and various applications in chemical engineering.

Analysis

Consider the free convective flow of grey gas, near equilibrium in the optically thin limit, through a porous medium bounded by an infinite vertical plate with constant suction. The plate is maintained at constant temperature T_w' and T_∞' is the temperature of the fluid far away from the plate. The x' axis is taken along the plate and y' axis normal to it. The flow in the medium is entirely due to buoyancy force caused by temperature difference between the wall and the fluid. Neglecting the viscous dissipation and Darcy's dissipation temrs, the flow can be shown to be governed by the following equations :

$$\frac{\partial v'}{\partial y'} = 0 \tag{1}$$

$$\frac{\partial u'}{\partial t'} + v' \frac{\partial u'}{\partial y'} = g\beta\,(T' - T_\infty') + \nu \frac{\partial^2 u'}{\partial y'^2} - \frac{\nu}{k'(t')}\, u' \tag{2}$$

and

$$\frac{\partial T'}{\partial t'} + v' \frac{\partial T'}{\partial y'} = \frac{K}{c_p\rho} \cdot \frac{\partial^2 T'}{\partial y'^2} - \frac{1}{\rho c_p} \cdot \frac{\partial q_r'}{\partial y'} \tag{3}$$

where u' and v' are components of velocity along x' and y' directions, g the acceleration due to gravity, β the coefficient of volume expansion, T' the temperature. ρ, ν, k, c_p respectively are density, kinemetic viscosity, thermal conductivity and specific heat of the fluid at constant pressure. k' and q_r' are permeability and heat flux respectively.

Following work of other workers[5–8] the permeability of the porous medium is assumed to be of the form

$$k'(t') = k_0'\,(1 + \in e^{iw't'}) \tag{4}$$

where k_0' is the mean permeability of the medium, w' is the frequency of fluctuation, t' is the time and $\in$ (<< 1) is a constant quantity.

Cogley *et al.*[11] showed that in the flow of grey gas near equilibrium in the opticlly thin limit, the radiative heat flux q_r' is given by

$$\frac{\partial q_r'}{\partial y'} = 4\,(T' - T_\infty')\; I' \tag{5}$$

where $I' = \int_0^\infty k_{\lambda w} \frac{\partial e_{b\lambda}}{\partial T'}\, d\lambda$, $k_{\lambda w}$ is the absorption coefficient at the wall and $e_{b\lambda}$ is Planck function.

The relation (5) has been used by many authors including Tekhar *et al.*[11] and Grief *et al.*[12]

The boundary conditions are

$$\begin{aligned} y' = 0 \;&:\; u' = 0, \quad T' = T_w' \\ y' \to \infty \;&:\; u' = 0, \quad T' = T_\infty' \end{aligned} \tag{6}$$

Integration of eqn. (1) gives

$$v' = -\, v_0$$

where $v_0 > 0$ is a constant with dimensions of velocity and negative sign indicates that the suction is towards the plate.

Introducing the following non-dimensional quantities :

$$y = y'\, v_0 / \nu \quad t = t'\, v_0^2 / 4\nu\,, \quad w = 4\nu\, w' / v_0^2\,,$$

$$u = u' / v_0\,, \quad \theta = (T' - T_\infty') / (T_w' - T_\infty')\,,$$

the eqn. (2) and (3) in view of (4) and (5), reduce to the following form

$$\frac{1}{4}\frac{\partial u}{\partial t} - \frac{\partial u}{\partial y} = Gr\,.\,\theta + \frac{\partial^2 u}{\partial y^2} - \frac{u}{k_0\,(1 + \in\, e^{iwt})} \tag{7}$$

$$\frac{1}{4}\frac{\partial \theta}{\partial t} - \frac{\partial \theta}{\partial y} = \frac{1}{Pr}\frac{\partial^2 \theta}{\partial y^2} - F\,.\,\theta \tag{8}$$

where

$$Gr = \frac{\nu\, g\, \beta\, (T_w' - T_\infty')}{v_0^3}, \quad \text{(Grashoff number)}$$

$$Pr = \mu \,.\, c_p / k, \quad \text{(Prandtl number)}$$

$$k_0 = k_0'\; v_0^2 / \nu^2 , \quad \text{(Permeability parameter)}$$

and

$$F = 4\, \nu\, I' / \rho \,.\, c_p \,.\, v_0^2 \quad \text{(Radiation parameter)}$$

The corresponding boundary conditions become

$$y = 0 : u = 0, \; \theta = 1 ,$$

$$y \to \infty : u = 0, \; \theta = 0 . \tag{9}$$

The partial differential eqn. (7) and (8) are reduced to ordinary one by assuming the following series expressions for velocity and temperature.

$$u\,(y, t) = u_0\,(y) + \in\, e^{iwt}\, u_1\,(y) + \ldots\ldots \tag{10}$$

$$\theta\;(y, t) = \theta_0\,(y) + \in\, e^{iwt}\, \theta_1\,(y) + \ldots\ldots. \tag{11}$$

Substituting eqn. (10) and (11) in eqn. (7) and (8) and equating the coefficients of like powers of $\in$ to zero, the following set of ordinary differential equations are obtained :

$$u_0'' + u_0' - \frac{1}{k_0}\, u_0 = -\, Gr \,.\, \theta_0 \tag{12}$$

$$u_1'' + u_1' - \left(\frac{iw}{4} + \frac{1}{k_0}\right) u_1 = -\, Gr \,.\, \theta_1 - \frac{1}{k_0}\, u_o \tag{13}$$

$$\frac{1}{Pr}\, \theta_0'' + \theta_0' - F \,.\, \theta_0 = 0 \tag{14}$$

$$\frac{1}{Pr}\, \theta_1' - \left(F + \frac{iw}{4}\right) \theta_1 = 0 \tag{15}$$

where the primes denote differentiation with respect to y.

The boundary conditions become

$$y = 0 : u_0 = 0,\ u_1 = 0,\ \theta_0 = 1,\ \theta_1 = 0\,,$$

$$y \to \infty : u_0 = 0,\ u_1 = 0,\ \theta_0 = 0,\ \theta_1 = 0\,. \tag{16}$$

Eqn. (12) to (15) are second order linear differential equations with constant coefficients, the solutions of which are straightforward. Solutions of (12) to (15), satisfying the boundary conditions (16), are substituted in eqn. (10) and (11), to give

$$u\,(y, t) = \frac{Gr}{P_1}\left[(e^{-r_1 y} - e^{-ay}) + \frac{\in\, e^{iwt}}{k_0}\left\{\frac{4i}{w}\,(e^{-r_2 y} - e^{-r_1 y}\right\}\right.$$

$$\left. - \frac{1}{\left(P_1 - \dfrac{iw}{4}\right)}\,(e^{-r_2 y} - e^{-ay})\right] \tag{17}$$

$$\theta\,(y, t) = e^{-ay} \tag{18}$$

where, $P_1 = a^2 - a - \dfrac{1}{k_0}$,

$$a = \left[Pr + \sqrt{(Pr^2 + 4Pr\,.\,F)}\right]/\,2\,, \tag{19}$$

$$r_1 = [1 + \sqrt{(1 + 4/k_0)}]\,/\,2\,,$$

$$r_2 = [1 + \sqrt{(1 + 4/k_0) + iw}]\,/\,2$$

It may be noted here that when radiation parameters, $F = 0$, the above solutions reduce to the solutions obtained by Singh and Kumar[8].

Taking the real part of the above solutions, the velocity field can be expressed in tems of fluctuating parts as

$$u\,(y, t) = u_0\,(y) + \in (M_r \cos wt - M_i \sin wt) \tag{20}$$

where $$M_r + i M_i = u_1(y)$$

and $$M_r = e^{-(1+\alpha)y/2}\left[(A-C)\sin\frac{\beta y}{2} - B\cos\frac{\beta y}{2}\right] + B\,e^{-ay},$$

$$M_i = e^{-(1+\alpha)y/2}\left[(A-C)\cos\frac{\beta y}{2} - B\sin\frac{\beta y}{2}\right] + Ce^{-ay} - Ae^{-r_1 y}$$

$$\alpha = \left[\frac{(1+4/k_0) + \sqrt{(1+4/k_0)^2 + w^2}}{2}\right]^{1/2},$$

$$\beta = \left[\frac{-(1+4/k_0) + \sqrt{(1+4/k_0)^2 + w^2}}{2}\right]^{1/2},$$

$$A = 4Gr/k_0\; P_1\; w\,,\quad B = 16Gr/k_0\;(16P_1^2 + w^2)\,,$$

$$C = 4Gr\,.\,w/k_0\; P_1\;(16P_1^2 + w^2)\,.$$

The expression for the transient velocity, for $wt = \frac{\pi}{2}$, is given by

$$u(y,\; \pi/2w) = u_0(y) - \epsilon\; M_1\,.$$

The fluctuating parts M_r, M_i and the transient velocity for $wt = \frac{\pi}{2}$ have been plotted in Fig. (1 & 2) respectively.

Skin friction : The skin-friction at the plate in terms of its amplitude and phase can now be calculated from eqn. (20), as

$$C_f = \frac{\tau_w}{\rho\,.\,v_0^2} = \left(\frac{\partial u}{\partial y}\right)_{y=0} = \frac{Gr}{P_1}\,(a - r_1) + \epsilon\;|N|\;\cos\,(wt + \alpha)$$

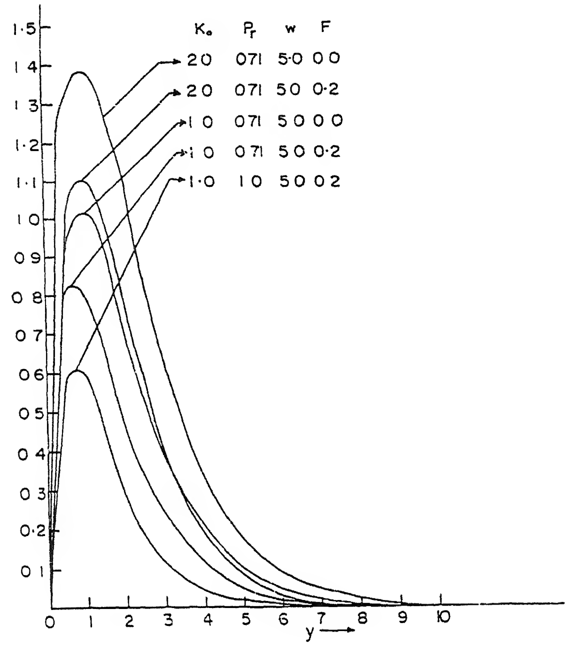

Fig. 1 – The velocity profiles for different values of K_0, Pr, W and F for $wt = \pi/2$.

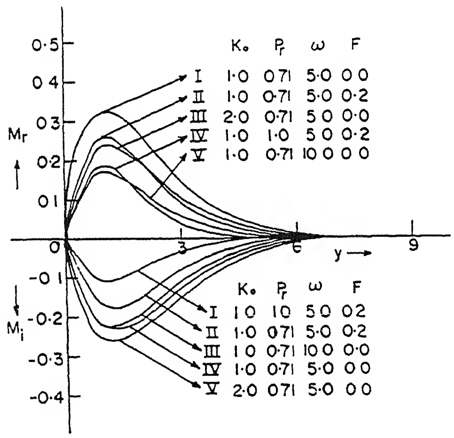

Fig. 2 – Fluctuating parts of velocity profiles.

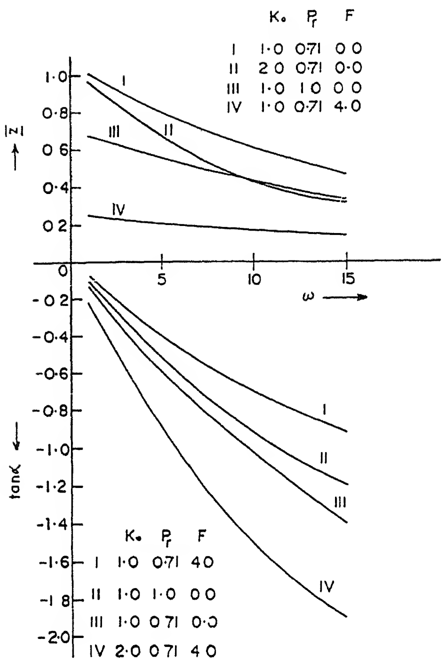

Fig. 3 – The phase and amplitude of the skin friction

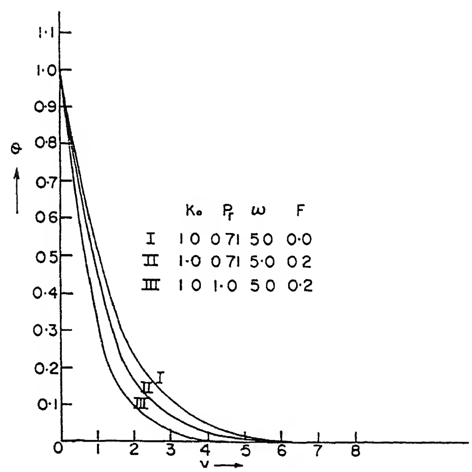

Fig. 4 – The temperature profiles for different values of K_0, Pr, w and F.

where

$$N = N_r + iN_i$$

$$N_r = \frac{\beta}{2}(A - C) + B(1+\alpha)/2 - Ba,$$

$$N_i = Ar_1 + \frac{B\beta}{2} - Ca - (A - C)(1+\alpha)/2$$

and

$$\tan\alpha = N_i / N_r.$$

Results and Discussion

The velocity profiles for $wt = \pi/2$ are shown in Fig. 1. It is observed that near the plate ($y << 1$) the velocity increases rapidly and then decreases slowly away from the plate. Also the velocity increases with permeability k_0 but decreases with Prandtl number Pr and radiation parameter F.

It may be noted from Fig. 2 that fluctuating parts of the velocity – M_r remains positive and M_i remains negative for all values of permeability k_0, Prandtl number Pr, frequency w and radiation parameter F. Also, M_r decreases with increase in k_0, Pr, w and F whereas M_i decreases as Pr or F or w decreases and as k_0 increases.

For the phase and amplitude of the skin-friction, we observe from Fig. 3 that the phase $\tan\alpha$ remains negative and decreases with increase in permeability k_0 but increases with Pr and F. This means that there is always a phase lag. Also the amplitude $|N|$ decreases with k_0, Pr and F.

The temperature distribution is plotted in Fig. 4. The temperature in thermal boundary layer decreases with increase in Prandtl number Pr or radiation parameter F.

Conclusions

It may be concluded from the above analysis that the effect of radiation is to decrease the velocity and temperature in the free convective boundary layer. But, with the increase in permeability parameter k_0, the velocity increases in the boundary layer.

References

1. Raptis, A., Tzivanidis, G. & Kafousias, N. (1981) *Tett. Heat & Mass Transfer* **8** : 417.
2. Raptis, A., Kafousias, N. & Massalas, C. (1982) *ZAMM* **62** : 489.
3. Raptis, A. (1983) *Int. J. Engg. Sci.* **21** : 345.
4. Raptis, A. & Perdikis, C.P. (1985) *Int. J. Engg. Sci.* **23** : 51.
5. Chandrasekhara, B.C., Namboodiri, P.M.S. & Hanumanthappa, A.R. (1984) *Warmeund-Stoffubertrangung* **18** : 17.
6. Vedhanayagam, M., Jain, P. & Fasirweather, G. (1987) *Int. Comm. Heat Mass Transfer* **14** : 495.
7. Singh, P., Misra, J.K. & Narayan, K.A. (1989) *Int. J. Numerical and Analytical Methods Geomechanics* **13** : 443.
8. Singh, K.D. & Suresh, K. (1993) *Jour. Math. Phy. Sci.* **27** : 141.
9. Takhar, H.S., Gorla, R.S.R. & Soundalgekar, V.M. (1996) *Int. J. Num. Methods for Heat and Fluid Flow* **16** : 77.
10. Rudraiah, N., Chandrasekhara, B.C., Veerabhadraiah, R. & Nagaraj, S.T. (1979) *PGSAM Series*, Asian Printers, Bangalore, p. 103.
11. Cogley, A.C., Vinceti, W.G. & Gilles, S.E. (1968) *AIAA J.* **6** : 551.
12. Greif, R., Habib, I.S. & Lin, J.C. (1971) *J. Fluid Mech.* **46** : 513.

PROC. NAT. ACAD. SCI. INDIA, 71 (A), III, 2001

Study of photoconductivity in (B_2O_3 – ZnS) Cu (0.1%) Cl (1%) composite

AKHILESH KUMAR*, SUNIL KUMAR SRIVASTAVA and S.G. PRAKASH

Department of Electronics & Communication, University of Allahabad, Allahabad-211 002, India.

**Department of Physics, Govt. of P.G. College, Rishikesh (Dehradun), India.*

Received July 15, 2000; Revised September 29, 2000; Accepted July 7, 2001

Abstract

The photoconductivity of (B_2O_3 – ZnS) Cu, Cl composites has been studied under various parameters such as field, light intensity, temperature and radiation wavelength etc. The (10% B_2O_3 – 90% ZnS) Cu (0.15%) Cl (1%) composite shows maximum photoconductivity. The *I–V* characteristics are linear up to 4V followed by saturation. For moderate temperatures, the photocurrent rises with temperature whereas with intensity it saturates.

(**Keywords** : photoconductivity/semi-conductors/composites)

Introduction

The interaction of photons having energy equal to or greater than the band gap, with bound electrons of lattice atoms, creates free electron hole pairs[1]. The increased carrier concentration in presence of light is function of various parameters such as intensity of illumination, energy of radiation, applied electric field, temperature[2] etc. These effects are well understood[3] by studying the variation of photocurrent as a function of above parameters. A good photosensitive material should not only show a large change in conductivity but also respond fast. If trapping centres are in abundance, the response time is slow. Trapping also increases the decay time, as the carriers are slowly released after removal of excitation source.

Although a lot of literature exists on the photoconducting properties of single crystals[4-5] relatively fewer measurements have been made on binder layers.

Photoconducing properties of a large number of materials have been investigated by several workers[6-7]. The temperature dependence of photocurrent provides a good information about the localized defect states and location of fermi level.

The nature of current *vs.* intensity curve gives an idea about the charge trapping and recombination processes taking place inside the material.

In current years properties of gallium-doped ZnO deposited onto glass by spray pyrolysis[8], optical and electrical characteristics of aluminium doped ZnO thin films prepared by Solgel technique[9], assembly and applications of the inorganic nanocrystals in polymer networks[10] etc. have been studied.

In the present study, an attempt has been made to study the photoconducting properties of (B_2O_3 – ZnS) Cu (0.1%) Cl (1%) binder layers under different parameters to get the optimum conditions.

Materials and Method

(i) *Preparation of sample* : For the preparation of sample, the two base materials *viz.* ZnS and B_2O_3 were taken in different proportions, say.

(i) 95% ZnS – 5% B_2O_3

(ii) 90% ZnS – 10% B_2O_3

(iii) 85% ZnS – 15% B_2O_3

Then copper impurity of concentration (0.05%, 0.1%, 0.15%, 0.2%) and chlorine (1%) was added in the form of NH_4 Cl aqueous solution into the mixture making it a homogeneous paste. The mixture was then slowly dried up at about 80°C. It was finely powdered and filled into silica tube with graphite corks loosely fitting the ends. For firing, a cylindrical furnace, both ends fitted with ruber corks is taken. Temperature was regulated by adjusting the external resistance put in the circuit and was measured by a (Cr–Al) temperature indicator. The sample was fired at 820°C for 45 min. under controlled atmospheric conditions.

(ii) *Fabrication of cell* : Cell was fabricated in the form of parallel plate capacitor by using polysterene as binder. The sample suspended in binder was pressed between two conducting glass plates. Conducting glass can be made by spraying stanic chloride ($SnCl_4$) solution on non-conduting glass plate held at 600°C. A thin layer of tin oxide (SnO_2) is thus deposited which is conducting and transparent.

(iii) *Measurements* : For measurement purpose a cell of area ~2.5 cm^2 with a thickness ~0.5 mm was mounted in a dark chamber and a d.c. field (50-100 V/cm) was applied and light from 300 W Hg lamp was allowed to fall on the surface of the cell. Photocurrent was measured through a nA meter under different parameters such as intensity, temperature,

field, wavelength of radiation etc. The temperature of cell is changed by changing the temperature of oven and intensity by changing the slit width. Optical filters are used for changing the wavelength of radiation.

Results and Discussion

Photoconducting properties of (5% B_2O_3 – 95% ZnS), (10% B_2O_3 – 90% ZnS) and (15% B_2O_3 – 85% ZnS) with different concentrations of Cu and Cl were studied. It was found that (10% B_2O_3 – 90% ZnS) sample with different concentrations of Cu shows maximum photoconductivity in comparison to other samples hence the photoconducting properties of (10% B_2O_3 – 90% ZnS) sample with different parameters was studied. Photoconductivity changes with the amount of Cu, and is maximum for 0.15% Cu. (Fig. 1).

(i) *Effect of field* : Fig. 2 shows variation of photocurrent with voltage. In presence of light initially photocurrent increases with increase in voltage later it saturates.

The saturation[1,11] of *Ip vs. V* curves at higher voltage may be explained on the basis of class II states, which are imperfection centres lying close to valence band and having higher capture cross section for holes than for electrons[12].

There are also other type of states i.e. class I states which have roughly similar cross section for electrons and holes. Under illumination there exist two fermi levels, one for electrons and other one for holes. By increasing light intensity the electron fermi levels and hole fermi levels are shifted towards conduction band and valence band respectively. At a particular voltage and intensity all the class II states may be converted into recombination levels. If the voltage is increased beyond these values more electrons will be injected into the material. There by raising the fermi level up towards the conduction band. The upward movement of the fermi level would convert some of the class II state into trapping level causing desensitization with increasing voltage.

(ii) *Effect of temperature* : Fig. 3 shows effect of temperature on photoconductivity of (10% B_2O_3 – 90% ZnS) Cu (0.15%) Cl (1%) sample[12]. Photocurrent increases with increase in temperature-graphs are linear but at higher voltages there is change of slope.

Fermi levels are shifted towards the middle of the gap with the increase in temperature.

Arrhenius plots i.e. variation of photocurrent with $1/T$ plots (Fig. 4) are straight lines with changing its slope at $1/T = 2.9 \times 10^{-3}/^{\circ}K$. Nature of the graphs do not change at different supply voltages.

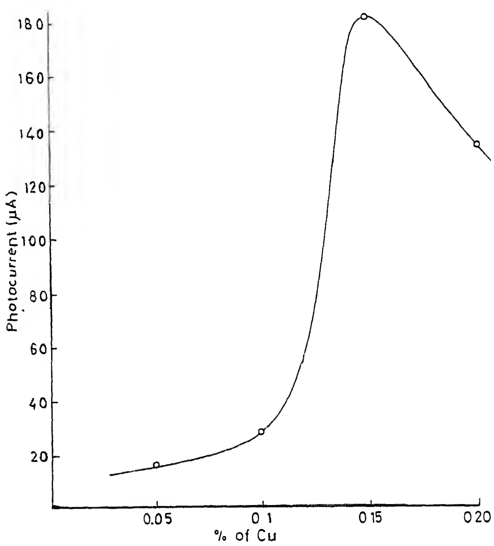

Fig. 1 – Variation of phtocurrent with % of Cu in the ZnS – B_2O_3 composites.

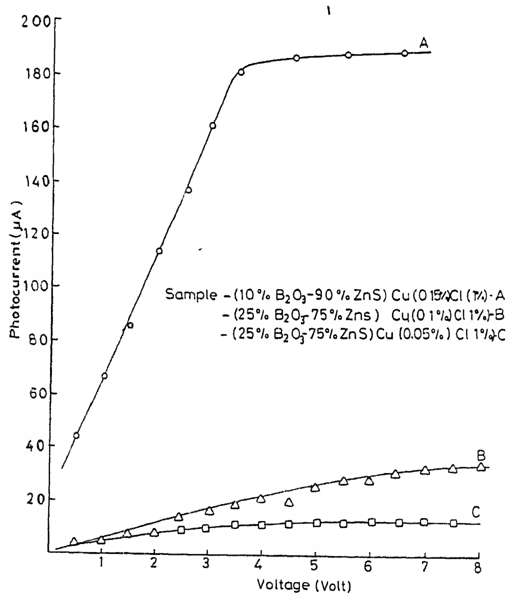

Fig. 2. – Variation of photocurrent with voltage for 3 composites with 0.15%, 0.1%, 0.05% of Cu.

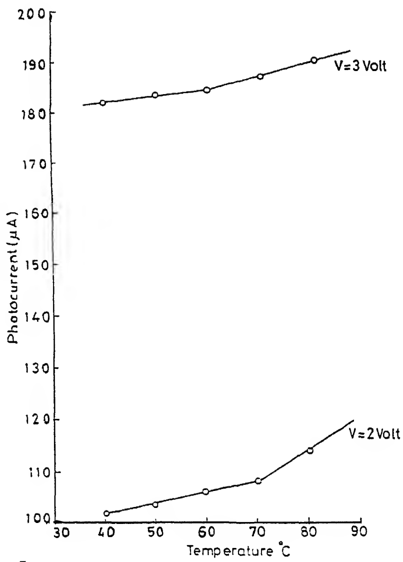

Fig. 3 – Variation of photocurrent with temperature for sample (10% B_2O_3 – 90% ZnS) Cu (0.15%) Cl (1%).

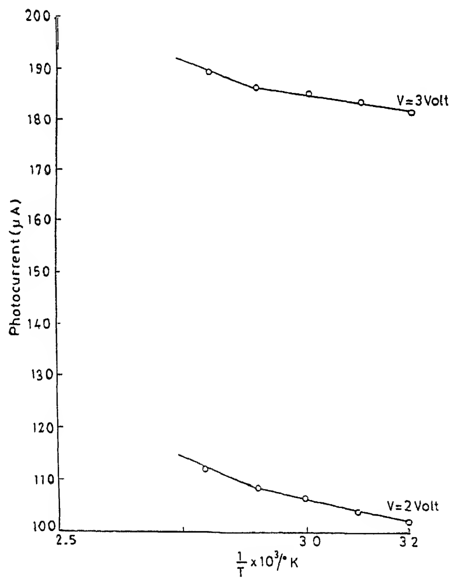

Fig. 4 – Arrhenius plots for sample (10% B_2O_3 – 90% ZnS) Cu (0.15%) Cl (1%).

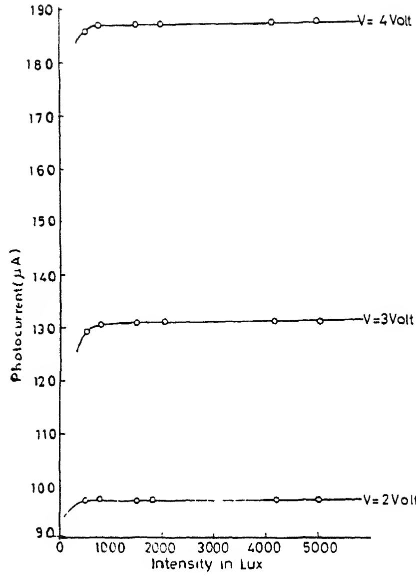

Fig. 5 – Variation of photocurrent with intensity for sample (10% B_2O_3 – 90% ZnS) Cu (0.15%) Cl (1%).

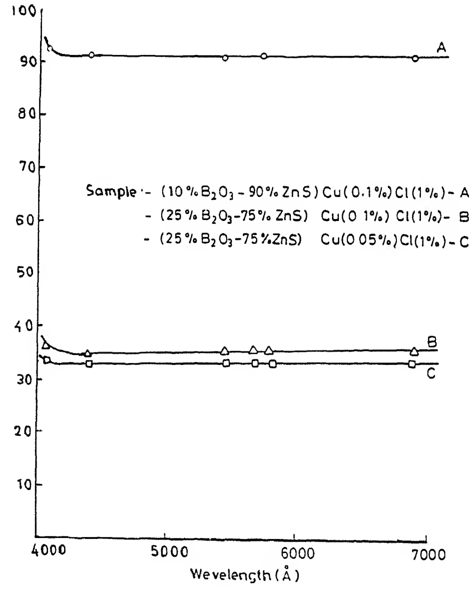

Fig. 6 – Variation of photocurrent with wavelength.

(iii) *Effect of intensity* : Fig. 5 shows variation of photocurrent with intensity of illumination. Initially photocurrent increases with increase in intensity later it becomes constant. This means that at a particular intensity all charge carriers are released.

(iv) *Effect of wavelength* : Fig. 6 shows variation of photocurrent with wavelength. Initially photocurrent decreases with increase in wavelength then becomes constant, The dip in photocurrent may be due to absorption of radiation by non- radiative centres.

Conclusions

The (B_2O_3 – ZnS) composites show maximum photoconductivity for (10% B_2O_3 – 90% ZnS) Cu (.15%) Cl (1%) composition. The $I - V$ characteristics are linear upto 4V, followed by saturation. For moderate temperature, the photocurrent rises with temperature, whereas it saturates with rise in intensity.

References

1. Bube, R.H (1967) *Photoconductivity of solids*, John Wiley & Sons, New York, p. 211.
2. Aldrich, R.E., Hon, S.L. & Horvill, M.L. (1971) *J. Appl. Phys.* **42** : 493.
3. Rose, A. (1951) *R.C.A. Review*, **12** : 362.
4. Mark, Peter (1964) *J. Phys. Chem. Solids* **25** : 911.
5. Shmilevich, A.M., Stys, L.E., Chemeresyuk, G.G. & Serdyuk, V.V. (1981) *Sov. Phys. – Semicond.* **15** : 489.
6. Glew, R.W. (1977) *Thin Solid Films* **46** : 59.
7. Kenawy, M.A. & Zayed, H.A. (1990) *J. Mater. Sci.* **1** : 115.
8. Tiburcio-Silver, A., Sanchez-Jaurz, A. & Avilagarcia, A. (1998) *Sol. Energy Mater. Sol. Cells (Netherlands)*, **55** : 3.
9. Jimenez, A.E., Gonzalez, Sot, J.A., Vrueta & Saurez, R. (1998) *Para. J. Cryst. Growth (Netherlands)* **192 : 430.**
10. Thiang, J M., Yang, Y., Yang, B., Liu, S.Y. & Shen, J.C. (1998) *Thin Solid Films (Switzerland)* **327** : 536.
11. Devi, Sadhana & Prakash, S.G. (1994) *Indian J. Pure & Applied Phys.* **32** : 930.
12. Rose, A. (1963) *Concept of photoconductivity and allied problems*, Wiley, New York, p. 43.

PROC. NAT. ACAD. SCI. INDIA, 71 (A), III, 2001

Study of drinking water quality in Gorakhpur city

Received : July 1, 1997; Revised : June 12, 1998, Re-revised : March 18, 1999;
Accepted : April 23, 1999

Abstract

Water samples from different sources were analysed for physico- chemical and bacteriological properties. It was observed that the water available in Gorakhpur City was moderately hard and contained appreciable amount of iron. The water available from water works and from tubewell source could be safely used for drinking purpose but those from shallow hand pumps and open wells should be avoided due to high level of turbidty, iron, chloride and coliform density.

(**Keywords**: physico-chemical & bacteriological properties/ water quality.)

Water is essential for maintenance of all forms of life. It is estimated that water available for human consumption is only three percent of total quantity of water available on this planet. The demand for water is always increasing as a result of continued population growth and rapid agricultural and industrial expansion. It is high time that apart from judicious planning and management of this precious resource, the issue of its quality determination be seriously taken up for its safe and efficient use.

The studies on water (Fig. 1) for human consumption have been taken up extensively in developed countries but the data for developing countries including India is rather scanty[1-13]. In the present work, the study on the quality of water for human consumption has been taken up in the city of Gorakhpur (Fig. 1) by determining its physico-chemical and bacteriological characteristics. The city of Gorakhpour is located in the eastern part of State of Uttar Pradesh of India. It is situated on the banks of river Rapti within alluvial plain and abundant quality of water is available at shallow depth so that general public prefers to draw water from hand pumps and tubewells instead of depending on water supplied from city water works which is available in limited localities.

The quality of water is generally expressed in terms of different physico-chemical and bacteriological parameters. The physical parameters of interest are turbidity, colour, taste and odour where as pH, alkalinity, chloride, hardness, sodium, potassium, calcium manganese, mercury, selenium, iron, arsenic, sulphates, phenolic compounds, nitrates, fluoride etc. represent the main chemical characteristics. As far as the question of bacteriological characterization goes, coliform density is used as an indicator of faecal

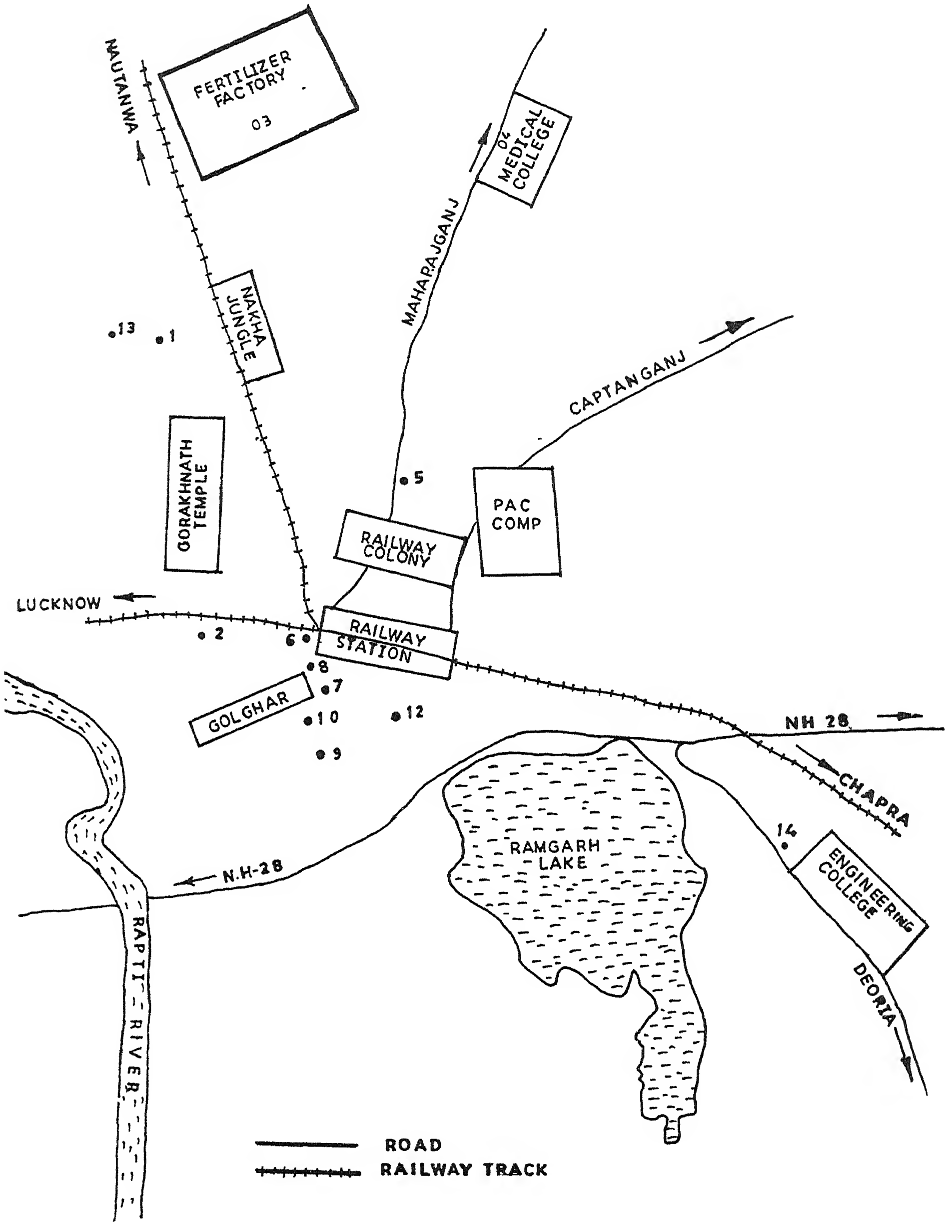

Fig. 1 – Schematic locational map of Gorakhpur City showing sampling locations.

Table 1 – Details of sample collection.

Sampling point	Location	Source type	Sanitary condition
1.	Rajendra Nagar	Deep borewell	Good
2.	Humayunpur	Shallow handpump	Good
3.	Fertilizer Colony	Water works	Good
4.	Medical College	Mark II handpump	Bad
5.	Shahpur Square	Shallow handpump	Fair
6.	Dharamshala	Shallow handpump	Bad
7.	Golghar	Shallow handpump	Bad
8.	Head Post Office	Shallow handpump	Bad
9.	Nakas Chowk	Mark II handpump	Good
10.	Maya Bazar	Water works	Fair
11.	Gorakhnath	Water works	Fair
12.	University Office	Water works	Fair
13.	Luxhipur	Open well	Bad
14.	Engineering College	Shallow hand pump	Good

Table 2 – Details of experimental methodology employed for determining physico-chemical and bacteriological parameters of interest.

S.No.	Parameter of interest	Experimental methodology
1.	pH	Glass electrode method
2.	Turbidity	Nephelometric turbidity method
3.	Alkalinity	Indicator method
4.	Hardness	EDTA titrimetric method
5.	Chloride	Agentometric method
6.	Sodium	Flame photometric method
7.	Potassium	Flame photometric method
8.	Calcium	Flame photmetric method
9.	Iron	Phenanthroline method
10.	Manganese	Persulfate method
11.	Nitrate	UV-spectrophotometric method
12.	Suplhate	Turbidimetric method
13.	Fluoride	Alizarin photometric method
14.	Coliform density	Multiple tube fermentation method

Table 3 – Arithmatic mean and standard deviation of different parameters

Sampling Stos	pH	Turbidity (NTU)	Alkanity as $CaCO_3$ (mg/l)	Chloride mg/l	Hardness mg/l	Sodium mg/l	Potassium mg/l	Calcium mg/l	Iron mg/l	Manganese mg/l	Nitrate mg/l	Sulphate mg/l	Fluoride mg/l	MPH per 100 ml
1	8 20±0 20	1.20±0 715	104 2±13 7	25 2±5.2	678.8±12.4	10±4	5±2	8±0	0 1±0 0	NT*	0 35±0 20	111±9	0 19±0 08	0±0
2	7 92±0 11	1.96±0 27	114 2±9.5	50.8±2.3	96 8±5 4	23±1	4±0	8±0	0.2±0 0	NT*	2.97±0.95	135±6	0.21±0 13	0±0
3	8 29±0 21	3.88±0 438	126.8±5.3	43.6±13.4	120.0±25 2	31±10	10±1	16±0	0.6±0.1	NT*	1.25±0 66	107±2	0 03±0 03	0±0
4	8.15±0 36	6.46±0 705	122.8±20.6	53 0±14.8	138.2±44 6	28±3	5±1	30±2	0 4±0.1	NT*	2.47±12 05	180±5	0 06±0 00	6±6
5	7 77±0 17	3.32±1 163	107 6±5.8	73.2±10.2	127 8±16 4	55±3	4±0	44±3	0.5±0.1	NT*	10 90±2 55	146±13	0 29±0 11	16±14
6	7 64±0 23	4.10±1.57	271.6±18 3	349 2±9 1	145.6±13 8	102±5	13±2	54±0	0 4±0.1	NT*	12.66±0 96	186±6	0 10±0 06	5±6
7	8 20±0 18	3.98±0 75	178 6±24 6	460.0±17.7	138 0±5 3	120±10	4±0	38±0	0.4±0 0	NT*	12 64±0.95	138±3	0 36±0 13	1±1
8	7 68±0 21	4 70±0 86	186.6±10 2	359 4±5.1	150 6±12 2	101±7	4±1	46±0	0.5±0 1	NT*	12 76±1.27	115±6	0 20±0 05	945±443
9	8.22±0 13	3 46±1 02	161.2±22.2	261.6±48.0	108.0±5 9	84±5	5±0	46±0	0.5±0.2	NT*	414±0.34	193±9	0 07±0 03	0±0
10	8.27±0.09	1 96±0 76	156.4±6.6	93 0±30.7	117 0±6 4	77±4	5±3	38±2	0.4±0.1	NT*	3.87±3.00	181±11	0 06±0 03	0±0
11	8 24±0 24	1 58±0 56	135 4±5.0	59 2±15.2	106 8±14.6	74±2	6±1	30±0	0.2±0 0	NT*	2.13±0 40	109±6	0 22±0 11	0±0
12	8 17±0 11	1 88±0 544	116 8±6.0	51.8±15.2	108.2±1.3	26±2	4±1	25±0	0.2±0.0	NT*	3 01±0.78	105±10	0 14±0 09	13±28
13.	7 83±0 15	7 20±0 363	187 2±10.5	117.6±5 6	108.0±21 9	39±8	4±1	29±0	0.4±0.1	NT*	12.66±2.18	176±38	0 14±0 08	174±61
14	8.00±0 25	3 70±0 717	117 2±7 8	92 8±8.0	105.2±8.5	53±7	3±1	30±0	1 3±0.1	NT*	4.20±1.20	155±11	0 29±0 13	0±0

* Note traced.

Table 4 – Drinking Water Standard (See Ref. 16).

(a) Physical and chemical standards : The physical and chemical water quality of water should not exceed the limits shown in the table below:

S.No.	Characteristics	Acceptable*		Cause for Rejection**	
1	2	3		4	
1.	Turbidity (Unit on NTU Scale)	2.5	(5)	10	(10)
2.	Color (Unit on Pt-Co Scale)	5.0		25	
3.	Taste and odor	unobjectionable		Unobjectionable	
4.	pH	7.5 to 8.5 (6.5-8.5)		6.5 to 9.2 (NR)	
5.	Total dissolved solids(mg/l)	500	(400)	1500	(2000)
6.	Total hardness (mg/l) as	200	(300)	600	(600)
7.	Chloride (as Cl) mg/l	200	(250)	1000	(1000)
8.	Sulfate (as SO_{12}) mg/l	200	(200)	400	(400)
9.	Fluorides (as F) mg/l	1.0	(1.0)	1.5	(1.5)
10.	Nitrates (as NO_3) mg/l	45	(45)	45	(100)
11.	Calcium (as Ca) mg/l	75	(75)	200	(200)
12.	Magnesium (as Mg) mg/l	30	(30)	150	(100)
13.	Iron (as Fe) mg/l	0.1	(0.03)	1.0	(1.0)
14.	Manganese (as Mn) mg/l	0.05	(0.03)	0.5	(0.3)
15.	Copper (as Cu) mg/l	0.05	(0.05)	1.5	(1.5)
16.	Zinc (as Zn) mg/l	5	(5)	15	(15)
17.	Phenolic compounds (as Phenol) mg/l	0.001	(0.001)	0.002	(0.0032)
18.	Anionic detergents (mg/l)	0.2	(0.2)	1.0	(1.0)
19.	Mineral oil (mg/l)	0.01	(0.01)	0.3	(0.3)
Toxic Materials					
20.	Aresenic (as As) mg/l	0.05	(0.05)	0.05	(NR)
21.	Cadmium (as Cd) mg/l	0.01	(0.01)	0.01	(NR)
22.	Chromium (as Cr^{-6}) mg/l	0.05	(0.05)	0.05	(NR)
23.	Cyanide (as CN) mg/l	0.05	(0.05)	0.05	(NR)
24.	Lead (as Pb) mg/l	0.1	(0.05)	0.1	(NR)
25.	Selenium (as Se) mg/l	0.01	(0.01)	0.01	(NR)
26.	Mercury (total as Hg) mg/l	0.001	(0.001)	0.001	(NR)

Values in parenthisis are the Ref. 16.

Values IS-10500, 1991 with January, 1993 amendments.

(b) Bacteriological standards : Coliform count in any sample of 100 ml should be zero.

Water in the distribution system shall satisfy all the three criteria indicated below :

(1) *E. Coli* count in 100 ml of any sample should be zero.

(2) Coliforms organism not more than 10 per 100 ml shall be present in any sample.

(3) Coliform organism should not be more detectable in 100 ml of any two consecutive samples or more than 50% of the samples collected for the year.

*The figure indicated under the column acceptable are the limits up to which the water is generally acceptable to the consumers.

*Figures in excess of those mentioned under 'acceptable' render the water not acceptable but still may be tolerated in the absence of alternative and better source but upto the limits indicated under column "cause for rejection" above which the supply will have to be rejected.

pollution rather the pathogens themselves. The assessment of microbial safety of water, therefore, is expressed in terms of coliform (MPN) in 100 ml of water.

A total set of five samples from fourteen locations selected at random were collected and analysed for various water quality parameters. Table 1 gives detail of the sample collected in terms of the location of the source, the type of source and the sanitary conditions prevailing around the source. If the area near the source was clean and hygenic, the sanitary condition was termed good and in case a platform was provided near the source but drainage facility was not adequate, the sanitary condition was termd fair. The term bad condition was given to those sources which were not provided with platform and had very bad drainage facility or a big public drainage was passing through nearby area.

The water samples were collected in plastic bottles. The bottles were first rinsed with distilled water and then with sample water before actual collection. Water from the source of interest was allowed to run for two min. before taking samples to ensure flushing of stagnant water if any in the domestic water supply pipes or the handpumps. For open well, the samples was collected by dipping the sampling bottle tied with string taking care all along that the bottle did not touch the sides of the well. The water samples for bacteriological analysis were collected in 100 ml sterilised glass bottles.

The physico-chemical and bacteriological analysis was carried out by employing standard methods[14] using reagent which were prepared and stored exercising all precautions mentioned in the above stated standard methods. Table 2 gives details of the experimental methodology used for determining the water qualiy parameters of interest.

The arithmetic mean values and the associated standard deviation for the physico-chemical and bacteriological parameters of interest are shown in Table 3. The values were obtained from five sets of samples which were taken in the period between 22nd October 1996 and 8th January 1997 at intervals of two weeks. (Table 4).

The pH values of water samples analysed in the present work varied from 7.6 to 8.3 and were found to be within permissible limit. Turbidity which reflects on the appearance of water may not be important from health point of view but plays an important role in consumer satiafaction. The turbidity of typical treated water is expected to range between 0 to 2.5 NTU. In the present study, the tutbidities of water samples analysed varied from 1.2 to 7.2 NTU, the highest value was obtained from water sample taken from an open well and lowest from water samples taken from deep bore well.

Alkalinity which is the capacity of water to neutralize strong acid, itself is not harmful for human beings but the desired value for domestic water supply is expected[15] to be less than 100 mg/l[17]. In the present work, alkalinity of water samples ranged from 104.2 to

271.6 mg/l, the highest value being shown from water samples taken from shallow hand pump source. Hardness which understood in terms of capacity of water to precipitate soap, was found to vary between 67.6 and 150 mg/l of equivalent calcium carbonate thereby indicating that the water available in the city of Gorakhpur could be categorised as moderately hard.

The chloride content which generally reflects the presence of sodium chloride and is some times used as an indicator of pollution give a noticeable salty taste to water if its concentration rises above 250 mg/l. In the present work, chloride concentration ranged from 25.2 to 460 mg/l. The high values were obtained again from water samples taken from shallow hand pumps.

The concentration of sodium, potassium, calcium, manganese, sulphates, nitrates and fluorides were also tested and were observed to be within the permissible limits[16,17]. However, the concentration of iron was observed to be on the higher side. Iron though present in biologically significant proteins, is not a cause for concern as far as the general health of population goes but it has a nuisance value since it precipitates as ferric hydroxide, a rusty coloured silt which makes water unpalatable and causes stain to the laundry and plumbing fixtures.

The most common and widespread danger associated with drinking water is contamination either by sewage, other waste or human and animal excrement which have been known to cause water borne diseases. The universally acceptable principle for monitoring and assessing the microbial safety of water supply is through the measurement of coliform density (MPN). In the present work, the water samples from open well and shallow hand pump showed high level of coliform density.

In the present work a modest attempt was made to evaluate the standard of drinking water available to the citizens of Gorakhpur City and it was observed that the water available to them was moderately hard and had appreciable concentration of iron. It is recommended that people should draw water from sources having deep boring but should avoid drawing of water from open wells and shallow hand pumps.

References

1. Gupta, M.K., Singh, Vibha, Rajwansi, Poonam & Srivastava, Shalini (1994) *Indian Jour. of Environ. Health* **36**: 43.
2. Mittal, S.K. (1994) *Indian Jour. of Environ. Health* 36:51.
3. Nagpal, J.L. & Arora, H.C. (1991) *Jour. of Indian Water Works Assoc.* 23:113.

4. Narayana A.C. & Suresh G.C. (1989) *Indian Jour. of Environ. Health* **31**:228.

5. Nawlake, W.G. (1994) *Jour. of Indian Water Works Assoc.* **26**:9.

6. Ozha, D P. & Jain, P.C. (1993) *Jour. of Indian Water Works Assoc.* **25**:31.

7. Gupta, S.C. (1981) *Indian Jour. of Environ. Health* **23**:195.

8 Lakshman, A.P , Krishna Rao, T & Vishwanathan S. (1986) *Indian Jour. of Environ. Health* **28**:39.

9 Phirke, P M., Balasubramaniyan, R & Verma, S.R. (1969) *Indian Jour. of Environ. Health* **11**:323.

10 Sivakumar, M. & Ramamoorthy, M.V. (1977) *Indian Jour. of Environ. Health* **19**:199.

11 Kumar, V.P., Malhotra, I. & Mathur, R.P. (1993) *Proceedings of International Conference on Environmental Management*, Geo-Water and Engineering Aspects, Wallong Australia, 219.

12. Kanan, G.K. & Chaurasia, Sadhana (1996) *Jour. of Indian Water Works Assoc.* **28**:225.

13. Sirkar, A.G., Bhatanagar, Amita & Khanna, Manju (1996) *Jour of Indian Water Works Assoc.* **28**:215.

14. *Standard Methods for Examination of Water and Waste Water Quality*, Jointly published by APHA, AWWA, WPCF, New York, 16th Edition (1985).

15 Trivedi, R.K. & Goel, P.K. (1986) *Chemical and Biological Methods for Water Pollution Studies*, Environmental Publication, Karad, India.

16. *Manual of Water Supply and Treatment*, Ministry of Urban Development, Govt. of India, New Delhi (1991).

17. *Drinking Water*, IS-10500-1991, Bureau of Indian Standard, New Delhi (1991).

ALOK SRIVASTAVA*, AMITABH K. SRIVASTAVA, P.P. SRIVASTAVA** and S.C. PRASAD+

**Mahindra United World College of India, Paud, Pune, India*

Civil Engineering Department, M.N.R. Engineering College, Allahabad, India

***The National Academy of Sciences, India, 5, Lajpatrai Road, Allahabad-211 002, India*

+Author for correspondence.